Maastricht University

The antioxidant flavonoid 7-mono-O (B-hydroxyethyl)-rutoside : from clinic to concept

Citation for published version (APA):

Jacobs, H. (2011). *The antioxidant flavonoid 7-mono-O (B-hydroxyethyl)-rutoside : from clinic to concept*. [Doctoral Thesis, Maastricht University]. Universitaire Pers Maastricht. https://doi.org/10.26481/dis.20110701hj

Document status and date:
Published: 01/01/2011

DOI:
10.26481/dis.20110701hj

Document Version:
Publisher's PDF, also known as Version of record

Please check the document version of this publication:

• A submitted manuscript is the version of the article upon submission and before peer-review. There can be important differences between the submitted version and the official published version of record. People interested in the research are advised to contact the author for the final version of the publication, or visit the DOI to the publisher's website.
• The final author version and the galley proof are versions of the publication after peer review.
• The final published version features the final layout of the paper including the volume, issue and page numbers.

Link to publication

General rights
Copyright and moral rights for the publications made accessible in the public portal are retained by the authors and/or other copyright owners and it is a condition of accessing publications that users recognise and abide by the legal requirements associated with these rights.

• Users may download and print one copy of any publication from the public portal for the purpose of private study or research.
• You may not further distribute the material or use it for any profit-making activity or commercial gain
• You may freely distribute the URL identifying the publication in the public portal.

If the publication is distributed under the terms of Article 25fa of the Dutch Copyright Act, indicated by the “Taverne” license above, please follow below link for the End User Agreement:

www.umlib.nl/taverne-license

Take down policy
If you believe that this document breaches copyright please contact us at:

repository@maastrichtuniversity.nl

providing details and we will investigate your claim.

Download date: 05 May. 2023

The antioxidant flavonoid

7-mono-O-(β-hydroxyethyl)-rutoside

From clinic to concept

Hilde Jacobs

© Hilde Jacobs, Maastricht 2011
ISBN 978-94-6159-064-0
Universitaire Pers Maastricht

Lay-out: Hilde Jacobs
Production: Datawyse Boekproducties, Maastricht

The studies presented in this thesis were performed within NUTRIM School for Nutrition, Toxicology and Metabolism which participates in the Graduate School VLAG (Food Technology, Agrobiotechnology, Nutrition and Health Sciences), accredited by the Royal Netherlands Academy of Arts and Sciences.

Financial support for printing of this thesis was kindly provided by DSM Resolve (Geleen), Greiner Bio-One B.V. (Alphen a/d Rijn), Grace Davison Discovery Sciences, and Morssinkhof-Rymoplast (Lommel, België).

The antioxidant flavonoid
7-mono-O-(β-hydroxyethyl)-rutoside
From clinic to concept

PROEFSCHRIFT

ter verkrijging van de graad van doctor
aan de Universiteit Maastricht,
op gezag van de Rector Magnificus, Prof. mr. G.P.M.F. Mols,
volgens het besluit van het College van Decanen,
in het openbaar te verdedigen
op vrijdag 1 juli 2011 om 14.00 uur

door

Hilde Jacobs

geboren te Lommel op 4 mei 1984

UNIVERSITAIRE PERS MAASTRICHT

Promotor

Prof.dr. A. Bast

Copromotores

Dr. G.R.M.M. Haenen
Prof.dr. W.J.F. van der Vijgh, em. Vrije Universiteit Amsterdam

Beoordelingscommissie

Prof.dr. J.W.M. Heemskerk (voorzitter)
Dr. R. Peters (DSM Resolve, Geleen)
Prof.dr. G.J. Peters (Vrije Universititeit, Amsterdam)
Prof.dr. H.A.J. Struijker-Boudier
Prof.dr. V.C.G. Tjan-Heijnen

It always seems impossible until it is done...

CONTENTS

CHAPTER 1	General introduction	**9**
CHAPTER 2	Characterization of the glutathione conjugate of the semisynthetic flavonoid monoHER	**25**
CHAPTER 3	An essential difference in the reactivity of the glutathione adducts of the structurally closely related flavonoids monoHER and quercetin.	**43**
CHAPTER 4	An essential difference between the flavonoids monoHER and quercetin in their interplay with the endogenous antioxidant network	**57**
CHAPTER 5	The semisynthetic flavonoid monoHER sensitises human soft tissue sarcoma cells to doxorubicin-induced apoptosis via inhibition of nuclear factor-kB	**77**
CHAPTER 6	Identification of the metabolites of the antioxidant flavonoid 7-mono-O-β-hydroxyethyl)-rutoside in mice.	**89**
CHAPTER 7	Differences in the metabolic profile of the antioxidant flavonoid 7-mono-O-(β-hydroxyethyl)-rutoside between men and mice. Possible implications for its cardioprotective effect.	**107**
CHAPTER 8	Summary and general discussion	**129**
	Samenvatting en algemene discussie	**137**
	Dankwoord	**143**
	Curriculum vitae	**149**
	List of publications	**151**

Chapter 1

General introduction

Clinical and preclinical pharmacology of the antioxidant flavonoid 7-mono-O-(β-hydroxyethyl)-rutoside (monoHER)

Chemical structure and antioxidant properties of monoHER

7-mono-O-(β-hydroxyethyl)-rutoside (monoHER) is a semisynthetic flavonoid and a constituent of Venoruton, a registered drug that is used in the treatment for chronic venous insufficiency. Venoruton also contains other structurally related hydroxyethylrutosides (HERs), i.e. diHER, triHER and tetraHER. These HERs are derived from the naturally occurring flavonoid rutin by substituting its hydroxyl groups with O-β-hydroxyethyl groups. Of these semisynthetic flavonoids, monoHER appeared to be the most powerful antioxidant (Haenen *et al.*, 1993; van Acker *et al.*, 1993).

Like most flavonoids, monoHER consists of three rings referred to as the A, B and C rings (Figure 1). In addition, it contains an ortho-dihydroxy group in the B ring (catechol), and a C2-C3 double bond and 4-oxo function in the C ring, which contribute to its high antioxidant activity (van Acker *et al.*, 1996). Further characteristic structural features of monoHER are the rutinose group (glucose + rhamnose) at the 3-O position in the C ring and the hydroxyethyl group at the 7-O position in the A ring.

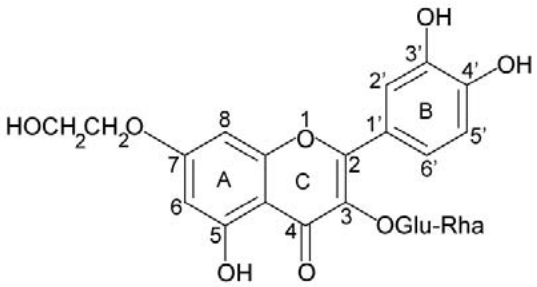

Figure 1. Structural formula of monoHER and numbering of relevant carbon atoms.

Preclinical studies with monoHER

MonoHER and doxorubicin-induced cardiotoxicity

Doxorubicin is a very effective antitumour agent, but its clinical use is limited by the occurrence of a cumulative dose-related cardiotoxicity, resulting in congestive heart failure (Bast *et al.*, 2007; Lipshultz *et al.*, 2005; Singal and Iliskovic,

1998). Doxorubicin-induced cardiotoxicity presumably results from free radicals, which are produced during redox-cycling of doxorubicin (Horenstein *et al.*, 2000; Julicher *et al.*, 1988; Xu *et al.*, 2001). Because of its favorable iron chelating and radical scavenging properties (Haenen *et al.*, 1993; van Acker *et al.*, 1993), monoHER was tested as a protector against doxorubicin-induced cardiotoxicity.

MonoHER protected almost completely (92.7%) against doxorubicin-induced cardiac damage in an isolated atrium model (van Acker *et al.*, 1993). In mice, cardioprotection was observed when monoHER was administered as an intraperitoneal (i.p.) dose of 500 mg/kg five times/week in combination with a weekly intravenously (i.v.) dose of 4 mg/kg doxorubicin for a period of six weeks (van Acker *et al.*, 1995). Cardiac damage was assessed by the changes in the electrocardiogram (ECG), recorded with a transmitter transplanted in the intraperitoneal cavity of the mice. The increase in the ST-interval of the ECG was used as a measure for doxorubicin-induced cardiotoxicity (Figure 2). At the end of the study (week 8) the ST-interval of the ECG had increased by 16.7 ± 2.7 msec in the doxorubicin-treated mice. At the same time, the ST-interval had increased by only 1.7 ± 0.8 msec in the monoHER co-medicated mice (van Acker *et al.*, 1995).

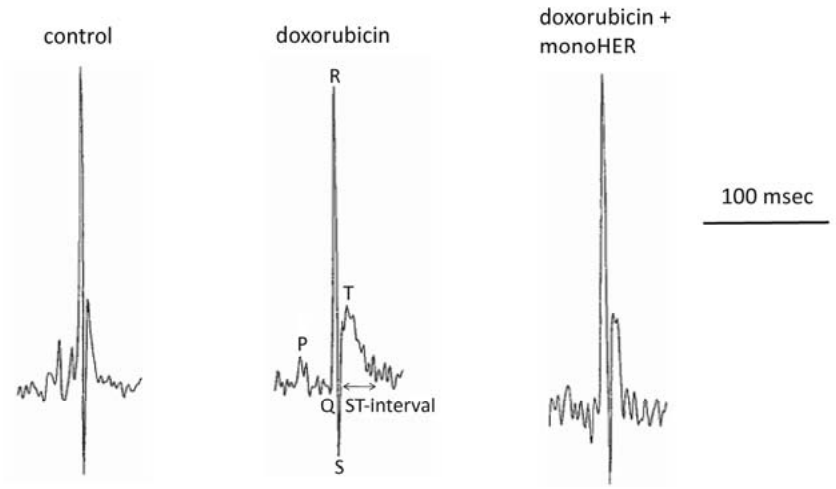

Figure 2. Typical ECG trace of a mouse before (control) and after receiving 4 mg/kg doxorubicin with(out) 500 mg/kg monoHER for 6 weeks (van Acker *et al.*, 2000).

A later performed study showed complete protection against doxorubicin-induced cardiac damage in mice, when monoHER was given as a single i.p. injec-

tion (500 mg/kg) only once a week 1 hour before doxorubicin administration (4 mg/kg, i.v.) (van Acker *et al.*, 2000) (Figure 3).

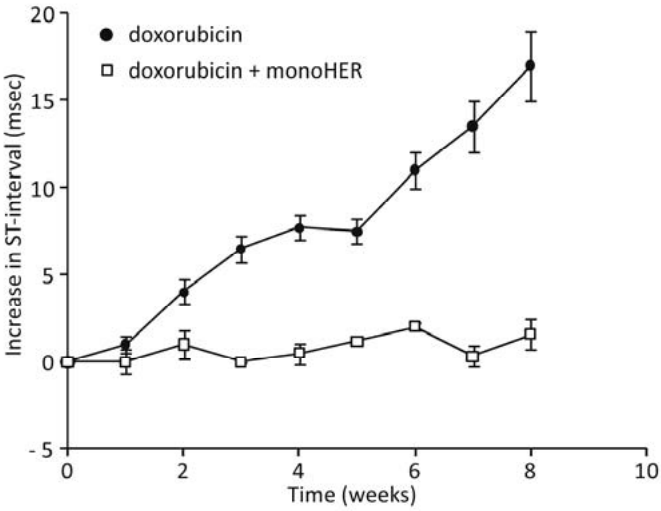

Figure 3. Protection by monoHER on the ST-interval lengthening of the ECG of mice treated with doxorubicin (van Acker *et al.*, 2000).

Since it is known that the long-term effect of doxorubicin on cardiac tissue may progress in time to more severe myocardial injury, resulting in cardiomyopathy or even chronic heart failure, it was investigated whether the cardioprotective effect of monoHER was maintained after a longer period of time (26 weeks). The cardioprotective effect lasted for a longer period of time than during the first 8 weeks. However, towards the end of 26 weeks of observation the cardioprotection by monoHER was not present anymore and toxicity became comparable to that in doxorubicin-treated animals (Bruynzeel *et al.*, 2007d). Continuation of weekly injections of monoHER (after 6 weeks of doxorubicin administration) for another 26 weeks even seemed to aggravate the development of doxorubicin-induced cardiotoxicity. This suggests that the dose and frequency of monoHER administration is crucial in obtaining an optimal antioxidant activity.

Because of the relative short half-life of monoHER (about 30 minutes), the time interval between monoHER and doxorubicin administration (1 hour) might be of influence on the cardioprotective effect of monoHER, i.e. could become better with a shorter time interval and worse when lengthening the time interval. However, data described by Bruynzeel et al. (2006) did not show a significant change in protection against doxorubicin-induced cardiac damage when

the time interval between monoHER and doxorubicin changed from 10 minutes to 2 hours.

Abou El Hassan et al. (2003a) investigated whether there is a pharmacokinetic interaction between monoHER and doxorubicin that might be involved in the protective effect of monoHER against doxorubicin-induced cardiotoxicity. The areas under the concentration-time curves (AUCs) of neither monoHER nor doxorubicin(ol) were affected by co-administration of the drugs. Also, no changes in other pharmacokinetic parameters such as initial and final half-lives, mean residence time, clearance and volume of distribution were observed after single or combined administration. This indicates that the cardioprotection observed in mice is not caused by a pharmacokinetic interaction between monoHER and doxorubicin.

MonoHER and the antitumour activity of doxorubicin

In order to use monoHER in clinical practice as a protector against doxorubicin-induced cardiotoxicity, monoHER should not influence the antitumour activity of doxorubicin. *In vitro*, it was found that monoHER did not significantly influence the IC_{50} (which is the concentration of the drug that gives a 50% inhibition of cell growth) of doxorubicin in the human ovarian cancer cell lines A2780 and OVCAR-3, and the human breast cancer cell line MCF-7 (Table 1). Similarly, *in vivo*, monoHER did not reduce the antitumour activity of doxorubicin in A2780 and OVCAR-3 subcutanous xenografts in nude mice (van Acker *et al.*, 1997). Thus, both *in vitro* and *in vivo*, monoHER protected against the toxic effect of doxorubicin on cardiac cells without interfering with the cytostatic effect on cancer cells.

Table 1. IC_{50} values of growth inhibition of various tumour cell lines by doxorubicin in the absence and presence of monoHER (van Acker *et al.*, 1997).

	A2780 (10^{-8} M)	**MCF-7** (10^{-7} M)	**OVCAR-3** (10^{-7} M)
Doxorubicin	2.05 ± 0.66	2.09 ± 0.75	3.28 ± 1.70
Doxorubicin + monoHER (50 µM)	2.57 ± 1.95	1.11 ± 0.04	4.29 ± 1.95
Doxorubicin + monoHER (100 µM)	2.00 ± 1.82	2.10 ± 0.22	5.67 ± 2.37

Data are expressed as mean ± SD of at least three independent experiments performed in triplicate.

To obtain more insight in the mechanism underlying the selective protective effects of monoHER, it was investigated whether monoHER (1 mM) affects doxorubicin-induced apoptosis in neonatal rat cardiac myocytes (NeRCaMs), human

umbilical vein endothelial cells (HUVECs) and the ovarian cancer cell lines A2780 and OVCAR-3. Doxorubicin-induced cell death was effectively reduced by monoHER in heart, endothelial and A2780 cells. OVCAR-3 cells were highly resistant to doxorubicin-induced apoptosis (Bruynzeel *et al.*, 2007b). Experiments with the broad caspase-inhibitor zVAD-fmk showed that doxorubicin-induced apoptosis was caspase-dependent in HUVECs and A2780 cells, whereas caspase-independent mechanisms seemed to be important in NeRCaMs. MonoHER suppressed doxorubicin-dependent activation of the mitochondrial apoptotic pathway in normal and A2780 cells as illustrated by p53 accumulation and activation of caspase-9 and -3 cleavage (Bruynzeel *et al.*, 2007b). These data indicate that monoHER might act by suppressing the activation of molecular mechanisms that mediate either caspase-dependent or -independent cell death. However, the concentration of monoHER needed (1 mM) indicates that the *in vitro* inhibition of the antitumour effect of doxorubicin is not relevant for the clinical application of monoHER.

MonoHER and doxorubicin-induced inflammation

Some studies support the suggestion that inflammation induced by doxorubicin plays a role in its cardiotoxic effects (Deepa and Varalakshmi, 2006; Hecker, 1990; Hou *et al.*, 2005). To investigate whether doxorubicin could induce an inflammatory response *in vitro*, HUVECs were incubated with increasing concentrations of doxorubicin. Doxorubicin affected both the viability and proliferation capacity of endothelial cells (Abou El Hassan *et al.*, 2003c). Doxorubicin also increased the adhesion of neutrophils, which was accompanied by the overexpression of VCAM and E-selectin. MonoHER was able to protect against these doxorubicin-induced inflammatory effects (Abou El Hassan *et al.*, 2003c) (Figure 4).

In addition, *in vivo,* it was demonstrated by Bruynzeel *et al.* (2007a) that treatment with doxorubicin induces an increase of N^{ε}-(carboxymethyl) lysine (CML) in intramyocardial arteries in mice. The induced increase in CML, which can be regarded as a biomarker for local endogenous stress, was found to be reduced by the anti-inflammatory agents, ketoprofen and dexamethasone, and by monoHER. These findings confirme the role of inflammation in doxorubicin-induced cardiotoxicity and indicate that monoHER has, besides its radical scavenging and iron chelating properties, anti-inflammatory properties that could also be involved in the protection against cardiac damage.

The anti-inflammatory effect of monoHER was also observed in a study on ischemia-reperfusion in mice (De Celle *et al.*, 2004). In this study, heart ischemia was induced for 30 minutes by ligating the left anterior descending coronary

artery. Afterwards, the ligature was removed and reperfusion was allowed. MonoHER (500 mg/kg) was given i.p. 1 hour before ischemia. This treatment significantly attenuated myocardial neutrophil influx and significantly reduced infarct size after reperfusion (De Celle *et al.*, 2004).

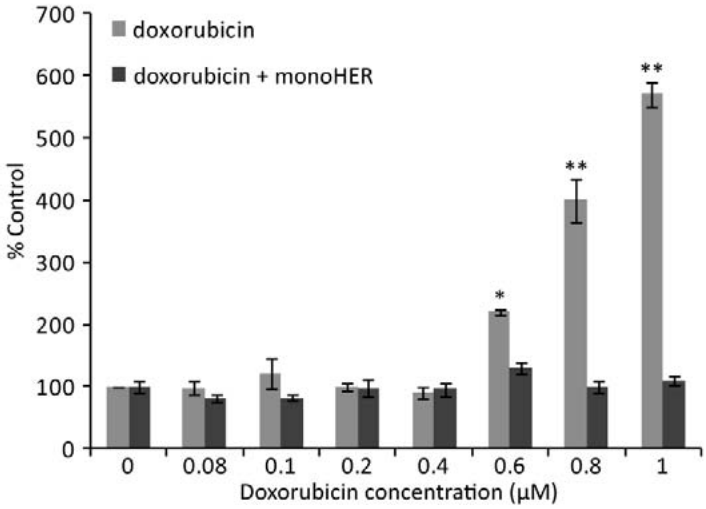

Figure 4. Overexpression of VCAM 24 h after incubation with doxorubicin. The combined treatment with monoHER prevented the concentration-dependent doxorubicin-induced overexpression of the adhesion molecule (Abou El Hassan *et al.*, 2003c).

Other pharmacological properties of monoHER

Several other pharmacological properties of monoHER have been described. As an effective antioxidant, monoHER protected erythrocytes in β-thalassemic mice against oxidative damage involved in their premature destruction (de Franceschi *et al.*, 2004). It has also been shown that monoHER has an effect on certain enzymes that intervene in the metabolism of mucopolysaccharides in human and bovine veins. The presence of monoHER (1 mg/ml) inhibited the enzyme β-glucuronidase extracted from human veins for 12.5% and for 70.3% when extracted from bovine veins, while monoHER did not significantly influence the activity of the enzyme N-acetylglucosaminidase obtained from both veins (Niebes and Laszt, 1971). MonoHER also affected prostaglandin synthesis in guinea pig lung tissue and human skin (Gosta, 1973). It has also been shown that monoHER has antioedematous properties in rats by inhibiting the action of bradykinine, histamine and carrageenin (Lecomte and Van Cauwenberge, 1974). Moreover, monoHER showed antithrombotic effects (Hladovec, 1977a; Mirkovitch, 1977), it prevented endothelial injury caused by nicotine and citrate (Hladovec, 1977b; Hladovec, 1978), it increased skin capillary resistance in a rat

model (Gabor, 1981) and reduced microvascular permeability in frogs (Kendall *et al.*, 1993).

Metabolism, bio-availability and pharmacokinetics of monoHER

Metabolic experiments with monoHER in the 1970s revealed that the major excretion route of monoHER in rats and mice is via bile by feces (Barrow and Griffiths, 1971; Barrow and Griffiths, 1974a; Barrow and Griffiths, 1974b; Hackett and Griffiths, 1977a; Hackett and Griffiths, 1979). The minor excretion route was by urine. Also enterohepatic cycling has been described (Hackett and Griffiths, 1977b).

More recently, Abou El Hassan *et al.* (2003b) investigated the bioavailability of monoHER in mice after different routes of administration. Concentrations of monoHER in plasma and heart were measured by HPLC with electrochemical detection (HPLC-ECD) (Abou El Hassan *et al.*, 2001; El Hassan *et al.*, 2001). After oral administration, monoHER could not be detected in plasma, which indicates that monoHER has a very poor oral bioavailability (Abou El Hassan *et al.*, 2003b). The i.p. and subcutaneous (s.c.) bioavailabilities were about 30 and 40%, respectively. In the same study, the pharmacokinetics of monoHER were determined (Table 2). Between 5 and 15 minutes after i.p. administration of 500 mg/kg monoHER, the maximal concentration (C_{max}) was reached in both plasma and heart tissue. Thereafter, monoHER disappeared from plasma and heart tissue with a half-life ($t_{1/2}$) of about 30 minutes. A C_{max} of about 131 µM was obtained in plasma, and the plasma area under the curve (AUC^{∞}) was 6.3 µmol min/ml. These values were used as end-points for a subsequent phase I study with monoHER.

Table 2. Summary of the pharmacokinetic parameters of monoHER in plasma and heart tissue of mice treated with 500 mg/kg i.p.(Abou El Hassan *et al.*, 2003b).

Parameter	Plasma	Heart
C_{max} (nmol/ml or /g wet tissue)	131	35.3
t_{max} (min)	5-15	5-15
$t_{1/2final}$ (min)	28.5	25.7
AUC^{∞} (µmol min/ml or /g wet tissue)	6.3	1.6
$AUC^{0\text{-}120min}$ (µmol min/ml or /g wet tissue)	6.1	1.6
MRT (min)	43.6	43.0

Clinical studies with monoHER

Phase I study in healthy volunteers

Toxicity studies of monoHER in several animal models revealed neither acute nor chronic toxic effects nor teratogenic effects after oral administration of monoHER (Berte, 1974; Chesterman *et al.*, 1973; Davies and Collins, 1973a; Davies and Collins, 1973b; Davies and Collins, 1973c; Hunter *et al.*, 1973; Lueschner, 1974a; Lueschner, 1974b; Lueschner, 1974c).

To evaluate the possible side effects of monoHER and to investigate the pharmacokinetics of monoHER in men, a phase I clinical trial was performed (Willems *et al.*, 2006). The study was performed as a single blind, randomized trial in healthy volunteers. MonoHER was administered as an i.v. infusion in 10 minutes. For formulation of the drug, the required amount of monoHER was dissolved in 100 ml 5% dextrose for intravenous use, adjusted to pH 9.3 using 4 M sodium hydroxide. After dissolution of the drug, the solution was readjusted to pH 8.4 with 1 M hydrochloric acid. The final solution was filtered through a 0.2-µm filter. This solution was chemically stable for at least 24 hours at room temperature (Abou El Hassan *et al.*, 2000). Because 10% of the registered drug Venoruton is monoHER and 1500 mg of Venoruton could be administered intravenously to patients without any side effect (Neumann *et al.*, 1992), the starting dose of monoHER was 100 mg/m^2. Dose escalation by 100% of the preceding dose took place after finishing each dose level until the protecting pharmacokinetic values for C_{max} and AUC^{∞} (as observed in mice after 500 mg/kg monoHER, i.p.) were reached and/or serious side effects were observed.

Up to the highest dose of 1500 mg/m^2, monoHER was well-tolerated and no serious side-effects were observed. At this dose, the pharmacokinetic endpoints were obtained, i.e. a mean peak plasma concentration of 360 ± 69.3 µM and a mean AUC^{∞} of 6.8 ± 2.1 µmol min/ml. The data also showed that monoHER is rapidly distributed and eliminated from the plasma compartment, which corresponds with a rapid uptake in and elimination from heart tissue as found in mice. From this phase I study, it could be concluded that 1500 mg/m^2 of monoHER is a feasible and safe dose to be used in further clinical studies.

Phase II study in cancer patients treated with doxorubicin

Based on the promising results with monoHER observed in preclinical experiments, a phase II study was performed to investigate the cardioprotective effect of monoHER on doxorubicin-induced cardiotoxicity in cancer patients (Bruynzeel *et al.*, 2007c). This study was performed in eight patients with metastatic cancer (Table 3). The patients were treated with doxorubicin preceded by a 10

minutes i.v. infusion of 1500 mg/m^2 monoHER. Endomyocardial biopsies were evaluable in five patients. To assess cardiac damage, four of the five patients underwent an endomyocardial biopsy at a cumulative dose of 300 mg/m^2 and one at 375 mg/m^2 doxorubicin. Of them, three patients were treated with a time-interval of 1 hour between monoHER and doxorubicin, one patient with a time-interval of 10 minutes and one patient with a time-interval of 2 hours.
No difference in biopsy score was found between these patients. Moreover, comparison of the mean biopsy score of the five patients with the mean score from historical data of patients who received a similar cumulative dose of doxorubicin, indicated that monoHER did not significantly protect against doxorubicin-induced cardiotoxicity in these cancer patients. An intriguing observation in this clinical study was that three of the four patients diagnosed with soft tissue sarcomas experienced objective remissions, while the fourth had stable disease (Table 3).

Table 3. Patient characteristics (Bruynzeel *et al.*, 2007c).

No.	Age/sex	Diagnosis	Total dose of doxorubicin (mg/m^2)	Response on doxorubicin	Biopsy
1	62/F	Breast cancer	100	PD	N
2	54/F	Adrenal cortical cancer	150	PD	N
3	25/M	Malignant peripheral nerve sheet tumour	480	PR	Y
4	64/M	Malignant fibrous histiocytoma	450	PR	Y
5	55/F	Breast cancer	100	PD	N
6	48/F	Breast cancer	300	SD	Y
7	45/F	Malignant fibrous histiocytoma	300	PR	Y
8	56/F	Malignant fibrous histiocytoma	375	SD	Y

Abbreviations: PD = progressive disease; PR = partial remission; SD = stable disease.

This 75% response rate is much higher than expected. The objective response rate obtained with doxorubicin in soft tissue sarcomas patients without prior chemotherapy is normally approximately 25% (Santoro *et al.*, 1995). It is therefore suggestive that monoHER enhances the antitumour activity of doxorubicin in soft tissue sarcomas. Both the lack of clear cardioprotection and the potentiation of the antitumour effect by monoHER observed in this clinical phase II study are in contrast with the results obtained in the earlier animal studies.

Aim and outline of the thesis

As described in **Chapter 1**, the outcome of the clinical phase II study with monoHER revealed two unexpected findings, which are in contrast to the preclinical observations with monoHER:

1. MonoHER did not significantly protect against doxorubicin-induced cardiotoxicity in cancer patients.
2. It appeared that monoHER enhances the antitumour activity of doxorubicin in soft tissue sarcoma patients.

To explain these unexpected clinical findings, we go back 'from clinic to concept' in this thesis.

First, the *antioxidant properties* of monoHER and its interaction with other antioxidants are further investigated. During their antioxidant activity, i.e., the scavenging of free radicals, flavonoids are converted into potentially harmful thiol-reactive oxidation products. Therefore, the thiol reactivity of the oxidation product of monoHER is studied, and the glutathione (GSH) conjugate of monoHER is characterized **(Chapter 2)**. Moreover, the reactivity of the GSH-monoHER conjugate is investigated **(Chapter 3)**. To protect against free radical damage the human body has an intricate network of antioxidants that passes over the reactivity from one antioxidant to another in a controlled way. The interplay of monoHER with this endogenous antioxidant network is investigated, and its position is compared with that of the well-studied flavonoid quercetin **(Chapter 4)**.

The results of the clinical phase II study suggest that *monoHER enhances the antitumour activity of doxorubicin* in soft tissue sarcomas. To elucidate the molecular mechanism behind this remarkable finding, the effect of monoHER on the cytotoxicity of doxorubicin is studied in human soft tissue sarcoma cell lines. Moreover, the potential involvement of GSH depletion and nuclear factor-kB (NF-kB) inactivation is investigated **(Chapter 5)**.

In mice, monoHER has been successfully used as a protector against doxorubicin-induced cardiotoxicity. However, most monoHER has already been cleared from the body at the time that doxorubicin concentrations are still high. This suggests that not only the parent compound monoHER itself, but also *monoHER metabolites* could be responsible for the observed cardioprotective effects in mice. Therefore, the metabolism of monoHER is investigated in mice. Moreover, the potential meaning of the identified metabolites in the cardioprotective effect of monoHER is discussed **(Chapter 6)**.

In humans, monoHER did not significantly protect the heart against damage caused by doxorubicin. To explain the different biological effects of monoHER in

mice and men, it is hypothesized that metabolites of monoHER that contribute to the observed cardioprotection in mice are not (or to a lesser extend) formed in men. Therefore, the metabolism of monoHER is also investigated in healthy volunteers and the identified metabolites are compared with those found in mice **(Chapter 7)**.

Finally, the most important findings are discussed and the future perspectives are given **(Chapter 8)**.

References

Abou El Hassan MA, Kedde MA, Bast A, van der Vijgh WJ (2001) Determination of monohydroxyethylrutoside in heart tissue by high-performance liquid chromatography with electrochemical detection. *J Chromatogr B Biomed Sci Appl* **757:** 191-196

Abou El Hassan MA, Kedde MA, Zwiers UT, Bast A, van der Vijgh WJ (2003a) The cardioprotector monoHER does not interfere with the pharmacokinetics or the metabolism of the cardiotoxic agent doxorubicin in mice. *Cancer Chemother Pharmacol* **51:** 306-310

Abou El Hassan MA, Kedde MA, Zwiers UT, Tourn E, Haenen GR, Bast A, van der Vijgh WJ (2003b) Bioavailability and pharmacokinetics of the cardioprotecting flavonoid 7-monohydroxyethylrutoside in mice. *Cancer Chemother Pharmacol* **52:** 371-376

Abou El Hassan MA, Touw DJ, Wilhelm AJ, Bast A, van der Vijgh WJ (2000) Stability of monoHER in an aqueous formulation for i.v. administration. *Int J Pharm* **211:** 51-56

Abou El Hassan MA, Verheul HM, Jorna AS, Schalkwijk C, van Bezu J, van der Vijgh WJ, Bast A (2003c) The new cardioprotector Monohydroxyethylrutoside protects against doxorubicin-induced inflammatory effects in vitro. *Br J Cancer* **89:** 357-362

Barrow A, Griffiths LA (1971) The biliary excretion of hydroxyethylrutosides and other flavonoids in the rat. *Biochem J* **125:** 24P-25P

Barrow A, Griffiths LA (1974a) Metabolism of the hydroxyethylrutosides. II. Excretion and metabolism of 3',4',7-tri-O-(beta-hydroxyethyl) rutoside and related compounds in laboratory animals after parenteral administration. *Xenobiotica* **4:** 1-16

Barrow A, Griffiths LA (1974b) Metabolism of the hydroxyethylrutosides. III. The fate of orally administered hydroxyethylrutosides in laboratory animals; metabolism by rat intestinal microflora in vitro. *Xenobiotica* **4:** 743-754

Bast A, Haenen GR, Bruynzeel AM, Van der Vijgh WJ (2007) Protection by flavonoids against anthracycline cardiotoxicity: from chemistry to clinical trials. *Cardiovasc Toxicol* **7:** 154-159

Berte F (1974) Toxicite chronique chiens. *Internal Report Zyma SA*

Bruynzeel AM, Abou El Hassan MA, Schalkwijk C, Berkhof J, Bast A, Niessen HW, van der Vijgh WJ (2007a) Anti-inflammatory agents and monoHER protect against DOX-induced cardiotoxicity and accumulation of CML in mice. *Br J Cancer* **96:** 937-943

Bruynzeel AM, Abou El Hassan MA, Torun E, Bast A, van der Vijgh WJ, Kruyt FA (2007b) Caspase-dependent and -independent suppression of apoptosis by monoHER in Doxorubicin treated cells. *Br J Cancer* **96:** 450-456

Bruynzeel AM, Mul PP, Berkhof J, Bast A, Niessen HW, van der Vijgh WJ (2006) The influence of the time interval between monoHER and doxorubicin administration on the protection against doxorubicin-induced cardiotoxicity in mice. *Cancer Chemother Pharmacol* **58:** 699-702

Bruynzeel AM, Niessen HW, Bronzwaer JG, van der Hoeven JJ, Berkhof J, Bast A, van der Vijgh WJ, van Groeningen CJ (2007c) The effect of monohydroxyethylrutoside on doxorubicin-induced cardiotoxicity in patients treated for metastatic cancer in a phase II study. *Br J Cancer* **97:** 1084-1089

Bruynzeel AM, Vormer-Bonne S, Bast A, Niessen HW, van der Vijgh WJ (2007d) Long-term effects of 7-monohydroxyethylrutoside (monoHER) on DOX-induced cardiotoxicity in mice. *Cancer Chemother Pharmacol* **60:** 509-514

Chesterman H, Heywood R, Fuller R (1973) Z12007: preliminary toxicity study in the Beagle dog. *Internal Report Zyma SA.*

Davies R, Collins C (1973a) Acute oral toxicity to beagle dogs of Z12007. *Internal Report Zyma SA.*

Davies R, Collins C (1973b) Acute oral toxicity to mice of Z12007. *Internal Report Zyma SA*

Davies R, Collins C (1973c) Acute oral toxicity to rats of Z12007. *Internal Report Zyma SA*

De Celle T, Heeringa P, Strzelecka AE, Bast A, Smits JF, Janssen BJ (2004) Sustained protective effects of 7-monohydroxyethylrutoside in an in vivo model of cardiac ischemia-reperfusion. *Eur J Pharmacol* **494:** 205-212

de Franceschi L, Turrini F, Honczarenko M, Ayi K, Rivera A, Fleming MD, Law T, Mannu F, Kuypers FA, Bast A, van der Vijgh WJ, Brugnara C (2004) In vivo reduction of erythrocyte oxidant stress in a murine model of beta-thalassemia. *Haematologica* **89:** 1287-1298

Deepa PR, Varalakshmi P (2006) Influence of a low-molecular-weight heparin derivative on the nitric oxide levels and apoptotic DNA damage in adriamycin-induced cardiac and renal toxicity. *Toxicology* **217:** 176-183

El Hassan MA, Kedde MA, Bast A, van der Vijgh WJ (2001) High-performance liquid chromatography with electrochemical detection for the determination of 7-monohydroxyethylrutoside in plasma. *J Chromatogr B Biomed Sci Appl* **752:** 115-121

Gabor M (1981) The effect of O-(beta-hydroxyethyl)-rutosides (HR) on the skin capillary resistance of rats. *Arzneimittelforschung* **31:** 442-445

Gosta A (1973) Effects of HR and its derivates on prostaglandin biosynthesis in guinea pig lung tissue and human skin. *Internal Report Zyma SA*

Hackett AM, Griffiths LA (1977a) The disposition and metabolism of 3',4',7-tri-O-(beta-hydroxyethyl)rutoside and 7-mono-O-(beta-hydroxyethyl)rutoside in the mouse. *Xenobiotica* **7:** 641-651

Hackett AM, Griffiths LA (1977b) Enterohepatic cycling of O-(beta-hydroxyethyl) rutosides and their biliary metabolites in the rat. *Experientia* **33:** 161-163

Hackett AM, Griffiths LA (1979) The metabolism and excretion of 7-mono-0-(beta-hydroxyethyl) rutoside in the dog. *Eur J Drug Metab Pharmacokinet* **4:** 207-212

Haenen GR, Jansen FP, Bast A (1993) The antioxidant properties of five O-(-β–Hydroxyethyl)-Rutosides of the flavonoid mixture Venoruton. *Phlebology* **Suppl.1:** 10-17

Hecker JF (1990) Survival of intravenous chemotherapy infusion sites. *Br J Cancer* **62:** 660-662

Hladovec J (1977a) Antithrombotic effects of some flavonoids alone and combined with acetylsalicylic acid. *Arzneimittelforschung* **27:** 1989-1992

Hladovec J (1977b) Differentation of in vitro and in vivo effects of a flavonoid on endothelial cell counts. *Arzneimittelforschung* **27:** 1142-1144

Hladovec J (1978) Endothelial injury by nicotine and its prevention. *Experientia* **34:** 1585-1586

Horenstein MS, Vander Heide RS, L'Ecuyer TJ (2000) Molecular basis of anthracycline-induced cardiotoxicity and its prevention. *Mol Genet Metab* **71:** 436-444

Hou G, Dick R, Abrams GD, Brewer GJ (2005) Tetrathiomolybdate protects against cardiac damage by doxorubicin in mice. *J Lab Clin Med* **146:** 299-303

Hunter B, Bridges J, Cherry C (1973) Preliminary assessment of Z12007 toxicity to rats in oral administration for four weeks. *Internal Report Zyma SA.*

Julicher RH, Sterrenberg L, Haenen GR, Bast A, Noordhoek J (1988) The effect of chronic adriamycin treatment on heart kidney and liver tissue of male and female rat. *Arch Toxicol* **61:** 275-281

Kendall S, Towart R, Michel CC (1993) Effects of hydroxyethylrutosides on the permeability of microvessels in the frog mesentery. *Br J Pharmacol* **110:** 199-206

Lecomte J, Van Cauwenberge H (1974) [Some pharmacologic properties of mono-(O-beta-hydroxyethyl)-7-rutoside in the rat]. *Arch Int Pharmacodyn Ther* **208:** 317-327

Lipshultz SE, Lipsitz SR, Sallan SE, Dalton VM, Mone SM, Gelber RD, Colan SD (2005) Chronic progressive cardiac dysfunction years after doxorubicin therapy for childhood acute lymphoblastic leukemia. *J Clin Oncol* **23:** 2629-2636

Lueschner F (1974a) Uber den Einfluss von Z12007, Mono-7-HR, Charge 1020- in diesem Bericht kurz "Mono-7-HR" genannt- auf die trachtige Kaninchen und den Foetus bei Verabreichung per Magensonde. *Internal Report Zyma SA.*

Lueschner F (1974b) Uber den Einfluss von Z12007, Mono-7-HR, Charge 1020- in diesem Bericht kurz "Mono-7-HR" genannt- auf die trachtige Maus und den Foetus bei Verabreichung per Magensonde. *Internal Report Zyma SA.*

Lueschner F (1974c) Uber den Einfluss von Z12007, Mono-7-HR, Charge 1020- in diesem Bericht kurz "Mono-7-HR" genannt- auf die trachtige Ratte und den Foetus bei Verabreichung per Magensonde. *Internal Report Zyma SA.*

Mirkovitch (1977) The influence of monoHER on experimental venous thrombosis in dogs. *Internal Report*

Neumann HA, Carlsson K, Brom GH (1992) Uptake and localisation of O-(beta-hydroxyethyl)-rutosides in the venous wall, measured by laser scanning microscopy. *Eur J Clin Pharmacol* **43:** 423-426

Niebes P, Laszt L (1971) Influence in vitro of a series of flavonoids on certain enzymes in the metabolism of mucopolysaccharides in the human and bovine saphenous vein. *Angiologica* **8:** 297-302

Santoro A, Tursz T, Mouridsen H, Verweij J, Steward W, Somers R, Buesa J, Casali P, Spooner D, Rankin E, et al. (1995) Doxorubicin versus CYVADIC versus doxorubicin plus ifosfamide in first-line treatment of advanced soft tissue sarcomas: a randomized study of the European Organization for Research and Treatment of Cancer Soft Tissue and Bone Sarcoma Group. *J Clin Oncol* **13:** 1537-1545

Singal PK, Iliskovic N (1998) Doxorubicin-induced cardiomyopathy. *N Engl J Med* **339:** 900-905

van Acker FA, van Acker SA, Kramer K, Haenen GR, Bast A, van der Vijgh WJ (2000) 7-monohydroxyethylrutoside protects against chronic doxorubicin-induced cardiotoxicity when administered only once per week. *Clin Cancer Res* **6:** 1337-1341

van Acker SA, Boven E, Kuiper K, van den Berg DJ, Grimbergen JA, Kramer K, Bast A, van der Vijgh WJ (1997) Monohydroxyethylrutoside, a dose-dependent cardioprotective agent, does not affect the antitumor activity of doxorubicin. *Clin Cancer Res* **3:** 1747-1754

van Acker SA, Kramer K, Grimbergen JA, van den Berg DJ, van der Vijgh WJ, Bast A (1995) Monohydroxyethylrutoside as protector against chronic doxorubicin-induced cardiotoxicity. *Br J Pharmacol* **115:** 1260-1264

van Acker SA, Towart R, Husken BC, De Jong J, van der Vijgh WJ, Bast A (1993) The protective effect of Venoruton and its main constituents on acute doxorubicin-induced cardiotoxicity. *Phlebology* **Suppl. 1:** 31-32

van Acker SA, van den Berg DJ, Tromp MN, Griffioen DH, van Bennekom WP, van der Vijgh WJ, Bast A (1996) Structural aspects of antioxidant activity of flavonoids. *Free Radic Biol Med* **20:** 331-342

Willems AM, Bruynzeel AM, Kedde MA, van Groeningen CJ, Bast A, van der Vijgh WJ (2006) A phase I study of monohydroxyethylrutoside in healthy volunteers. *Cancer Chemother Pharmacol* **57:** 678-684

Xu MF, Tang PL, Qian ZM, Ashraf M (2001) Effects by doxorubicin on the myocardium are mediated by oxygen free radicals. *Life Sci* **68:** 889-901

Chapter 2

Characterization of the glutathione conjugate of the semisynthetic flavonoid monoHER

Hilde Jacobs
Wim J.F. van der Vijgh
Ger H. Koek
Guy J.J. Draaisma
Mohamed Moalin
Gino P.F van Strijdonck
Aalt Bast
Guido R.M.M. Haenen

Free Radical Biology and Medicine 2009; 46:1567-1573

Abstract

Flavonoids protect against oxidative stress by scavenging free radicals. During this protection flavonoids are oxidized. The formed oxidized flavonoids are often reactive. Consequently, protection by flavonoids can result in the formation of toxic products. In this study the oxidation of 7-mono-O-(β-hydroxyethyl)-rutoside (monoHER), which is a constituent of the registered drug Venoruton, was studied in the absence and presence of glutathione (GSH). MonoHER was oxidized by horseradish peroxidase/H_2O_2. Spectrophotometric and HPLC analysis showed that in the presence of GSH, a monoHER-GSH conjugate was formed, which was identified as 2'-glutathionyl monohydroxyethylrutoside by mass spectrometric analysis and ^{1}H NMR. Preferential formation of this glutathione adduct in the B ring at C2' was confirmed by molecular quantum chemical calculations. This conjugate was also detected in the bile fluid of a healthy volunteer after i.v. administration of monoHER, demonstrating its formation *in vivo*. These results indicate that in the process of offering protection against free radicals, monoHER is converted into an oxidation product that is reactive towards thiols. The formation of this thiol-reactive oxidation product is potentially harmful. Thus, the supposed beneficial effect of monoHER as an antioxidant may be accompanied by the formation of products with an electrophilic, toxic potential.

Introduction

Flavonoids form a class of benzo-γ-pyrone derivatives which occur naturally in fruits, vegetables and plant-derived beverages such as tea and wine (Nichenametla *et al.*, 2006; Ren *et al.*, 2003). They have a wide spectrum of biological activities (Boots *et al.*, 2008; Choi *et al.*, 2001; Cushnie and Lamb, 2005; Naasani *et al.*, 2003; Park *et al.*, 2007; van Acker *et al.*, 2000a). The interest in these polyphenolic compounds was stimulated by the potential health benefits arising from their antioxidant activity, which is mainly the result of their high tendency to scavenge reactive oxygen species. However, during their antioxidant function, flavonoids are converted into oxidation products that take over part of the reactivity of the radical they have scavenged. In this way, electrophilic compounds are formed that are able to damage vital cellular components (Bast and Haenen, 2002; Haenen and Bast, 2002). Thus, despite all their apparently useful antioxidant properties, flavonoids can also become toxic as a result of their protection (Galati *et al.*, 2002). This holds true especially for flavonoids containing a catechol-like 3', 4'-dihydroxy substituent pattern in their B ring (Boots *et al.*, 2002).

A well-established example of such a flavonoid is quercetin, which is one of the most prominent flavonoids in our diet. In the process of offering protection against free radicals, quercetin is chemically converted into an oxidation product (Laughton *et al.*, 1989; Metodiewa *et al.*, 1999) that reacts with glutathione (GSH), thereby forming 2 glutathionyl adducts at position C6 and position C8 of the A ring (Awad *et al.*, 2000; Boots *et al.*, 2003; Galati *et al.*, 2001). This high reactivity towards thiols can result in GSH depletion and loss of protein function (Boots *et al.*, 2005). Thus, although a highly reactive species is being neutralized, during the same process potentially toxic products are formed, a phenomenon known as the quercetin paradox (Boots *et al.*, 2007).

The flavonoid of interest to us is the semisynthetic flavonoid 7-mono-O-(β-hydroxyethyl)-rutoside (monoHER). MonoHER is a constituent of the registered drug Venoruton (Haenen *et al.*, 1993; van Acker *et al.*, 1993), which is used in the treatment of chronic venous insufficiency (Petruzzellis *et al.*, 2002). Venoruton (oxerutins) is a standardized mixture of the semisynthetic flavonoids mono-, di-, tri- and tetra-hydroxyethylrutosides. These flavonoids are obtained by substituting the hydroxyl groups with hydroxyethyl groups in the naturally occurring flavonol rutin. The most important pharmacological action of Venoruton is the reduction of microvascular permeability with a consequent pre-

vention of edema (Wadworth and Faulds, 1992). In patients with chronic venous insufficiency, Venoruton improves microvascular perfusion and microcirculation and reduces erythrocyte aggregation. The preparation also has a possible protective effect on the vascular endothelium (Wadworth and Faulds, 1992). MonoHER is the most powerful antioxidant of Venoruton and has in addition to its radical-scavenging and iron-chelating properties, an anti-inflammatory capacity (Abou El Hassan *et al.*, 2003; Bruynzeel *et al.*, 2007a). Preclinical experiments have shown that monoHER is a potential protective agent against cardiotoxicity induced by the anticancer agent doxorubicin (DOX) (van Acker *et al.*, 2000). Because of these promising results, clinical trials are being performed in patients receiving doxorubicin to study the influence of monoHER on DOX-induced cardiotoxicity (Bruynzeel *et al.*, 2007b; Willems *et al.*, 2006). Because the flavonoids monoHER and quercetin have many structural characteristics in common, it is expected that a kind of quercetin paradox also exists for monoHER. This may have implications for the applicability of monoHER.

The objective of this study was therefore to investigate the thiol-reactivity of the oxidation product of monoHER. MonoHER oxidation was induced by horseradish peroxidase/H_2O_2 and the reactivity of its oxidation product with glutathione was determined. The product formed in the reaction with glutathione was isolated and further identified by MS and ^{1}H NMR. Molecular quantum chemical calculations were performed to theoretically explain the preferential formation of the 2'-monoHER-GSH adduct. Furthermore, the bile fluid of a healthy volunteer who received monoHER by intravenous infusion was analyzed to investigate the *in vivo* formation of the monoHER-GSH conjugate.

Materials and methods

Chemicals

MonoHER was kindly provided by Novartis Consumer Health (Nyon, Switzerland). Stock solutions of the drug were freshly prepared in a methanol/25 mM phosphate buffer (pH 3.33) mixture (4/1, v/v). Hydrogen peroxide, horseradish peroxidase (HRP) and reduced GSH were purchased from Sigma (St. Louis, MO, USA). Stock solutions of these chemicals were freshly prepared in a 145 mM phosphate buffer, pH 7.4. Trifluoroacetic acid (TFA) and deuterium oxide (D_2O) were purchased from Sigma-Aldrich (Steinheim, Germany). Acetonitrile HPLC grade, methanol and dimethyl sulphoxide (DMSO) were obtained from Biosolve

(Valkenswaard, The Netherlands) and formic acid was acquired from Merck (Darmstadt, Germany).

One-electron oxidation of monoHER

The incubation mixtures contained monoHER (50 µM), HRP (1.6 nM) and H_2O_2 (33 µM) in a 145 mM phosphate buffer (pH 7.4), unless noted otherwise. When the oxidation of monoHER was performed in the presence of GSH, the incubation mixture additionally contained 40 µM GSH. After 5 min of incubation at 37°C, the incubation mixtures were analyzed spectrophotometrically and by HPLC.

Spectrophotometric analysis

Spectrophotometric analysis was performed with a Varian Carry 50 scan spectrophotometer (Varian, Mulgrave, VIC, Australia). All absorption spectra were recorded from 220 to 500 nm with a scan speed of 960 nm/min, using quartz cuvettes. The UV/Vis scans were started before and 5 min after the addition of HRP.

High-performance liquid chromatography analysis

HPLC was performed using a HP 1100 series HPLC system (Agilent Technologies, Palo Alto, CA, USA). Analytical separations were achieved using a Supelcosil LC 318 column (5 µm, 25 cm x 4.6 mm) (Supelco, Bellefonte, PA, USA). The mobile phase consisted of water containing 0.1% (v/v) TFA with linear gradients of 5% acetonitrile at t = 0 to 20% acetonitrile at 5 min followed by an increase to 30% acetonitrile at 10 min. Finally 90% acetonitrile was used from 18 min onwards for 5 min. The column was reequilibrated with 5% acetonitrile for 5 min. A flow rate of 2 ml/min and an injection volume of 20 µl were used. Detection was carried out with a diode array detector. The chromatograms presented are based on detection at 355 nm.

Solid-phase extraction

The GSH adduct formed upon incubation of monoHER with HRP in the presence of GSH was isolated by solid-phase extraction (SPE). SPE was performed with a Sep-Pak C18 column (WAT 051910, Waters Corp., Milford, MA, USA). The column was washed with 100% acetonitrile followed by Milli-Q water (pH 3.5). After application of 100 µl of the incubation mixture, the column was washed a

second time with Milli-Q water (pH 3.5). Next, the GSH adduct was eluted with water containing 5% acetonitrile. After the fraction was collected, the purity was checked with HPLC. Identical fractions of several extractions were pooled and the combined eluate was evaporated to dryness under vacuum (50°C) and used for further analysis by MS and ^{1}H NMR analysis.

Mass spectrometry

A representative amount of the dried eluate was reconstituted in a 50% methanol/1% formic acid (v/v) mixture and introduced into the mass spectrometer (MS). Mass spectrometric measurements were performed with a Finnigan LCQ (Thermo Electron Corp., San Jose, CA, USA) in the negative electrospray mode using a spray voltage of 4.5 kV and a capillary temperature of 200 °C with nitrogen as the sheath and auxiliary gas.

^{1}H NMR spectroscopy

^{1}H NMR measurements were performed in D_2O at 25°C on a Varian Mercury VX 400 MHZ NMR (Varian).

Molecular quantum chemical calculations

Molecular quantum chemical calculations were performed with the software program Spartan '06 (Wavefunction, Irvine, CA, USA) to explain the experimental results. The calculations were carried out at the *ab initio* level. The Hartree-Fock method with the 3-21G basis set was used for the equilibrium geometry and lowest unoccupied molecular orbital (LUMO) calculations of a simplified monoHER-quinone (a methyl group was used to replace the large substituents attached to the A7-O and C3-O). In this way, the preferential site in the monoHER-quinone for nucleophilic attack by the thiol (-SH) group of glutathione was calculated.

Analysis of the monoHER-glutathione adduct in the bile fluid of a healthy volunteer

To evaluate the possible *in vivo* conjugation of monoHER with glutathione, bile fluid of a healthy 33-year-old male volunteer who received an intravenous monoHER infusion was analyzed for the presence of the monoHER-GSH adduct. The volunteer signed an informed consent for the study, which had been approved by the Medical Ethical Review Committee of the University Hospital.

Formulation of the drug

The monoHER infusion was formulated under aseptic conditions by the Department of Pharmacy, University Hospital Gasthuisberg, Leuven, Belgium. The required amount of monoHER was dissolved in 100 ml 5% dextrose for intravenous use, adjusted to pH 9.3 using 4 M sodium hydroxide. After dissolution of the drug, the solution was readjusted to pH 8.4 with 1 M hydrochloric acid. The final solution was filtered through a 0.2-µm filter.

Administration of the drug

MonoHER was administered as an intravenous infusion for 15 min at a dose of 1500 mg/m^2.

Bile aspiration

Before and at 2 h after monoHER infusion, the bile fluid from the healthy volunteer was collected via oral intubation of a tube with a balloon, which was maneuvered into the second part of the duodenum (Koek *et al.*, 2004). The balloon serves to prevent mixing of gastric contents or food with duodenal contents. The aspiration was performed until about 10 ml was collected. The bile fluid was divided in portions of 1 ml and frozen at -80°C.

Sample preparation and HPLC analysis

Aliquots of bile fluid were mixed with twice the volume of DMSO/methanol (1/4, v/v). The mixture was vortexed and centrifuged (17060 g, 15 min). The supernatant was removed and injected onto the HPLC column. To verify the presence of the monoHER-GSH conjugate in the bile fluid, blank bile fluid (collected before monoHER infusion) spiked with 60 µM monoHER-GSH adduct (synthesized as described above) was analyzed by the same procedure.

High-performance liquid chromatography analysis of the bile samples was performed on a HP 1100 series HPLC system (Agilent Technologies). Analytical separations were achieved using a YMC-Pack ODS-AQ column (3 µm, 150 x 4.6 mm) (YMC Europe GmbH, Dinslaken, Germany). The mobile phase consisted of water containing 0.1% (v/v) TFA with a linear gradient of 15% acetonitrile at t = 0 to 30% acetonitrile at 20 min. Ninety percent acetonitrile was used from 25 min onward for 1 min. The column was reequilibrated with 15% acetonitrile during 5 min. A flow rate of 1 ml/min and an injection volume of 10 µl were used. Detection was carried out with a diode array detector. The chromatograms presented are based on detection at 355 nm.

Results

Spectrophotometric and HPLC analysis of the one-electron oxidation of monoHER

The UV/Vis spectrum of the parent compound monoHER (50 μM) is depicted in Figure 1A. Two absorption maxima are observed, one at 258 nm and another one at 355 nm. The HPLC chromatogram of monoHER recorded at 355 nm shows one major peak (t_R = 6.7 min) (Figure 1B).

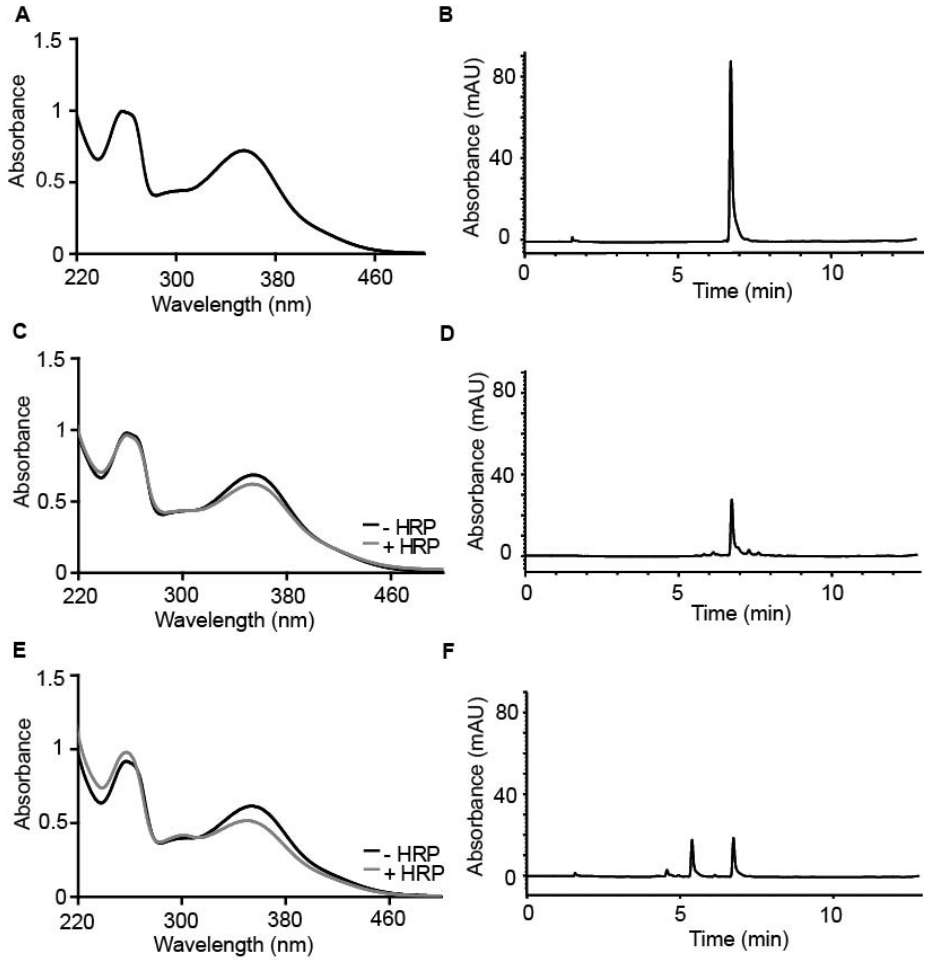

Figure 1. UV scans (left) and HPLC chromatograms (right) of the incubation mixture containing (A and B) 50 μM monoHER or (C-F) 50 μM monoHER, 1.6 nM horseradish peroxidase (HRP), and 33 μM H_2O_2 in the absence (C and D) or presence (E and F) of 40 μM glutathione. The UV scans were recorded before and 5 min after the addition of HRP. The various incubation mixtures were injected on the HPLC system 5 min after the addition of HRP.

Addition of the enzyme HRP to 50 µM monoHER changes the UV/Vis spectrum in time (Figure 1C). Four isosbestic points are observed at 249, 272, 305, and 412 nm, suggesting the conversion of monoHER into an oxidation product. MonoHER consumption is confirmed by HPLC analysis (Figure 1D). In the chromatogram, the peak height of monoHER (t_R = 6.7 min) decreases by approximately 67% after 5 min of incubation with HRP.

Spectrophotometric and HPLC analysis of the glutathione adduct of monoHER

The changes in the UV/Vis spectrum over time after addition of 40 µM GSH to the incubation mixture containing monoHER and HRP are shown in Figure 1E. Four isosbestic points are observed at 265, 280, 311, and 500 nm. These isosbestic points differ from the isosbestic points observed during the oxidation of monoHER. Comparison of the entire spectrum of the incubation mixtures with GSH (Figure 1E) and without GSH (Figure 1C) also indicates that the products formed, either in the presence or absence of GSH, are not identical. This is confirmed by HPLC analysis (Figure 1F). In the presence of glutathione, the peak height of monoHER in the chromatogram decreases and a second peak appears, eluting at a position different from that of the parent compound with a retention time of 5.4 min. Based on analogy with oxidized quercetin and other oxidized phenolic compounds (Boots *et al.*, 2003; Galati *et al.*, 2001), it is tentatively concluded that this second peak represents an adduct that is formed between oxidized monoHER and GSH. To confirm the formation of a monoHER-GSH adduct, the formed product was isolated and further characterized by MS and ^{1}H NMR.

Mass spectrometric analysis of the monoHER-glutathione adduct

MS analysis of the purified metabolite shows an M - 1 peak at *m/z* 958 (data not shown). This mass corresponds to the molecular weight of a mono-GSH adduct with monoHER.

^{1}H NMR characterization of the monoHER-glutathione adduct

To elucidate the chemical structure of the monoHER-GSH conjugate, the formed product was characterized by ^{1}H and COSY NMR. The aromatic regions of the ^{1}H NMR spectra of the parent compound monoHER (Figure 2A) and the monoHER-GSH adduct (Figure 2B) measured in D_2O at 25 °C are shown in Figure 2.

Identification of the various ^{1}H NMR resonances was done on the basis of the ^{1}H NMR chemical shifts and their splitting patterns. The doublets at 6.78 and 7.37 ppm are assigned to H5' and H6', respectively. The singlets at 6.23, 6.41, and 7.44 ppm are from H8, H6, and H2', respectively. These results were confirmed by the software program ACD/HNMR Predictor (version 8.09). Comparison of the ^{1}H NMR spectrum of the monoHER-GSH adduct to the ^{1}H NMR spectral characteristics of the parent compound monoHER clearly reveals the loss of the H2' ^{1}H NMR signal. Splitting patterns of all other aromatic protons are similar to those of monoHER itself. On the basis of these ^{1}H NMR characteristics it can be concluded that the GSH adduct of the oxidized flavonoid is formed in the B ring at C2'. This adduct can therefore be identified as 2'- glutathionyl monohydroxyethylrutoside (2'-monoHER-GSH adduct). The coupling of the protons was confirmed by COSY NMR (data not shown).

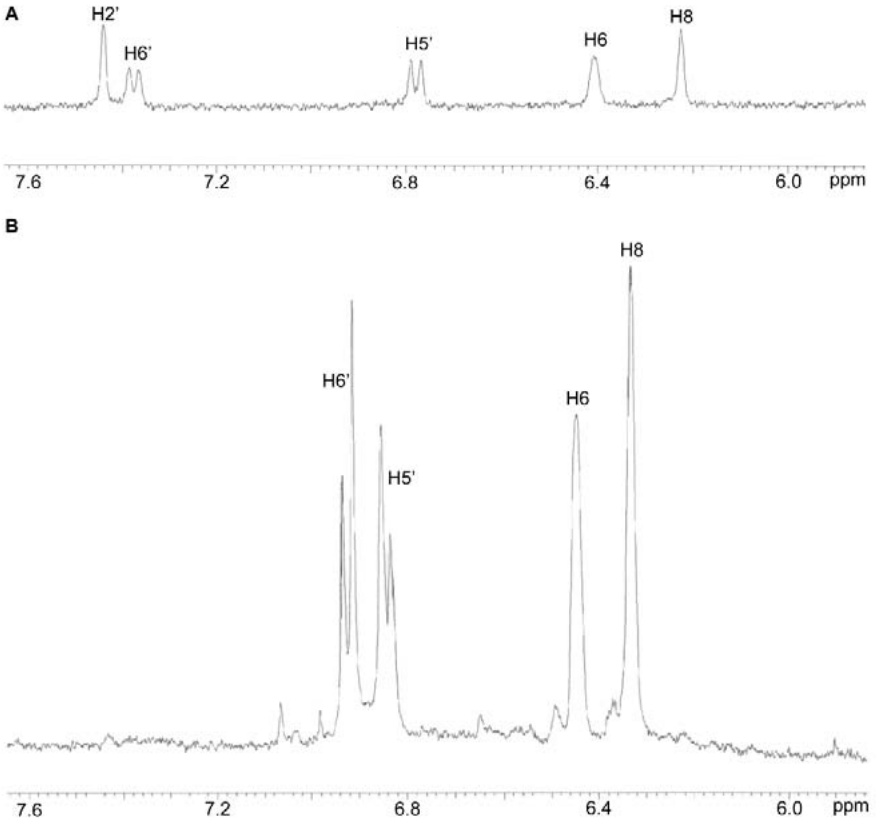

Figure 2. Aromatic parts of the ^{1}H NMR spectra of (A) the parent compound monoHER and (B) the metabolite formed during the incubation of monoHER with horseradish peroxidase/H_2O_2 in the presence of GSH.

Molecular quantum chemical calculations

Molecular quantum chemical calculations were carried out to clarify the preferential formation of the monoHER-GSH adduct at the C2' position in the B ring. After Hartree-Fock 3-21G calculations on the equilibrium geometry of the simplified monoHER-quinone, a LUMO map was generated to visualize the LUMO distribution. Figure 3A shows that the LUMO is a π* orbital and that it is localized over the B ring and part of the C ring. Subsequently, an electron density surface was generated onto which the absolute value of the LUMO (|LUMO|) was mapped (Figure 3B). By convention, colors tending toward red indicate small absolute values for the LUMO (near 0), whereas colors tending toward blue indicate large absolute values. The |LUMO| has the highest value over the C2' site at the B ring, with a maximum relative value of 0.024. The C5' site has a lower maximum value of 0.017. This indicates that C2' is the preferential site for nucleophilic attack, which is consistent with the experimental results.

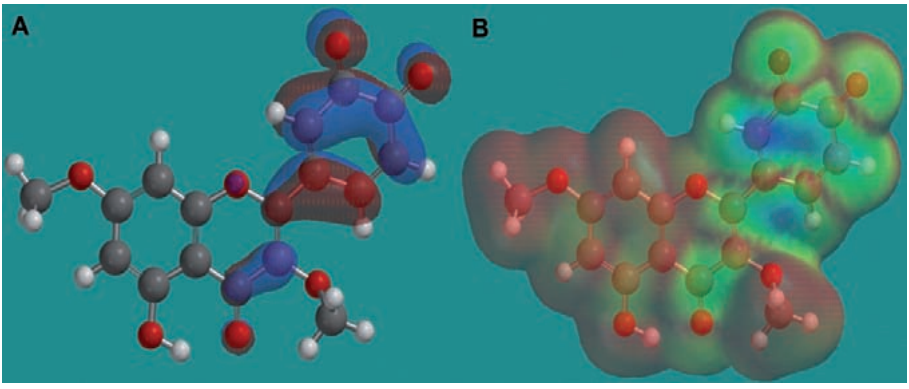

Figure 3. (A) LUMO map of the simplified monoHER-quinone. The LUMO is localized over the B ring and a part of the C ring. (B) Electron density surface of the absolute values of the LUMO for the monoHER-quinone. Blue indicates a high value for the orbital, and red indicates a low value. High values for the LUMO are seen over C2', indicating that this is a potential site for nucleophilic attack.

Excretion of the monoHER-glutathione adduct in the bile fluid of a healthy volunteer

High-performance liquid chromatographic analysis of bile fluid from a healthy volunteer, who received monoHER (1500 mg/m^2) via intravenous infusion, revealed the presence of the monoHER-GSH conjugate (retention time 3.1 min) (Figure 4A).

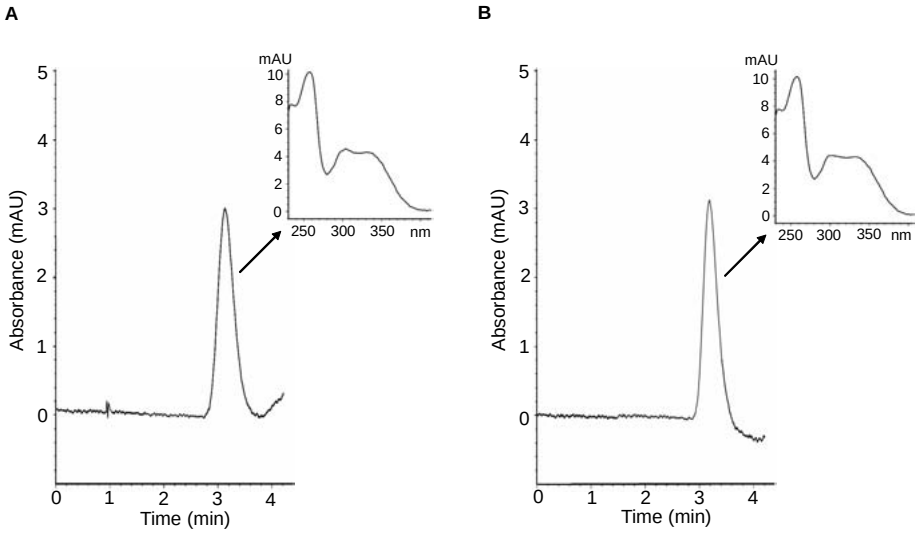

Figure 4. (A) The first part of the HPLC chromatogram of human bile fluid collected 2 h after iv administration of 1500 mg/m^2 monoHER. The DAD spectrum of the peak with a retention time of 3.1 min is shown. (B) The first part of the HPLC chromatogram of blank human bile fluid (collected before monoHER infusion) spiked with 60 µM synthesized monoHER-GSH conjugate. The DAD spectrum of the monoHER-GSH conjugate with a retention time of 3.1 min is shown.

Peak identification was performed by spiking blank bile fluid (collected before monoHER infusion) with the previously synthesized monoHER-GSH adduct. The peak that consequently appears in the spiked blank bile fluid has the same retention time as the peak present in the bile fluid collected after monoHER infusion (Figure 4B). Also, the DAD spectrum of the peak at 3.1 min is identical to the characteristic spectrum of the synthesized monoHER-GSH adduct (Figure 4). This confirms the presence of the monoHER-GSH conjugate in the bile fluid. These data demonstrate, for the first time, that the monoHER-GSH adduct is also formed *in vivo*.

Discussion

Previous studies have documented that oxidation products of some dietary phenolic compounds are electrophilic and readily react with nucleophiles such as glutathione (Boots *et al.*, 2003; Galati *et al.*, 1999). A well-documented example of such a compound is the flavonoid quercetin, which is converted into an oxidation product that reacts with glutathione, thereby forming two adducts

in which GSH is attached to the A ring, i.e., 6-GSQ and 8-GSQ (Awad *et al.*, 2000; Boots *et al.*, 2003; Galati *et al.*, 2001).

In this study, the oxidation product of monoHER was obtained through oxidation by horseradish peroxidase/H_2O_2. Spectrophotometric and HPLC analysis of the reaction mixture confirmed the oxidation of monoHER. In the presence of GSH, one major product different from the oxidation product was detected. MS analysis showed that this product had an M - 1 peak at *m/z* 958. This mass corresponds to the molecular weight of a mono-GSH adduct with monoHER. ^{1}H NMR analysis identified this monoHER-GSH conjugate as 2'-glutathionyl monohydroxyethylrutoside, representing a glutathione adduct originating from glutathione conjugation at the B ring of monoHER. Preferential formation of this adduct is in line with the results of the theoretical calculations for the |LUMO| with Spartan '06. Moreover, conjugation of monoHER with glutathione also occurs *in vivo*, as shown by the presence of this conjugate in the bile fluid of a healthy volunteer after i.v. administration of monoHER.

The semisynthetic flavonoid monoHER has many structural characteristics in common with quercetin. Both flavonoids belong to the subclass of the flavonols and contain a catechol-like 3', 4'-dihydroxy substituent pattern in their B ring. This catechol moiety is most likely responsible for their potent antioxidant activity (Heijnen *et al.*, 2002). They also contain the C2-C3 double bond and the 4-oxo function in the C ring, which contribute to their high antioxidant function (Lien *et al.*, 1999; Rice-Evans *et al.*, 1996; van Acker *et al.*, 1996). In contrast with quercetin, monoHER has a rutinose group attached to position 3 of the C ring, and the hydroxylgroup at position 7 of the A ring is substituted with a hydroxyethyl group. These small differences in their chemical structures (Figures 5 and 6) can explain their different oxidation products and subsequent interaction with glutathione. MonoHER glutathionyl formation occurs at the B ring, whereas the glutathionyl formation with quercetin occurs at the A ring.

After oxidation of quercetin, four tautomeric forms of the oxidation product can exist, one *o*-quinone isomer and three quinone methide isomers (Awad *et al.*, 2000). Owing to the relatively high abundance of the quinone methide-type 2 intermediate (calculations with Spartan '06 showed that this quercetin tautomer had an abundance of more than 99%), glutathionyl adduct formation occurs at positions C6 and C8 of the quercetin A ring, i.e., 6-GSQ and 8-GSQ (Figure 5).

In the chemical structure of monoHER, the C3-OH group is substituted by a rutinose group. This restricts the overall conjugation of the π system. Because the rearrangement of the proton of the 3-OH group to generate a 3-keto group cannot occur, the formation of quinone methide tautomers is prevented, lead-

ing merely to the formation of the *o*-quinone isomer. Elimination of the possibilities for quinone methide formation by the absence of the C3-OH group restricts glutathionyl adduct formation to the B ring. This is in line with our experimental results, which indicate that only one GSH conjugate is formed after monoHER oxidation in the presence of GSH, i.e., 2'-monoHER-GSH (Figure 6).

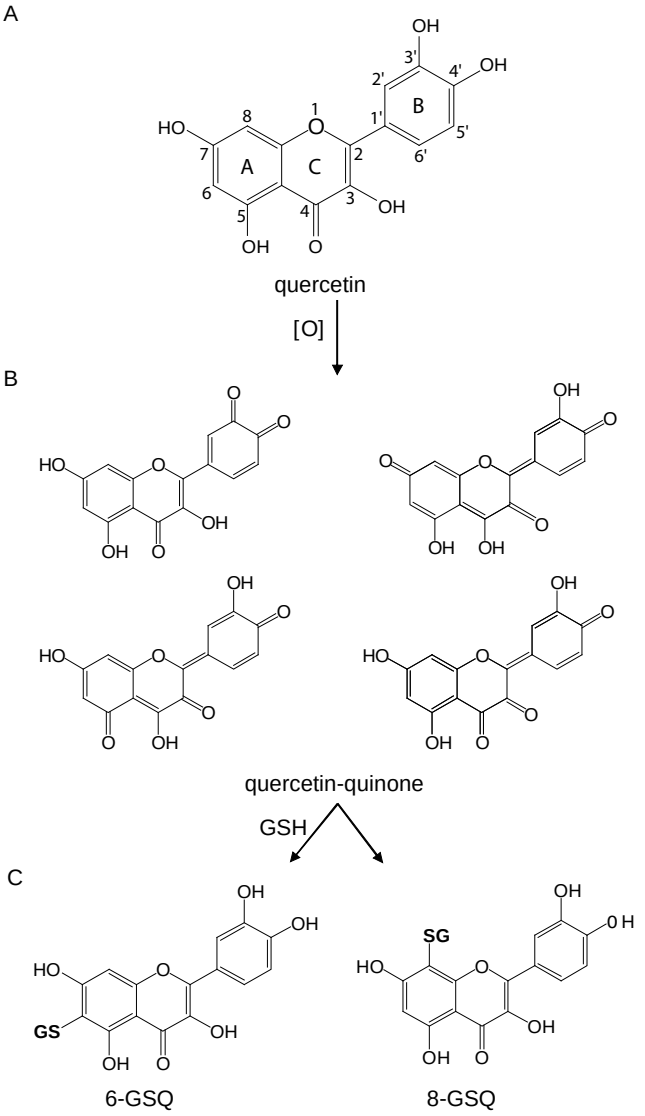

Figure 5. Oxidation of quercetin, followed by the possible reaction of its major oxidation product with GSH. (A) After oxidation of quercetin, (B) four tautomeric forms of the oxidation product can exist, one *o*-quinone isomer and three quinone methide isomers. (C) Glutathionyl adduct formation occurs at positions C6 and C8 of the A ring, i.e., 6-GSQ and 8-GSQ.

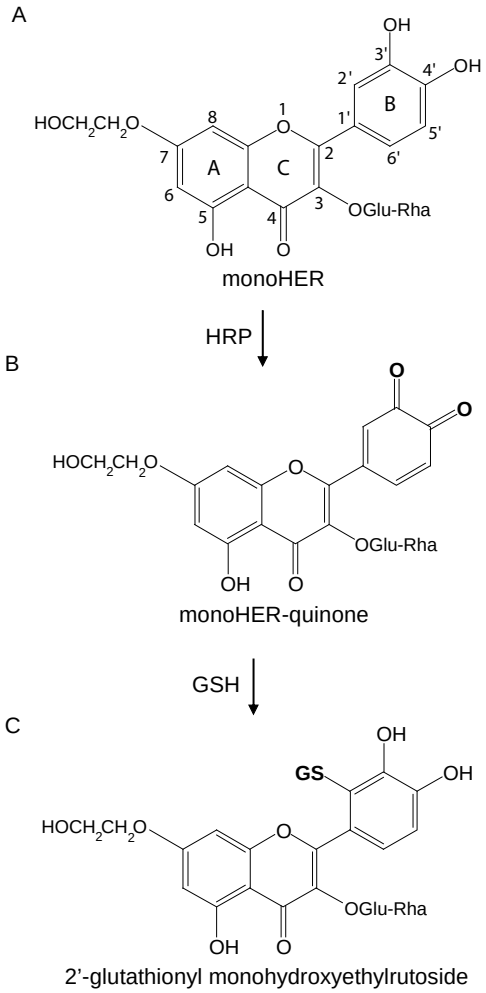

Figure 6. Oxidation of monoHER, followed by the possible reaction of its oxidation product with GSH. (A) In the presence of HRP monoHER becomes oxidized and (B) the monoHER-quinone is formed. (C) This monoHER-quinone reacts with GSH, thereby forming the 2'-monoHER-GSH adduct.

Theoretically, the B ring of monoHER has two possible sites for nucleophilic attack of glutathione, i.e., C2' and C5'. Molecular quantum chemical calculations of the LUMO with Spartan '06 show that the LUMO is localized over the B ring and a part of the C ring. Comparing the relative values of the LUMO of the two possible sites for nucleophilic attack in the B ring of monoHER, it can be seen that the C2' site has a higher |LUMO| (0.024) than the C5' site (0.017). This

indicates that the C2' atom is more susceptible to nucleophilic attack and explains the preferential formation of 2'-glutathionyl monoHER.

For quercetin it has been found that in the process of offering protection against free radicals, thiol-reactive oxidation products that can cause cell damage are formed (Boots *et al.*, 2007). This phenomenon is coined as the quercetin paradox. When monoHER exerts its antioxidant function (i.e., scavenging free radicals), it is also converted into an oxidation product. This study illustrates that this oxidation product of monoHER shows reactivity towards thiols, which is evidenced by the formation of the 2'-monoHER-GSH adduct. In addition to its formation *in vitro*, this GSH conjugate is also formed *in vivo*, as seen by its presence in the bile fluid of a healthy volunteer who received monoHER by intravenous infusion. Previous reports have indicated that GSH conjugates are formed *in vitro* (Awad *et al.*, 2000; Boots *et al.*, 2003; Galati *et al.*, 2001). Attempts have been made by other researchers to detect the *in vivo* formation of conjugates between flavonoids and glutathione (Jones *et al.*, 2004). To our knowledge, this study is the first to show that a flavonoid conjugate with glutathione really is formed *in vivo*.

The formation of electrophilic, thiol-reactive oxidation products can have some implications. First of all the formed oxidation product can react with the thiol GSH, which will reduce GSH levels and thus the antioxidant defense. In addition to the reaction with GSH, it is assumed that the oxidized antioxidant is also prone to react with essential thiol groups of critical proteins, potentially resulting in the loss of protein function (Boots *et al.*, 2005). Thus, the supposed beneficial effect of monoHER as an antioxidant could be eclipsed by the formation of products with an electrophilic, toxic potential. However, further research is necessary to determine the potential toxicological consequences.

References

Abou El Hassan MA, Verheul HM, Jorna AS, Schalkwijk C, van Bezu J, van der Vijgh WJ, Bast A (2003) The new cardioprotector Monohydroxyethylrutoside protects against doxorubicin-induced inflammatory effects in vitro. *Br J Cancer* **89:** 357-362

Awad HM, Boersma MG, Vervoort J, Rietjens IM (2000) Peroxidase-catalyzed formation of quercetin quinone methide-glutathione adducts. *Arch Biochem Biophys* **378:** 224-233

Bast A, Haenen GR (2002) The toxicity of antioxidants and their metabolites. *Environmental Toxicology and Pharmacology* **11:** 251-258

Boots AW, Balk JM, Bast A, Haenen GR (2005) The reversibility of the glutathionyl-quercetin adduct spreads oxidized quercetin-induced toxicity. *Biochem Biophys Res Commun* **338:** 923-929

Boots AW, Haenen GR, den Hartog GJ, Bast A (2002) Oxidative damage shifts from lipid peroxidation to thiol arylation by catechol-containing antioxidants. *Biochim Biophys Acta* **1583:** 279-284

Boots AW, Kubben N, Haenen GR, Bast A (2003) Oxidized quercetin reacts with thiols rather than with ascorbate: implication for quercetin supplementation. *Biochem Biophys Res Commun* **308:** 560-565

Boots AW, Li H, Schins RP, Duffin R, Heemskerk JW, Bast A, Haenen GR (2007) The quercetin paradox. *Toxicol Appl Pharmacol* **222:** 89-96

Boots AW, Wilms LC, Swennen EL, Kleinjans JC, Bast A, Haenen GR (2008) In vitro and ex vivo anti-inflammatory activity of quercetin in healthy volunteers. *Nutrition* **24:** 703-710

Bruynzeel AM, Abou El Hassan MA, Schalkwijk C, Berkhof J, Bast A, Niessen HW, van der Vijgh WJ (2007a) Anti-inflammatory agents and monoHER protect against DOX-induced cardiotoxicity and accumulation of CML in mice. *Br J Cancer* **96:** 937-943

Bruynzeel AM, Niessen HW, Bronzwaer JG, van der Hoeven JJ, Berkhof J, Bast A, van der Vijgh WJ, van Groeningen CJ (2007b) The effect of monohydroxyethylrutoside on doxorubicin-induced cardiotoxicity in patients treated for metastatic cancer in a phase II study. *Br J Cancer* **97:** 1084-1089

Choi JA, Kim JY, Lee JY, Kang CM, Kwon HJ, Yoo YD, Kim TW, Lee YS, Lee SJ (2001) Induction of cell cycle arrest and apoptosis in human breast cancer cells by quercetin. *Int J Oncol* **19:** 837-844

Cushnie TP, Lamb AJ (2005) Antimicrobial activity of flavonoids. *Int J Antimicrob Agents* **26:** 343-356

Galati G, Chan T, Wu B, O'Brien PJ (1999) Glutathione-dependent generation of reactive oxygen species by the peroxidase-catalyzed redox cycling of flavonoids. *Chem Res Toxicol* **12:** 521-525

Galati G, Moridani MY, Chan TS, O'Brien PJ (2001) Peroxidative metabolism of apigenin and naringenin versus luteolin and quercetin: glutathione oxidation and conjugation. *Free Radic Biol Med* **30:** 370-382

Galati G, Sabzevari O, Wilson JX, O'Brien PJ (2002) Prooxidant activity and cellular effects of the phenoxyl radicals of dietary flavonoids and other polyphenolics. *Toxicology* **177:** 91-104

Haenen GR, Bast A (2002) The use of vitamin supplements in self-medication. *Therapie* **57:** 119-122

Haenen GR, Jansen FP, Bast A (1993) The antioxidant properties of five O-(-β–Hydroxyethyl)-Rutosides of the flavonoid mixture Venoruton. *Phlebology* **Suppl.1:** 10-17

Heijnen CG, Haenen GR, Oostveen RM, Stalpers EM, Bast A (2002) Protection of flavonoids against lipid peroxidation: the structure activity relationship revisited. *Free Radic Res* **36:** 575-581

Jones DJ, Lamb JH, Verschoyle RD, Howells LM, Butterworth M, Lim CK, Ferry D, Farmer PB, Gescher AJ (2004) Characterisation of metabolites of the putative cancer chemopreventive agent quercetin and their effect on cyclo-oxygenase activity. *Br J Cancer* **91:** 1213-1219

Koek GH, Vos R, Flamen P, Sifrim D, Lammert F, Vanbilloen B, Janssens J, Tack J (2004) Oesophageal clearance of acid and bile: a combined radionuclide, pH, and Bilitec study. *Gut* **53:** 21-26

Laughton MJ, Halliwell B, Evans PJ, Hoult JR (1989) Antioxidant and pro-oxidant actions of the plant phenolics quercetin, gossypol and myricetin. Effects on lipid peroxidation, hydroxyl radical generation and bleomycin-dependent damage to DNA. *Biochem Pharmacol* **38:** 2859-2865

Lien EJ, Ren S, Bui HH, Wang R (1999) Quantitative structure-activity relationship analysis of phenolic antioxidants. *Free Radic Biol Med* **26:** 285-294

Metodiewa D, Jaiswal AK, Cenas N, Dickancaite E, Segura-Aguilar J (1999) Quercetin may act as a cytotoxic prooxidant after its metabolic activation to semiquinone and quinoidal product. *Free Radic Biol Med* **26:** 107-116

Naasani I, Oh-Hashi F, Oh-Hara T, Feng WY, Johnston J, Chan K, Tsuruo T (2003) Blocking telomerase by dietary polyphenols is a major mechanism for limiting the growth of human cancer cells in vitro and in vivo. *Cancer Res* **63:** 824-830

Nichenametla SN, Taruscio TG, Barney DL, Exon JH (2006) A review of the effects and mechanisms of polyphenolics in cancer. *Crit Rev Food Sci Nutr* **46:** 161-183

Park HH, Lee S, Oh JM, Lee MS, Yoon KH, Park BH, Kim JW, Song H, Kim SH (2007) Anti-inflammatory activity of fisetin in human mast cells (HMC-1). *Pharmacol Res* **55:** 31-37

Petruzzellis V, Troccoli T, Candiani C, Guarisco R, Lospalluti M, Belcaro G, Dugall M (2002) Oxerutins (Venoruton): efficacy in chronic venous insufficiency--a double-blind, randomized, controlled study. *Angiology* **53:** 257-263

Ren W, Qiao Z, Wang H, Zhu L, Zhang L (2003) Flavonoids: promising anticancer agents. *Med Res Rev* **23:** 519-534

Rice-Evans CA, Miller NJ, Paganga G (1996) Structure-antioxidant activity relationships of flavonoids and phenolic acids. *Free Radic Biol Med* **20:** 933-956

van Acker FA, Schouten O, Haenen GR, van der Vijgh WJ, Bast A (2000a) Flavonoids can replace alpha-tocopherol as an antioxidant. *FEBS Lett* **12:** 145-148

van Acker FA, van Acker SA, Kramer K, Haenen GR, Bast A, van der Vijgh WJ (2000) 7-monohydroxyethylrutoside protects against chronic doxorubicin-induced cardiotoxicity when administered only once per week. *Clin Cancer Res* **6:** 1337-1341

van Acker SA, Towart R, Husken BC, De Jong J, van der Vijgh WJ, Bast A (1993) The protective effect of Venoruton and its main constituents on acute doxorubicin-induced cardiotoxicity. *Phlebology* **Suppl. 1:** 31-32

van Acker SA, van den Berg DJ, Tromp MN, Griffioen DH, van Bennekom WP, van der Vijgh WJ, Bast A (1996) Structural aspects of antioxidant activity of flavonoids. *Free Radic Biol Med* **20:** 331-342

Wadworth AN, Faulds D (1992) Hydroxyethylrutosides. A review of its pharmacology, and therapeutic efficacy in venous insufficiency and related disorders. *Drugs* **44:** 1013-1032

Willems AM, Bruynzeel AM, Kedde MA, van Groeningen CJ, Bast A, van der Vijgh WJ (2006) A phase I study of monohydroxyethylrutoside in healthy volunteers. *Cancer Chemother Pharmacol* **57:** 678-684

Chapter 3

An essential difference in the reactivity of the glutathione adducts of the structurally closely related flavonoids monoHER and quercetin

Hilde Jacobs
Mohamed Moalin
Marike van Gisbergen
Aalt Bast
Wim J.F. van der Vijgh
Guido R.M.M. Haenen

Submitted

Abstract

During the scavenging of free radicals flavonoids are oxidized to electrophilic quinones. Glutathione (GSH) can trap these quinones, thereby forming GSH-flavonoid adducts. The aim of the present study was to compare the stability of the GSH-flavonoid adduct of 7-mono-O-(β-hydroxyethyl)-rutoside (monoHER) with that of quercetin. It was found that GSH-quercetin reacts with the thiol N-acetyl-L-cysteine (NAC) to form NAC-quercetin, whereas GSH-monoHER does not react with NAC. In addition, the adduct of the monoHER quinone with the dithiol dithiothreitol (DTT) is relatively stable, whereas the DTT-quercetin adduct is readily converted into quercetin and DTT disulfide. These differences in reactivity of the thiol-flavonoid adducts demonstrate that GSH-monoHER is much more stable than GSH-quercetin. This difference in reactivity was corroborated by molecular quantum chemical calculations. Thus, although both flavonoid quinones are rapidly scavenged by GSH, the advantage of monoHER is that it forms a stable conjugate with GSH, thereby preventing a possible spread of toxicity. These findings demonstrate that even structurally comparable flavonoids behave differently, which will be reflected in the biological effects of these flavonoids.

Introduction

Flavonoids are a class of naturally occurring polyphenolic compounds that are ubiquitously present in fruits, vegetables and plant-derived beverages such as tea and wine (Hertog *et al.*, 1993; Kuhnau, 1976). The interest in these substances has been stimulated by the potential health benefits arising from their antioxidant activity, which is mainly the result of their high tendency to scavenge reactive oxygen species (van Acker *et al.*, 2000a). However, during their antioxidant function, flavonoids are converted into oxidation products that usually retain a part of the reactivity of the species they have scavenged (Bast and Haenen, 2002; Galati *et al.*, 2002). In this way, electrophilic compounds are formed that are able to damage vital cellular compounds (O'Brien, 1991), i.e. the flavonoid quinone could react with protein thiols, which can lead to toxic effects such as increased membrane permeability (Yen *et al.*, 2003) or altered functioning of enzymes that contain critical SH-groups (Kalyanaraman *et al.*, 1987; Moore *et al.*, 1988). A well-established example of such a flavonoid is quercetin, which is one of the most prominent flavonoids in our diet. In the process of offering protection against free radicals, quercetin is chemically converted into a quinone (Laughton *et al.*, 1989; Metodiewa *et al.*, 1999) that readily reacts with glutathione (GSH), thereby forming two glutathionyl adducts at position C6 and position C8 of the A ring (Awad *et al.*, 2000; Boots *et al.*, 2003; Galati *et al.*, 2001).

The flavonoid of interest to us is the semisynthetic flavonoid 7-mono-O-(β-hydroxyethyl)-rutoside (monoHER) (Bast *et al.*, 2007; Haenen *et al.*, 1993; van Acker *et al.*, 2000). Like quercetin, monoHER is also chemically converted into an electrophilic quinone as a result of scavenging reactive species (Jacobs *et al.*, 2009). Recently, it was shown that this monoHER quinone can be trapped by the thiol GSH. The binding of the quinone to GSH is considered to be a detoxification mechanism to protect cells against harmful reactive species (Meister, 1994; Yu, 1994). Nevertheless, previous studies with quercetin have shown that this reaction is reversible (Boots *et al.*, 2005; Boots *et al.*, 2007). Thus, the formation of a GSH-quercetin conjugate might only provide a temporary protection against oxidized quercetin and even spread toxicity (Boots *et al.*, 2005). The chemical structure of quercetin and monoHER, both belonging to the group of flavonols, are closely related. Little is known about the stability of the 2'-GSH-monoHER adduct. This prompted us to study the reactivity of the 2'-GSH-

monoHER with other thiols in comparison with that of the GSH adducts of quercetin.

Materials and methods

Chemicals

7-mono-O-(β-hydroxyethyl)-rutoside (monoHER) was kindly provided by Novartis Consumer Health (Nyon, Switzerland). Quercetin, reduced glutathione (GSH), hydrogen peroxide (H_2O_2), horseradish peroxidase (HRP) and dithiothreitol (DTT) were purchased from Sigma (St. Louis, MO, USA). N-acetyl-L-cysteine (NAC) was acquired from Merck (Darmstadt, Germany). Trifluoroacetic acid (TFA) was acquired from Sigma-Aldrich (Steinheim, Germany). Acetonitrile HPLC grade and methanol were obtained from Biosolve (Valkenswaard, The Netherlands). 2'-GSH-monoHER was synthesized as described previously (Jacobs *et al.*, 2009).

Oxidation of monoHER and quercetin and subsequent formation of GSH-monoHER and GSH-quercetin

The procedures to oxidize monoHER and quercetin were similar to the ones used previously (Boots *et al.*, 2005; Jacobs *et al.*, 2009). Shortly, 100 µM monoHER was incubated for 5 minutes at 37°C together with 1.6 nM HRP and 33 µM H_2O_2 in a 145 mM phosphate buffer (pH 7.4). The GSH-monoHER adduct was formed by oxidizing 100 µM monoHER in the presence of 120 µM GSH. The NAC-monoHER adduct was formed by oxidizing 100 µM monoHER in the presence of 120 µM NAC. The DTT-monoHER adduct was formed by oxidizing 100 µM monoHER in the presence of 120 µM DTT. The incubation mixtures were analyzed by high-performance liquid chromatography (HPLC). Similar experimental conditions were used to oxidize quercetin and to form the subsequent thiol-adducts.

Reaction of GSH-monoHER and GSH-quercetin with NAC

The GSH-monoHER and the GSH-quercetin adducts were freshly prepared by oxidizing 100 µM monoHER or quercetin in the presence of 120 µM GSH, as described above. After 5 minutes of incubation at 37°C, the reaction was stopped by filtering the solution through a Sep-Pak C18 cartridge. In this way,

the enzyme is removed from the solution and the oxidation is stopped. Thereafter, 120 µM NAC was added to the obtained solution containing the GSH-monoHER or GSH-quercetin adduct. After an additional 5 minutes of incubation at 37°C, the incubation mixture was analyzed by HPLC.

High-performance liquid chromatography analysis

HPLC was performed using a HP 1100 series HPLC system (Agilent Technologies, Palo Alto, CA, USA). Analytical separations were achieved using a Grace Smart RP 18 column (5 µm, 150 mm x 4.6 mm) (Grace, Deerfield, IL, USA). The mobile phase consisted of water containing 0.1% (v/v) TFA with linear gradients of 5% acetonitrile at t = 0 to 20% acetonitrile at 5 min followed by an increase to 30% acetonitrile at 15 min. Finally 90% acetonitrile was used from 23 min onward for 3 min. The column was reequilibrated with 5% acetonitrile for 5 min. A flow rate of 2 ml/min and an injection volume of 20 µl were used. Detection was carried out with a diode array detector (DAD). Quantification of monoHER and quercetin was done based on detection at 355 nm and 375 nm, respectively.

Molecular quantum chemical calculations

Molecular quantum chemical calculations (ab initio level) were performed with the software program Spartan '06 (Wavefunction, Irvine, CA, USA) to explain the differences in reactivity between the GSH-monoHER and GSH-quercetin adducts. The activation energy for the first step of the reaction from GSH-adduct to quinone, i.e. deprotonation of the OH-group adjacent to the position where GSH is bound in the flavonoid, was determined by calculating the equilibrium geometry with the Hartree-Fock method using the 3-21G basis set. To omit complicated calculations because of the presence of long - hardly contributing - substituents, quercetin-3,7-OMe was used instead of monoHER, and MeSH instead of GSH for the calculations.

Statistics

All experiments were performed, at least, in triplicate. Data are expressed as mean ± SD or as a typical example. Statistical analysis was performed using student's t-test. P values ≤ 0.05 were considered statistically significant.

Results

Reaction of monoHER quinone and quercetin quinone with thiols

MonoHER and quercetin (100 µM) were incubated with a concentration of HRP/H_2O_2 that led to the oxidation of approximately 50% of both flavonoids in 5 minutes (Figure 1). Oxidation of monoHER or quercetin in the presence of glutathione (GSH) resulted in the formation of approximately 50 µM GSH-monoHER or GSH-quercetin. Similarly, oxidation of monoHER or quercetin in the presence of the thiol N-acetyl-L-cysteine (NAC) resulted in the formation of 50 µM NAC-monoHER or NAC-quercetin.

These results confirm that monoHER and quercetin are oxidized by HRP/H_2O_2 to quinones that readily react with thiols. Likewise, oxidation of monoHER in the presence of the dithiol dithiothreitol (DTT) resulted in the formation of a DTT-monoHER adduct. On the other hand, when quercetin was oxidized in the presence of DTT, no DTT-quercetin adduct was found and also no net consumption of quercetin.

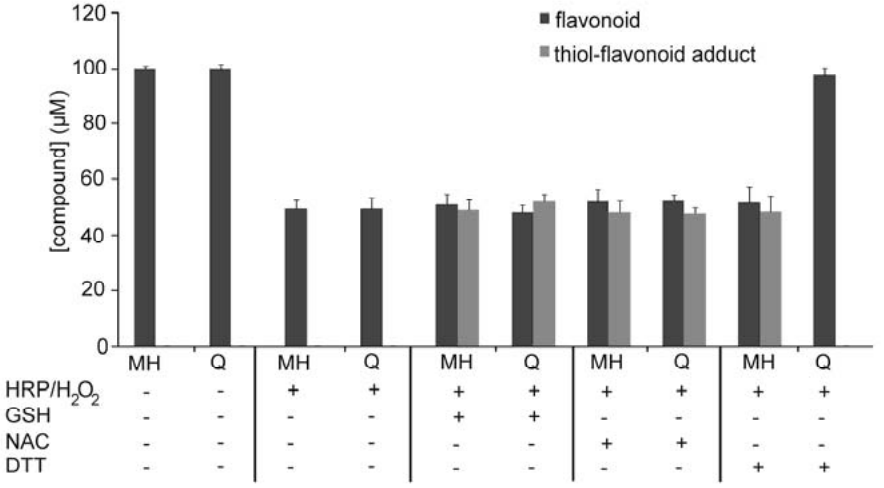

Figure 1. Oxidation of the flavonoids monoHER (MH) and quercetin (Q) by horseradish peroxidase (HRP) and H_2O_2 without or with the thiols glutathione (GSH), N-acetyl-L-cysteine (NAC) or dithiothreitol (DTT). The composition of the incubation mixtures was: (A) 100 µM monoHER or quercetin, (B) 100 µM monoHER or quercetin, 1.6 nM HRP and 33 µM H_2O_2, (C) 100 µM monoHER or quercetin, 1.6 nM HRP, 33 µM H_2O_2 and 120 µM GSH, (D) 100 µM monoHER or quercetin, 1.6 nM HRP, 33 µM H_2O_2 and 120 µM NAC and (E) 100 µM monoHER or quercetin, 1.6 nM HRP, 33 µM H_2O_2 and 120 µM DTT. The incubation mixtures were incubated for 5 minutes at 37°C. The remaining flavonoid and the formed thiol-flavonoid adducts were quantified by HPLC. Experiments were performed at least in triplicate and data are shown as mean ± SD.

Reaction of GSH-monoHER and GSH-quercetin with NAC

Subsequently, GSH-monoHER and GSH-quercetin were incubated with the thiol NAC for 5 minutes. As shown in Figure 2A, GSH-monoHER did not react with NAC, i.e., the concentration of the GSH-monoHER adduct remained the same and no NAC-monoHER was formed within the 5 minutes of incubation. In contrast, GSH-quercetin did react with NAC: the major part of the GSH-quercetin adduct was gradually converted into NAC-quercetin (Figure 2B).

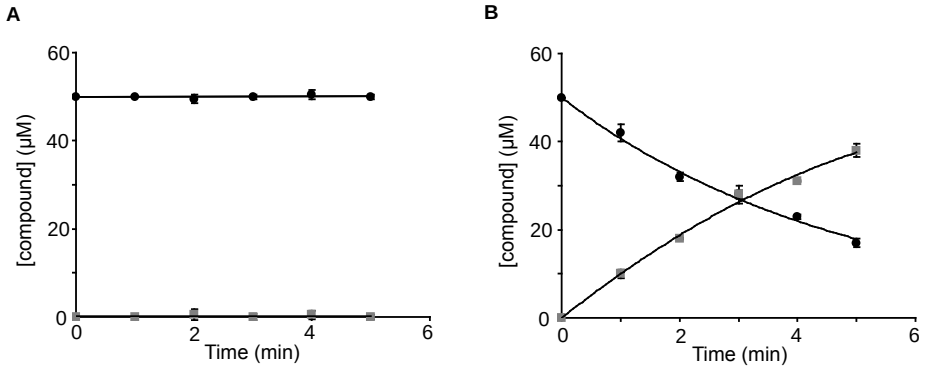

Figure 2. Reaction of the GSH-flavonoid (50 µM) with NAC (120 µM). (A) With GSH-monoHER, there is no consumption of GSH-monoHER (●) over time and no NAC-monoHER (■) is formed. (B) With GSH-quercetin, NAC-quercetin (■) is formed and the concentration of GSH-quercetin (●) decreases in time. Experiments were performed at least in triplicate and data are shown as mean ± SD.

Discussion

The flavonoids monoHER and quercetin are converted into quinones when they scavenge free radicals. The results of our study confirm that both the monoHER quinone and the quercetin quinone react with GSH to form the 2'-GSH-monoHER and 6- or 8-GSH-quercetin adducts, respectively (Boots *et al.*, 2003; Jacobs *et al.*, 2009). The flavonoid quinones also readily react with other thiols (Jacobs *et al.*, 2010), as also illustrated in the present study with NAC as a thiol.

The reaction of thiols with the flavonoid quinones is depicted in Figure 3. It is a Michael addition in which the thiol acts as a nucleophile. In this reaction, a Meisenheimer complex (Figure 3c) is formed as an intermediate that eventually, via deprotonation and subsequent protonation, forms the resulting thiol-flavonoid adduct (Figure 3e).

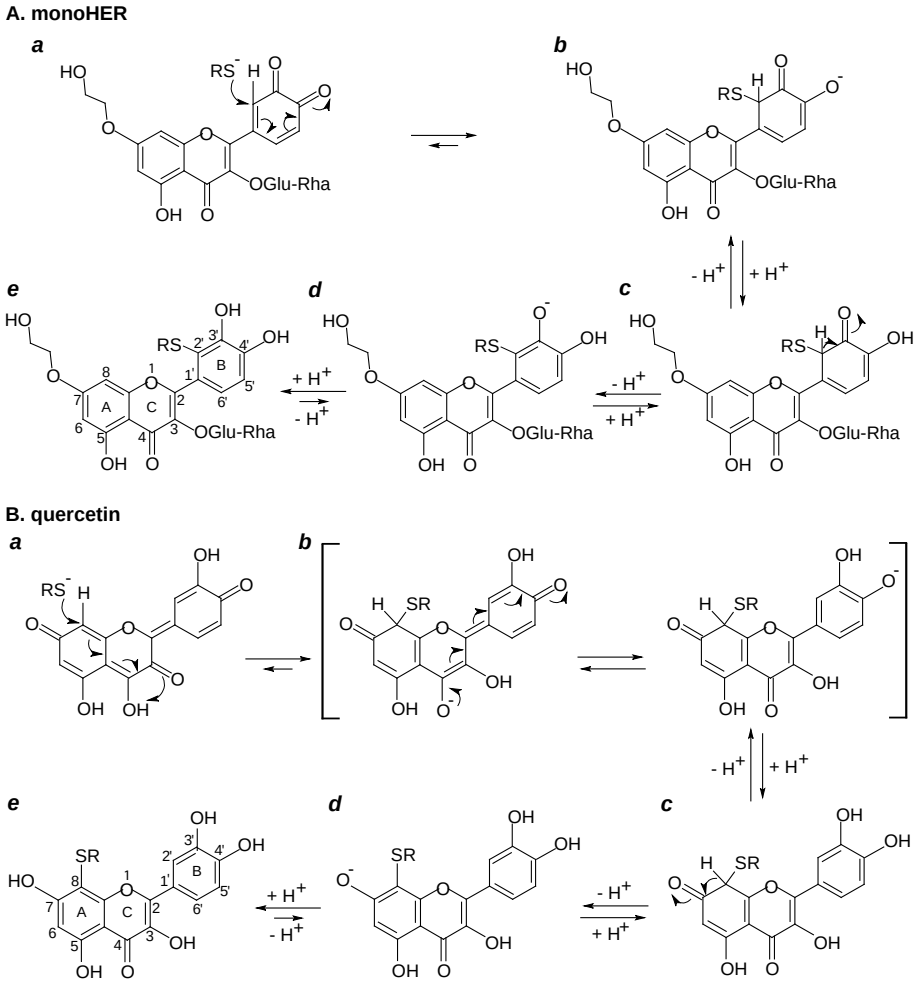

Figure 3. Reaction of the monoHER quinone (A) and the quercetin quinone (B) with monothiols (GSH or NAC). This reaction is a Michael addition. In the case of the monoHER quinone, first the nucleophilic thiolate (RS^-) attacks the monoHER quinone at the 2'-position in the B ring (a). By protonation a Meisenheimer complex is formed (c). After deprotonation (d) and subsequent protonation the resulting thiol-flavonoid adduct is formed (e). In the case of the quercetin quinone, the Michael addition starts with the nucleophilic attack of the thiolate (RS^-) at the 6- or 8-position in the A ring of the quercetin quinone. The subsequent reactions are comparable to those of monoHER.

As expected the monoHER quinone also reacts with the dithiol DTT to form a DTT-monoHER adduct (Figure 1). Intriguingly, it seems as if the quercetin quinone does not react with DTT, i.e. no DTT-quercetin adduct formation and no net consumption of quercetin were observed when quercetin was oxidized in the presence of DTT. Considering the reactivity of the quercetin quinone to-

wards thiols, the quercetin quinone has to react with DTT (e.g. in analogy with GSH and NAC, Figure 3A) to form a DTT-quercetin adduct. In contrast to GSH or NAC, DTT contains two thiol groups that easily form an intramolecular disulfide. That no DTT-quercetin adduct was detected in our experiments has to be due to the presence of these two thiol groups. As depicted in Figure 4, one of the thiol groups attacks the quercetin quinone to form DTT-quercetin. In a second reaction step, due to the presence of the free intramolecular SH-group in the DTT moiety, which has a high tendency to form a six-membered ring with an internal disulfide bond, the DTT-quercetin adduct is rapidly converted into quercetin and DTT disulfide. This rapid conversion of the DTT-quercetin adduct explains why, in contrast to DTT-monoHER, this adduct was not found when quercetin was oxidized in the presence of DTT. This reaction is comparable to the reactions of DTT with disulfides and other compounds that also proceed relatively fast with a DTT adduct as an intermediate (Haenen *et al.*, 1990).

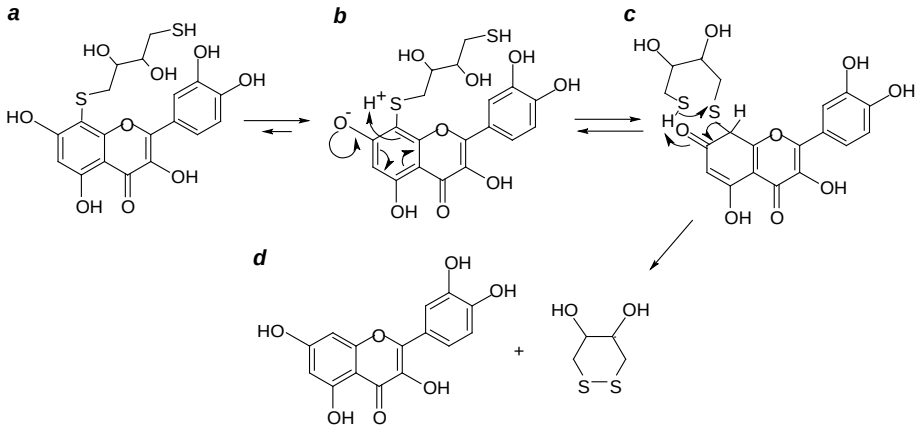

Figure 4. Conversion of DTT-quercetin (a) into quercetin and DTT-disulfide (d). The reaction starts with tautomerization by deprotonation of the 7-OH group of DTT-quercetin and the subsequent protonation of C8 (b). This results in the formation of a Meisenheimer complex (c), which ultimately results in the formation of quercetin and DTT disulfide (d).

In the reaction of thiols with the quercetin quinone, the thiol, and most probably also one of the thiol groups of DTT, is attached to the 6- or 8-position in the flavonoid A ring, whereas with monoHER the thiol is attached to the 2'-position in the B ring (Boots *et al.*, 2003; Jacobs *et al.*, 2009) (Figure 3). The conversion of DTT-quercetin into quercetin and DTT disulfide starts with the deprotonation of the 7-OH group in DTT-quercetin (Figure 4b). This is the group adjacent to the thiol-flavonoid bond. In the case of DTT-monoHER this would be the 3'-OH (Fig-

ure 3d). Quantum molecular calculations show that deprotonation of the 3'-OH of RSH-monoHER needs more activation energy (ca. 100 kJ/mol more) than deprotonation of the 7-OH of RSH-quercetin. This explains why the DTT-monoHER adduct is, unlike DTT-quercetin, not rapidly converted into monoHER and DTT disulfide.

A similar intriguing finding was that the GSH-quercetin adduct reacts with other thiols (e.g. NAC) whereas the GSH-monoHER adduct does not (Figure 2). The formation of the NAC-flavonoid adduct from the GSH-flavonoid adduct includes two sequential steps: (i) the reverse of the reaction depicted in Figure 3, i.e. the conversion of the GSH-flavonoid into the flavonoid quinone and GSH, and (ii) the reaction of the flavonoid quinone with NAC. In the first step, the OH group in the GSH-flavonoid adduct adjacent to the position where GSH is chemically bound has to be deprotonated first (Figure 3e → d). The deprotonation enables the formation of the Meisenheimer complex (Figure 3c) and ultimately the formation of the quinone and GSH. This deprotonation is similar to the deprotonation of the DTT-flavonoid adduct (Figure 4a → b) and requires more activation energy (ca. 100 kJ/mol) in GSH-monoHER than in GSH-quercetin. This explains why GSH-monoHER, in contrast to GSH-quercetin, is not converted into NAC-monoHER.

As explained above, to convert the GSH-flavonoid adduct into the NAC-flavonoid adduct, the flavonoid quinone has to be formed first. In the most abundant tautomer of the quercetin quinone (Figure 3B, a), the distance between the electron deficient carbonyl centers is maximal within the flavonoid backbone. In the ortho-quinone of monoHER two carbonyls are adjacent (Figure 3A, a), which is energetically unfavorable compared to the larger distance between these groups in the quercetin quinone (Jacobs *et al.*, 2010). This might also contribute to why the GSH-quercetin adduct is readily converted into GSH and the quercetin quinone that subsequently reacts with NAC, whereas the GSH-monoHER adduct is not.

Both the monoHER quinone and the quercetin quinone readily react with thiols, also when they are formed in a biological system (Jacobs *et al.*, 2010) (Figure 5). In the case of the quercetin quinone, this reaction has shown to be reversible. This indicates that after the quercetin quinone has reacted with GSH, the quinone may still react with other thiols, as demonstrated by the formation of the NAC-quercetin adduct. In tissues with GSH in abundance, like the liver, this is not likely to cause any problem because the quinone will be trapped again by GSH. However, in e.g. blood plasma, where GSH is practically absent, or when GSH has been depleted, the quercetin quinone might bind to essential thiols of vital proteins. This can cause toxicity such as increased membrane

permeability (Yen *et al.*, 2003) or impaired functioning of enzymes that depend on a critical thiol-group (Kalyanaraman *et al.*, 1987; Moore *et al.*, 1988). In this way, the GSH-quercetin adduct might serve as a transport or storage of oxidized quercetin, and even spread toxicity (Boots *et al.*, 2005).

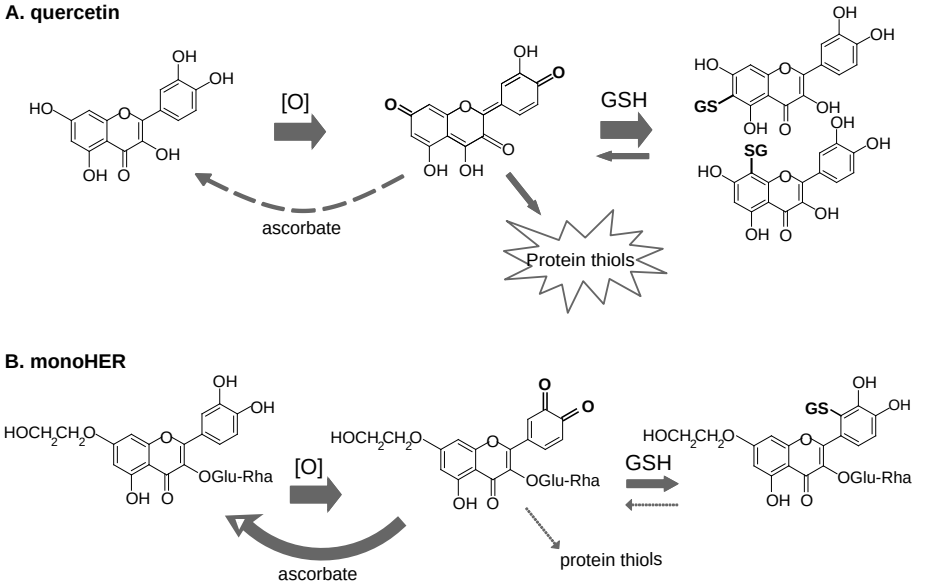

Figure 5. Schematic overview depicting the essential difference between quercetin and monoHER. When monoHER and quercetin protect against oxidative stress by scavenging free radicals, both flavonoids are oxidized, thereby forming flavonoid quinones. Both the monoHER quinone and the quercetin quinone can react with GSH to form a GSH-monoHER and a GSH-quercetin adduct, respectively. The GSH-quercetin adduct can be converted back into the quercetin quinone and GSH. Thereby, especially in tissue where GSH levels are low, the quercetin quinone might react with other thiols groups, such as protein thiols, which will cause toxicity. The GSH-monoHER adduct is more stable than the GSH-quercetin adduct. This means that once the monoHER quinone is bound to GSH it will not be transferred to other thiols, thereby preventing spread of toxicity. Moreover, it has been shown that the monoHER quinone, in contrast to the quercetin quinone, reacts with the antioxidant ascorbate rather than with thiols.

The GSH-monoHER adduct, in contrast to the GSH-quercetin adduct, is relatively stable. As shown in the present study, once the monoHER quinone is scavenged by GSH, it will not readily react with other thiols. Moreover, this GSH-monoHER adduct is highly water-soluble and is expected to be excreted by the body. The GSH-monoHER adduct has been detected *in vivo* in the bile fluid of healthy volunteers (Jacobs *et al.*, 2009). In this way, the toxic oxidation products are eliminated and there will be no spread of toxicity. In blood plasma, the monoHER quinone might, similarly to the quercetin quinone, also react with protein thiols

and cause toxicity. However, the monoHER quinone, in contrast to the quercetin quinone, reacts with ascorbate rather than with protein thiols (Jacobs *et al.*, 2010). In this way, the reactivity of the radicals becomes completely neutralized.

In general, flavonoids are treated as a group of antioxidants that have similar interactions with biological systems. Our study shows that GSH-monoHER is stable, whereas GSH-quercetin readily reacts with other thiols. This demonstrates that even structurally comparable flavonoids behave differently. This should be considered in evaluating the biological effects of flavonoids.

References

Awad HM, Boersma MG, Vervoort J, Rietjens IM (2000) Peroxidase-catalyzed formation of quercetin quinone methide-glutathione adducts. *Arch Biochem Biophys* **378:** 224-233

Bast A, Haenen GR (2002) The toxicity of antioxidants and their metabolites. *Environmental Toxicology and Pharmacology* **11:** 251-258

Bast A, Haenen GR, Bruynzeel AM, Van der Vijgh WJ (2007) Protection by flavonoids against anthracycline cardiotoxicity: from chemistry to clinical trials. *Cardiovasc Toxicol* **7:** 154-159

Boots AW, Balk JM, Bast A, Haenen GR (2005) The reversibility of the glutathionyl-quercetin adduct spreads oxidized quercetin-induced toxicity. *Biochem Biophys Res Commun* **338:** 923-929

Boots AW, Kubben N, Haenen GR, Bast A (2003) Oxidized quercetin reacts with thiols rather than with ascorbate: implication for quercetin supplementation. *Biochem Biophys Res Commun* **308:** 560-565

Boots AW, Li H, Schins RP, Duffin R, Heemskerk JW, Bast A, Haenen GR (2007) The quercetin paradox. *Toxicol Appl Pharmacol* **222:** 89-96

Galati G, Moridani MY, Chan TS, O'Brien PJ (2001) Peroxidative metabolism of apigenin and naringenin versus luteolin and quercetin: glutathione oxidation and conjugation. *Free Radic Biol Med* **30:** 370-382

Galati G, Sabzevari O, Wilson JX, O'Brien PJ (2002) Prooxidant activity and cellular effects of the phenoxyl radicals of dietary flavonoids and other polyphenolics. *Toxicology* **177:** 91-104

Haenen GR, De Rooij BM, Vermeulen NP, Bast A (1990) Mechanism of the reaction of ebselen with endogenous thiols: dihydrolipoate is a better cofactor than glutathione in the peroxidase activity of ebselen. *Mol Pharmacol* **37:** 412-422

Haenen GR, Jansen FP, Bast A (1993) The antioxidant properties of five O-(-b-Hydroxyethyl)-Rutosides of the flavonoid mixture Venoruton. *Phlebology* **Suppl.1:** 10-17

Hertog MG, Hollman PC, Katan MB, Kromhout D (1993) Intake of potentially anticarcinogenic flavonoids and their determinants in adults in The Netherlands. *Nutr Cancer* **20:** 21-29

Jacobs H, Moalin M, Bast A, van der Vijgh WJ, Haenen GR (2010) An Essential Difference between the Flavonoids MonoHER and Quercetin in Their Interplay with the Endogenous Antioxidant Network. *PLoS One* **5:** e13880

Jacobs H, van der Vijgh WJ, Koek GH, Draaisma GJ, Moalin M, van Strijdonck GP, Bast A, Haenen GR (2009) Characterization of the glutathione conjugate of the semisynthetic flavonoid monoHER. *Free Radic Biol Med* **46:** 1567-1573

Kalyanaraman B, Premovic PI, Sealy RC (1987) Semiquinone anion radicals from addition of amino acids, peptides, and proteins to quinones derived from oxidation of catechols and catecholamines. An ESR spin stabilization study. *J Biol Chem* **262:** 11080-11087

Kuhnau J (1976) The flavonoids. A class of semi-essential food components: their role in human nutrition. *World Rev Nutr Diet* **24:** 117-191

Laughton MJ, Halliwell B, Evans PJ, Hoult JR (1989) Antioxidant and pro-oxidant actions of the plant phenolics quercetin, gossypol and myricetin. Effects on lipid peroxidation, hydroxyl radical generation and bleomycin-dependent damage to DNA. *Biochem Pharmacol* **38:** 2859-2865

Meister A (1994) Glutathione-ascorbic acid antioxidant system in animals. *J Biol Chem* **269:** 9397-9400

Metodiewa D, Jaiswal AK, Cenas N, Dickancaite E, Segura-Aguilar J (1999) Quercetin may act as a cytotoxic prooxidant after its metabolic activation to semiquinone and quinoidal product. *Free Radic Biol Med* **26:** 107-116

Moore GA, Weis M, Orrenius S, O'Brien PJ (1988) Role of sulfhydryl groups in benzoquinone-induced Ca2+ release by rat liver mitochondria. *Arch Biochem Biophys* **267:** 539-550

O'Brien PJ (1991) Molecular mechanisms of quinone cytotoxicity. *Chem Biol Interact* **80:** 1-41

van Acker FA, Schouten O, Haenen GR, van der Vijgh WJ, Bast A (2000a) Flavonoids can replace alpha-tocopherol as an antioxidant. *FEBS Lett* **12:** 145-148

van Acker FA, van Acker SA, Kramer K, Haenen GR, Bast A, van der Vijgh WJ (2000) 7-monohydroxyethylrutoside protects against chronic doxorubicin-induced cardiotoxicity when administered only once per week. *Clin Cancer Res* **6:** 1337-1341

Yen GC, Duh PD, Tsai HL, Huang SL (2003) Pro-oxidative properties of flavonoids in human lymphocytes. *Biosci Biotechnol Biochem* **67:** 1215-1222

Yu BP (1994) Cellular defenses against damage from reactive oxygen species. *Physiol Rev* **74:** 139-162

Chapter 4

An essential difference between the flavonoids monoHER and quercetin in their interplay with the endogenous antioxidant network

Hilde Jacobs
Mohamed Moalin
Aalt Bast
Wim J.F. van der Vijgh
Guido R.M.M. Haenen

PLoS One 2010; 5:e13880

Abstract

Antioxidants can scavenge highly reactive radicals. As a result the antioxidants are converted into oxidation products that might cause damage to vital cellular components. To prevent this damage, the human body possesses an intricate network of antioxidants that pass over the reactivity from one antioxidant to another in a controlled way. The aim of the present study was to investigate how the semi-synthetic flavonoid 7-mono-O-(β-hydroxyethyl)-rutoside (monoHER), a potential protective agent against doxorubicin-induced cardiotoxicity, fits into this antioxidant network. This position was compared with that of the well-known flavonoid quercetin. The present study shows that the oxidation products of both monoHER and quercetin are reactive towards thiol groups of both GSH and proteins. However, in human blood plasma, oxidized quercetin easily reacts with protein thiols, whereas oxidized monoHER does not react with plasma protein thiols. Our results indicate that this can be explained by the presence of ascorbate in plasma; ascorbate is able to reduce oxidized monoHER to the parent compound monoHER before oxidized monoHER can react with thiols. This is a major difference with oxidized quercetin that preferentially reacts with thiols rather than ascorbate. The difference in selectivity between monoHER and quercetin originates from an intrinsic difference in the chemical nature of their oxidation products, which was corroborated by molecular quantum chemical calculations. These findings point towards an essential difference between structurally closely related flavonoids in their interplay with the endogenous antioxidant network. The advantage of monoHER is that it can safely channel the reactivity of radicals into the antioxidant network where the reactivity is completely neutralized.

Introduction

The human body is endowed with a wide range of antioxidants to protect cells from damage induced by free radicals and other reactive species. Glutathione (GSH) is one of the most important endogenous hydrophilic antioxidants (Meister, 1994a). It is synthesized in many different cell types from its constituting amino acids glutamic acid, cysteine and glycine, and is therefore not required in the human diet (Meister, 1994a). The actual antioxidant property of GSH is attributable to the thiol group that is present in its cysteine moiety. As an effective nucleophile, GSH also plays an important role in the protection against electrophilic compounds (Yu, 1994).

Like GSH, ascorbic acid (vitamin C) is also an important hydrophilic antioxidant. In contrast to GSH, ascorbic acid cannot be synthesized by humans and, as a consequence, is required in the human diet (Meister, 1994b). It directly scavenges $O_2^{\bullet-}$ and $^{\bullet}OH$ and various other radicals.

Phenolic antioxidants comprise α-tocopherol (the most active form of vitamin E) and flavonoids. Like ascorbic acid and most other vitamins, α-tocopherol has to be obtained exclusively from the diet. It is the major lipid-soluble lipoprotein antioxidant (Niki, 1987). α-Tocopherol is localized in biomembranes and functions as an efficient inhibitor of lipid peroxidation. Flavonoids, on the other hand, are not essential nutrients but they form an integral part of the human diet as they are found in fruits, vegetables, nuts and plant-derived beverages such as tea and wine (Hertog *et al.*, 1993; Kuhnau, 1976). They have a wide range of biological activities (Landis-Piwowar and Dou, 2008; Liu *et al.*, 2010; Rathee *et al.*, 2009), but are most commonly known for their antioxidant activity. Quercetin is one of the most frequently studied dietary flavonoids (Formica and Regelson, 1995; Hertog *et al.*, 1993). It can scavenge highly reactive species, an activity that is implicated in its health benefits (Amic *et al.*, 2007; Boots *et al.*, 2008).

The flavonoid of interest to us, that closely resembles the chemical structure of quercetin, is the semi-synthetic flavonoid 7-mono-O-(β-hydroxyethyl)-rutoside (monoHER). MonoHER is the most powerful antioxidant constituent of the registered drug Venoruton® (Haenen *et al.*, 1993), which is used in the treatment of chronic venous insufficiency (Petruzzellis *et al.*, 2002). *In vitro* screening has shown that monoHER is the most potent protector against cardiotoxicity induced by the anticancer agent doxorubicin within a series of flavonoids (Haenen *et al.*, 1993). Preclinical experiments have confirmed that mono-

HER is indeed a potential protective agent against doxorubicin-induced cardiotoxicity (van Acker *et al.*, 2000; van Acker *et al.*, 1995). Because of these promising results, clinical trials are being performed to study the protection of intravenously administered monoHER against doxorubicin-induced cardiotoxicity in cancer patients (Bruynzeel *et al.*, 2007; Willems *et al.*, 2006). The antioxidant activity of monoHER is supposed to be involved in its protection. Because of its excellent radical scavenging properties monoHER can effectively protect the heart against free radicals produced by doxorubicin.

During the scavenging of highly reactive species, antioxidants donate an electron or a hydrogen atom to the radical involved, thereby converting the radical into a relatively stable non-radical. In this way the reactivity of the radical is annihilated. However, in this reaction the antioxidant itself is converted into an oxidation product that takes over part of the reactivity of the radical. This oxidized antioxidant might cause damage to vital cellular components (Bast and Haenen, 2002). For example, when α-tocopherol scavenges free radicals it is oxidized to produce the corresponding tocopheroxyl radicals (Mukai *et al.*, 1991). These radicals can recombine with other radicals, such as peroxyl radicals, thereby neutralizing them (Upston *et al.*, 1999). However, when these tocopheroxyl radicals cannot be eliminated, lipid peroxidation is aggravated, a phenomenon referred to as tocopherol-mediated peroxidation (Bowry *et al.*, 1992; Upston *et al.*, 1999).

To prevent damage by reactive oxidation products of antioxidants, the human body has a refined network of antioxidants that pass over the reactivity from one antioxidant to another in a controlled way, thereby gradually diminishing the reactivity of the radical and recycling the antioxidants. In this way, it has been shown that ascorbate can regenerate α-tocopherol from tocopheroxyl radicals, thereby preventing tocopherol-mediated peroxidation (Mukai *et al.*, 1991; Niki, 1987; Packer *et al.*, 1979). This illustrates that antioxidants act in synergy to annihilate radicals. Besides preventing damage induced by harmful oxidation products, regeneration is important because it restores the antioxidant network.

The regeneration of α-tocopherol by ascorbate is well documented, however, not much is known on the regeneration of flavonoids. When quercetin protects against free radicals, thiol-reactive oxidation products of quercetin are formed that can cause damage to vital cellular components, a phenomenon known as the quercetin paradox (Boots *et al.*, 2007). Recently it was found that the oxidation product of monoHER is also reactive towards thiols (Jacobs *et al.*, 2009). This might have implications for the applicability of monoHER. However,

as mentioned above, antioxidants do not act in isolation to protect against oxidative damage.

The aim of the present study was to determine how monoHER fits into the antioxidant network and to get insight in the regeneration of flavonoids. Particularly, the reactivity of oxidized monoHER towards thiols and ascorbate was investigated. In addition a comparison with quercetin was made.

Materials and methods

Ethics Statement

For the study spare, anonymised human blood plasma obtained from the Academic Hospital Maastricht was used according to the procedure approved by the medical ethical review board of the hospital.

Chemicals

7-mono-O-(β-hydroxyethyl)-rutoside (monoHER) was kindly provided by Novartis Consumer Health (Nyon, Switzerland). Stock solutions of the drug were freshly prepared in a methanol/25 mM phosphate buffer (pH 3.33) mixture (4/1, v/v). Quercetin was purchased from Sigma (St. Louis, MO, USA) and stock solutions were freshly prepared in methanol. Bovine serum albumin (BSA), reduced glutathione (GSH), hydrogen peroxide (H_2O_2), horseradish peroxidase (HRP), L-ascorbic acid (vitamin C) and 5,5´-dithiobis-(2-nitrobenzoic acid) (DTNB) were also purchased from Sigma (St. Louis, MO, USA). Trifluoroacetic acid (TFA) was acquired from Sigma-Aldrich (Steinheim, Germany). Acetonitrile HPLC grade and methanol were obtained from Biosolve (Valkenswaard, The Netherlands). 2'-GSH-monoHER was synthesized as described previously (Jacobs *et al.*, 2009).

Oxidation of monoHER

MonoHER was oxidized as described before (Jacobs *et al.*, 2009). Shortly, 50 µM monoHER was incubated for 5 minutes at 37 °C together with 1.6 nM HRP and 33 µM H_2O_2 in a 145 mM phosphate buffer (pH 7.4). The GSH-monoHER adduct was formed by oxidizing 50 µM monoHER in the presence of 40 µM GSH. To investigate the influence of ascorbate on the oxidation of monoHER and on the formation of the GSH-monoHER adduct, ascorbate (final concentration of 40

µM, unless noted otherwise) was added to the incubation mixtures. The reactions were monitored spectrophotometrically and by HPLC. MonoHER consumption was determined at 355 nm, ascorbate consumption at 270 nm.

Spectrophotometric analysis

Spectrophotometric analysis was performed with a Varian Carry 50 spectrophotometer (Varian, Mulgrave, VIC, Australia). All absorption spectra were recorded from 220 to 500 nm with a scan speed of 960 nm/min, using quartz cuvettes. The UV/Vis scans were started 30, 150 and 300 seconds after the addition of HRP.

High-performance liquid chromatography analysis

High-performance liquid chromatography (HPLC) was performed using a HP 1100 series HPLC system (Agilent Technologies, Palo Alto, CA, USA). Analytical separations were achieved using a Supelcosil LC 318 column (5 µm, 25 cm x 4.6 mm) (Supelco, Bellefonte, PA, USA). The mobile phase consisted of water containing 0.1% (v/v) TFA with linear gradients of 5% acetonitrile at t = 0 to 20% acetonitrile at 5 min followed by an increase to 30% acetonitrile at 10 min. Finally 90% acetonitrile was used from 18 min onward for 5 min. The column was reequilibrated with 5% acetonitrile for 5 min. A flow rate of 2 ml/min and an injection volume of 20 µl were used. Detection was carried out with a diode array detector (DAD). The chromatograms presented are based on detection at 355 nm (absorption maximum of monoHER).

Measurement of thiol reactivity

To determine the thiol reactivity of oxidized monoHER and quercetin, free SH-groups were measured using the DTNB [5, 5´-dithiobis-(2-nitrobenzoic acid)] assay. The incubation mixtures contained 50 µM monoHER, 1.6 nM HRP, 33 µM H_2O_2 and 40 µM GSH (or 400 µM BSA) in a 145 mM phosphate buffer (pH 7.4). When the oxidation was performed in the presence of ascorbate, the incubation mixture additionally contained 40 µM of ascorbate. After 0 or 5 minutes of incubation at 37 °C, thiol content was measured by adding DTNB (final concentration of 0.6 mM) to the incubation mixtures. The formation of TNB was measured spectrophotometrically at 412 nm. Similar experiments with 50 µM monoHER were performed in human blood plasma to determine the reactivity

towards plasma protein thiols. Identical experimental conditions were used to determine thiol reactivity of oxidized quercetin.

Molecular quantum chemical calculations

Molecular quantum chemical calculations (ab initio level) were performed with the software program Spartan '06 (Wavefunction, Irvine, CA, USA) to corroborate the experimental results. The Møller Plesset, RI-MP2 with the 6-31G* basis set was used to calculate the relative abundance of the tautomers of oxidized quercetin. The Hartree-Fock method with the 3-21G basis set was used for calculating the equilibrium geometry and the energies of the lowest unoccupied molecular orbital (LUMO) of the quercetin quinone methide and a simplified monoHER quinone (the rutin group at C3-O and the ethoxygroup at C7-O were replaced by methyl groups) and the highest occupied molecular orbital (HOMO) of GSH and ascorbate, unless depicted otherwise. In addition, a LUMO map for the monoHER quinone and the quercetin quinone methide were generated to get a visual on the LUMO distribution.

Statistics

All experiments were performed, at least, in triplicate. Data are expressed as mean ± SD or as a typical example. Statistical analysis was performed using student's t-test. P values ≤ 0.05 were considered statistically significant.

Results

GSH reacts with oxidized monoHER to form 2'-GSH-monoHER

UV and HPLC analysis (Figure 1A and Figure 2A) show that oxidation of 50 µM monoHER by HRP/H_2O_2 leads to the consumption of monoHER at a rate of 5.5 ± 0.4 µM/min (Figure 3). In the presence of 40 µM GSH, all the oxidized monoHER is recovered as 2'-GSH-monoHER at a rate of 5.5 ± 0.3 µM/min (Figure 3). This is concluded from the appearance of the characteristic UV spectrum of 2'-GSH-monoHER (Figure 1B) and HPLC analysis of the incubation mixture (Figure 2B). In the HPLC chromatogram a second peak emerges, eluting at a position identical to that of the synthesized 2'-GSH-monoHER adduct. These data demonstrate that the monoHER quinone is formed as a primary oxidation product and that this oxidation product forms an adduct with GSH.

Ascorbate reduces oxidized monoHER to monoHER

As shown by UV and HPLC analysis, addition of 40 µM ascorbate to the incubation mixture containing monoHER and HRP/H_2O_2 prevents monoHER consumption (Figure 1C and Figure 2C). At the same time the ascorbate concentration decreases, as seen in the spectrum as a decrease of the absorption at 270 nm. When monoHER is omitted from the incubation mixture, there is no detectable ascorbate consumption. These findings suggest that monoHER is regenerated from its oxidation product by ascorbate.

The average rate of ascorbate consumption in the presence of monoHER (4.3 ± 0.3 µM/min) is 23% less than monoHER consumption in the absence of ascorbate (5.5 ± 0.4 µM/min) (Figure 3). Addition of more ascorbate (final concentration of 100 µM) to the incubation mixture reduces the ascorbate consumption to 1.5 ± 0.1 µM/min, 72% less than monoHER consumption without ascorbate. This indicates that the enzyme HRP is also partially inhibited by ascorbate, as has been shown previously (Boots *et al.*, 2003). The extent of inhibition depends on the ascorbate concentration.

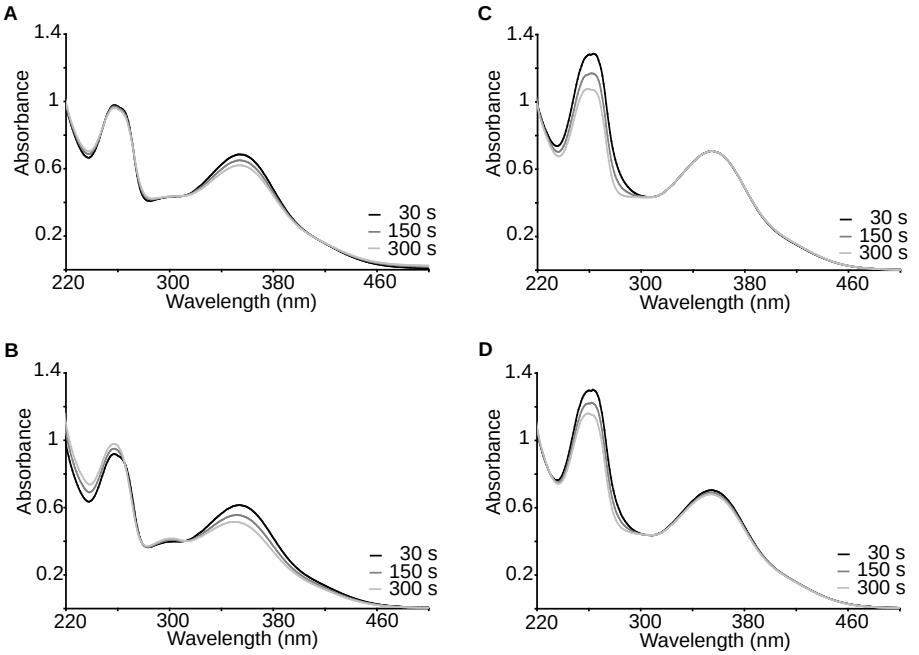

Figure 1. Spectrophotometrical analyses. Spectrophotometrical analysis of the incubation mixture containing (A) 50 µM monoHER, 1.6 nM horseradish peroxidase (HRP) and 33 µM H_2O_2. The same experiment was carried out in (B) the presence of 40 µM GSH, (C) 40 µM ascorbate and (D) both 40 µM GSH and 40 µM ascorbate. The UV/Vis scans were recorded 30, 150 and 300 seconds after the addition of HRP. A typical example is shown.

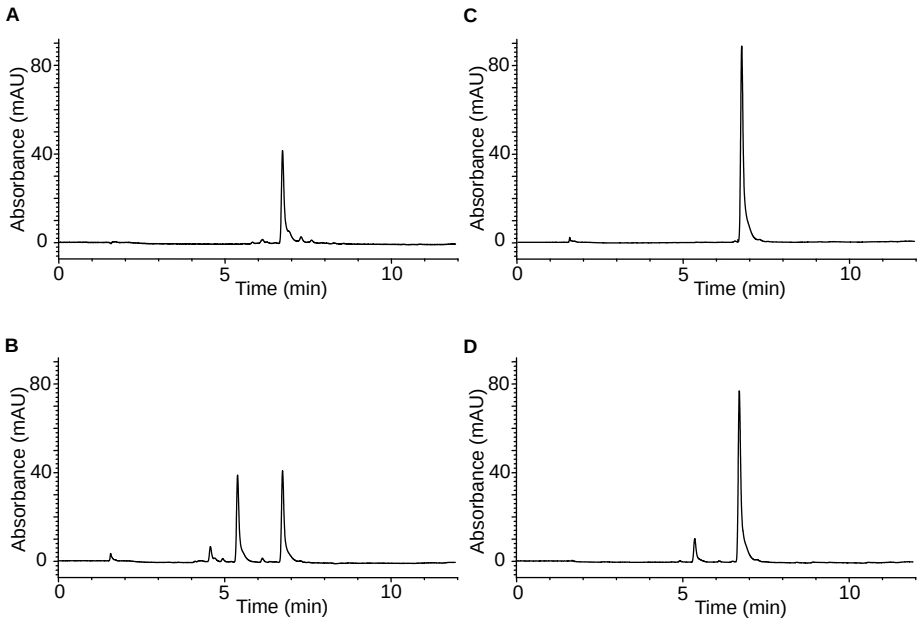

Figure 2. HPLC analyses. HPLC analysis of the incubation mixture containing (A) 50 µM monoHER, 1.6 nM horseradish peroxidase (HRP) and 33 µM H_2O_2. The same experiment was carried out in (B) the presence of 40 µM GSH, (C) 40 µM ascorbate and (D) both 40 µM GSH and 40 µM ascorbate. The different incubation mixtures were injected on the HPLC system 5 minutes after the addition of HRP. A typical example is shown. The retention time of monoHER is 6.7 min and that of 2'-GSH-monoHER is 5.4 min. The initial peak height of monoHER before oxidation was 88 mAU, corresponding to a concentration of 50 µM. After 5 minutes of oxidation the monoHER concentrations in the incubation mixtures A, B, C and D were 22.5 µM, 22.5 µM, 50 µM and 43.5 µM, respectively.

Competition between GSH and ascorbate for oxidized monoHER

To investigate the competition between GSH and ascorbate, monoHER was oxidized in the presence of both compounds (Figure 1D and Figure 2D). Comparison of the rate of 2'-GSH-monoHER formation (1.3 ± 0.1 µM/min) and the rate of ascorbate consumption (3.0 ± 0.3 µM/min) (Figure 3) indicates that oxidized monoHER reacts two to three times faster with ascorbate than with GSH. These results are in contrast with those found for quercetin. In a comparable competition experiment with quercetin it was found that oxidized quercetin predominantly reacts with GSH (Boots *et al.*, 2003).

As shown in Figure 4A, both oxidized monoHER and oxidized quercetin, produced *in situ* by HRP/H_2O_2-mediated oxidation, decrease the thiol content of the incubation mixture containing 40 µM GSH to approximately 50% in 5 minutes. The presence of ascorbate (40 µM) does not affect the consumption of thiols by oxidized quercetin (Figure 4B). In contrast, ascorbate significantly de-

creases the thiol consumption induced by oxidized monoHER (Figure 4B). This confirms that oxidized monoHER preferentially reacts with ascorbate, whereas oxidized quercetin preferentially reacts with GSH.

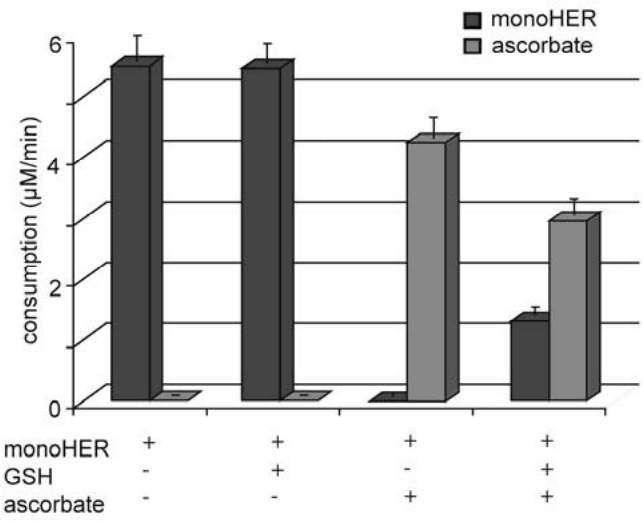

Figure 3. MonoHER and ascorbate consumption rates. Consumption of monoHER and ascorbate in the incubation mixtures containing 50 µM monoHER, 1.6 nM HRP and 33 µM H_2O_2 in the presence of either 40 µM GSH, 40 µM ascorbate or both 40 µM GSH and 40 µM ascorbate. The incubation time was 5 minutes. All measurements were carried out in triplicate and data are expressed as mean ± SD.

Competition between protein thiols and ascorbate for oxidized monoHER and oxidized quercetin

Next, monoHER and quercetin were oxidized in human blood plasma. In human blood plasma GSH is practically absent and ascorbate concentrations are 40-60 µM (Brubacher *et al.*, 2000). The generation of oxidized quercetin decreases the thiol content of plasma, i.e. protein thiols, by approximately 40% (Figure 4C). In contrast, the generation of oxidized monoHER has no effect on the thiol content of human blood plasma (Figure 4C). An additional experiment shows that oxidized monoHER is able to react with the thiol group of albumin, which is the most abundant plasma protein (Figure 4D). Ascorbate is able to prevent the reaction of oxidized monoHER with albumin (Figure 4D).

These results point towards an essential difference between monoHER and quercetin, i.e. oxidized monoHER rather reacts with ascorbate than with protein thiols, while oxidized quercetin preferentially reacts with protein thiols.

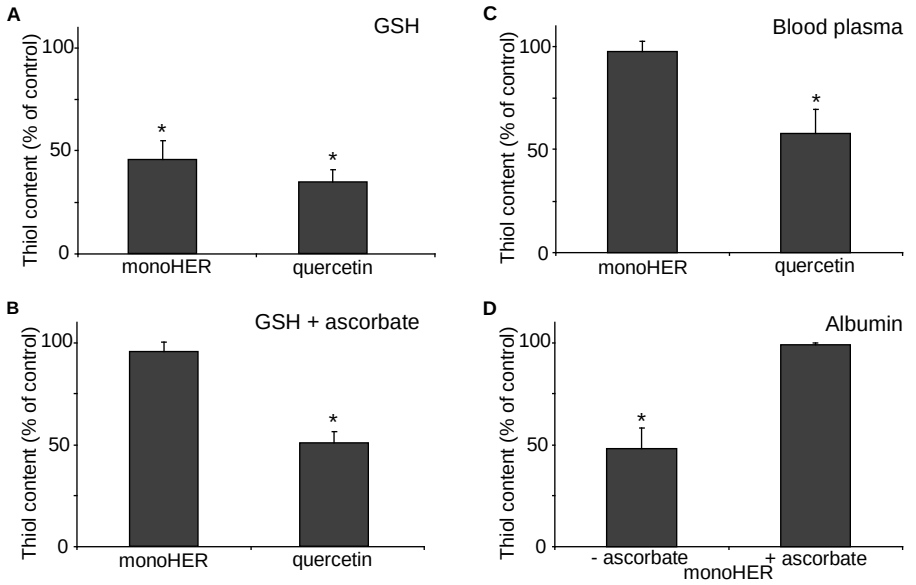

Figure 4. Reactivity of oxidized monoHER and oxidized quercetin towards thiols. Thiol content of the incubation mixture containing 50 µM monoHER or quercetin, 1.6 nM HRP and 33 µM H_2O_2 in the presence of either (A) 40 µM GSH, (B) both 40 µM GSH and 40 µM ascorbate, (C) human blood plasma or (D) 400 µM albumin (BSA) (with or without 40 µM ascorbate). The thiol content of the different incubation mixtures was measured 5 minutes after the addition of HRP. All measurements were carried out in triplicate and data are expressed as mean ± SD. *P<0.05 compared to control.

Explanation of the difference in reactivity between oxidized monoHER and oxidized quercetin

Molecular quantum chemical calculations show that the tautomer depicted in Figure 5A, a quinone methide, represents more than 99% of oxidized quercetin. In oxidized monoHER only the ortho-quinone, illustrated in Figure 5B, can be formed. Generation of a LUMO map of oxidized monoHER and oxidized quercetin shows that the LUMO of oxidized monoHER is restricted to the B ring and part of the C ring, while the LUMO of oxidized quercetin is delocalized over all the phenolic rings (Figure 5). The LUMO of the monoHER ortho-quinone and the quercetin quinone methide are 42.6 kJ/mol and 0.0605 kJ/mol, respectively, showing that oxidized monoHER is a harder electrophile than oxidized quercetin. The HOMO of ascorbate and GSH are -394 kJ/mol and -1.35 kJ/mol, respectively, showing that ascorbate is a harder nucleophile than GSH. According to Pearson's HSAB concept (Pearson, 1963), hard electrophiles react faster and form stronger bonds with hard nucleophiles, explaining the preferential reaction of oxidized monoHER with ascorbate over thiols.

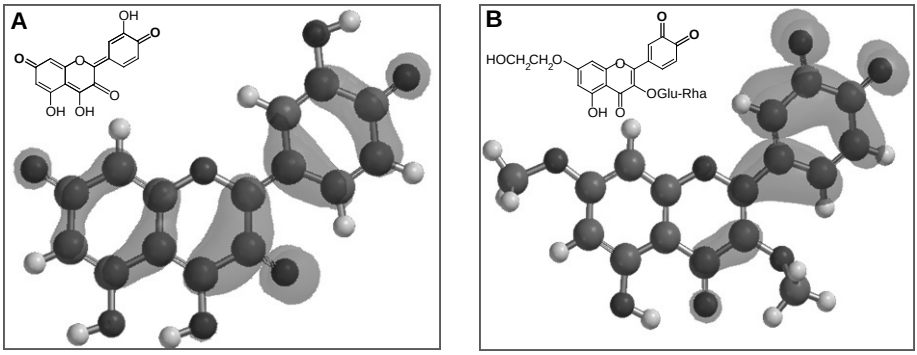

Figure 5. LUMO delocalization maps. LUMO delocalization map of (A) oxidized quercetin and (B) oxidized monoHER. In oxidized monoHER, the rutin group at C3-O and the ethoxygroup at C7-O were replaced by methyl groups and for quercetin, the most abundant tautomer (>99%) was used. The LUMO of oxidized monoHER is localized in the B ring and part of the C ring, while the LUMO of oxidized quercetin is distributed over all the phenolic rings (rings A, C and B).

Discussion

Paradoxically, free radical scavenging antioxidants are chemically converted into potentially harmful oxidation products when they protect against free radicals (Bast *et al.*, 1991). These oxidation products usually retain a part of the reactivity of the species they have scavenged, and might therefore cause damage to vital cellular targets (Bast and Haenen, 2002; Haenen and Bast, 2002). To protect cells against this damage the human body has a refined network in which the reactivity is transferred from one antioxidant to another, thereby gradually diminishing the reactivity (Bast *et al.*, 1991; Meister, 1994a).

The aim of the present study was to investigate how monoHER fits into this endogenous antioxidant network. The interaction of monoHER with the network was compared with that of quercetin, which chemically closely resembles monoHER. The results of this study show that oxidized monoHER is reduced by ascorbate to recycle the parent compound monoHER, while oxidized monoHER reacts with GSH to form a GSH-conjugate. The reactions of oxidized quercetin with ascorbate and GSH are similar to those of oxidized monoHER (Boots *et al.*, 2003). However, as shown in the present study, a major difference is that oxidized quercetin preferentially reacts with thiols, whereas oxidized monoHER preferentially reacts with ascorbate. This is an essential difference in the interplay of both flavonoids with antioxidants of the endogenous antioxidant network.

The different position of monoHER and quercetin in the network has to originate from an intrinsic difference in the chemical nature of their oxidation products. Quantum chemical calculations revealed that of the four possible tautomeric forms of oxidized quercetin, the tautomer shown in Figure 5A, has an abundance of more than 99%. In this tautomer the distance between the electron deficient carbonyl centers is maximal, which is energetically favorable and explains its high abundance. The high abundance of this specific tautomer is corroborated by the formation of adducts in the A ring, i.e. 6-GSH-quercetin and 8-GSH-quercetin, in the reaction of GSH with oxidized quercetin (Galati *et al.*, 2001).

In monoHER a rutinose is attached to the 3-OH group of the C ring and a hydroxyethyl group is attached to the hydroxyl group oxygen at position 7 of the A ring. These substitutions preclude the formation of quinone methide tautomers in oxidized monoHER. Therefore, only the ortho-quinone can be formed (Figure 5B). In this ortho-quinone two carbonyls are adjacent, which is energetically unfavorable compared to the larger distance between these groups in the preferential tautomer of oxidized quercetin. The presence of an ortho-quinone in the B ring is corroborated by the formation of an adduct in this ring, i.e. 2'-GSH-monoHER, in the reaction of oxidized monoHER with GSH (Jacobs *et al.*, 2009).

Apparently, the oxidation products of monoHER and quercetin are energetically different. The LUMO of oxidized monoHER is primarily concentrated in the B ring and therefore relatively high, while that of oxidized quercetin is spread over the whole molecule (Figure 5). This is reflected by a LUMO of oxidized quercetin (0.0605 kJ/mol) that is substantially lower than that of oxidized monoHER (42.6 kJ/mol). Pearson's HSAB concept assigns the terms 'hard' or 'soft' to chemical species to explain or predict the outcome of a chemical reaction (Pearson, 1963). 'Hard' applies to electrophiles (the reactants that accept binding electrons) that have LUMO of high energy or nucleophiles (the reactants that donate binding electrons) with a low HOMO energy. 'Soft', on the other hand, applies to electrophiles with a low LUMO value or nucleophiles with a high HOMO value. According to the HSAB concept, hard electrophiles react faster and form stronger bonds with hard nucleophiles, whereas soft electrophiles react faster and form stronger bonds with soft nucleophiles.

Based on their LUMO values, oxidized quercetin is a softer electrophile than oxidized monoHER. The reaction of GSH with both oxidized monoHER and quercetin is a Michael addition in which GSH acts as a nucleophile. The reaction with ascorbate is a redox reaction in which ascorbate finally donates two electrons to the oxidized products. GSH is a relatively soft nucleophile (HOMO value

of -1.35 kJ/mol) compared to ascorbate (HOMO value of -394 kJ/mol). This can explain the preferential reaction of the soft electrophile, oxidized quercetin, with thiols over ascorbate. Oxidized monoHER, on the other hand, is a harder electrophile than oxidized quercetin explaining its preference for the harder nucleophile ascorbate over GSH. Moreover, as depicted in Figure 6A, the active part of ascorbate can approach the active part of oxidized monoHER by a hydrogen bond and a π-π interaction between ascorbate and the ortho-quinone. The reaction between oxidized monoHER and ascorbate is presented step by step in Figure 6B.

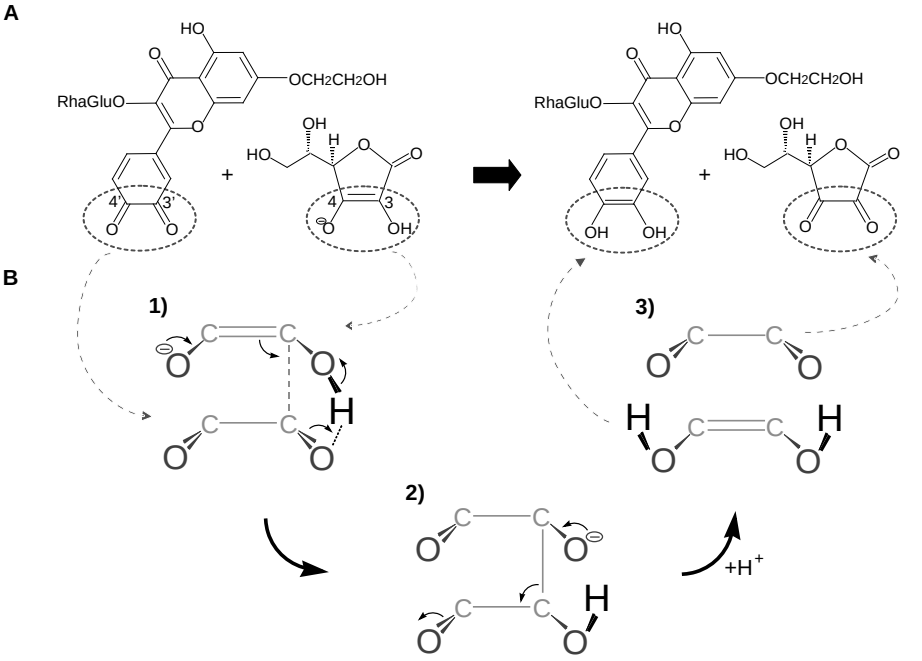

Figure 6. Chemical reaction of oxidized monoHER with ascorbate. (A) Chemical structure of oxidized monoHER (left) and ascorbate (right). The active part of ascorbate and the active part of oxidized monoHER are indicated by the dotted ellipses. (B) Suggested route for the reaction of oxidized monoHER with ascorbate. Only the active parts are shown to illustrate the suggested mechanism more clearly. (1) The active part of ascorbate (top) approaches the active part of oxidized monoHER (bottom) due to a π-π interaction and a hydrogen bond. The π-electrons of ascorbate are used to create a new bond. The C3 of ascorbate will most likely attack the C3' of the monoHER quinone because it is more electron deficient than the C4' according to Spartan '06. (2) After the attack, a transition state, with an *sp3* bond between ascorbate and oxidized monoHER, is suggested to be formed. (3) This intermediate rapidly decomposes into monoHER and oxidized ascorbate. The driving force of this reaction is the restoration of the highly conjugated π-system of monoHER.

Based on our findings, the following concept is proposed. Flavonoids easily pick up the reactivity of radicals due to their superior scavenging activity. This reactivity is directed in different ways by the two flavonoids studied (Figure 7). Quercetin directs this reactivity towards thiols. Conjugation of oxidized quercetin with GSH is primarily a cellular defense mechanism to alleviate the harmful consequences of the reactive quinone metabolite (O'Brien, 1991). However, this will reduce GSH levels and thus weaken the endogenous antioxidant network. Moreover, in e.g. blood plasma, where GSH is practically absent, or when GSH has been depleted, oxidized quercetin will react with protein thiols. This causes toxicity such as increased membrane permeability (Yen *et al.*, 2003) or impaired functioning of enzymes that contain a critical thiol-group (Kalyanaraman *et al.*, 1987; Moore *et al.*, 1988). In contrast to quercetin, monoHER preferentially directs its acquired reactivity towards ascorbate. In human blood plasma, oxidized monoHER, contrary to oxidized quercetin, does not react with plasma protein thiols. Ascorbate present in plasma reduces oxidized monoHER to the parent compound and prevents that oxidized monoHER reacts with thiols. The oxidized ascorbate formed in this recycling of monoHER can also be regenerated in the network, e.g. by dehydroascorbate reductase that uses NADH as cofactor. In this way, the reactivity is completely neutralized and the antioxidant network is restored. Thus, the advantage of monoHER is that it can function as a catalyst that safely channels the reactivity of radicals into the endogenous antioxidant network. This advantage might have been involved in the superior effect of monoHER over other structurally related flavonoids (van Acker *et al.*, 1993) in our screening procedure for protection against doxorubicin-induced cardiotoxicity. To conclude, our study demonstrates that structurally related flavonoids, belonging to the same subgroup and displaying a comparable radical scavenging activity, can have a different impact on health.

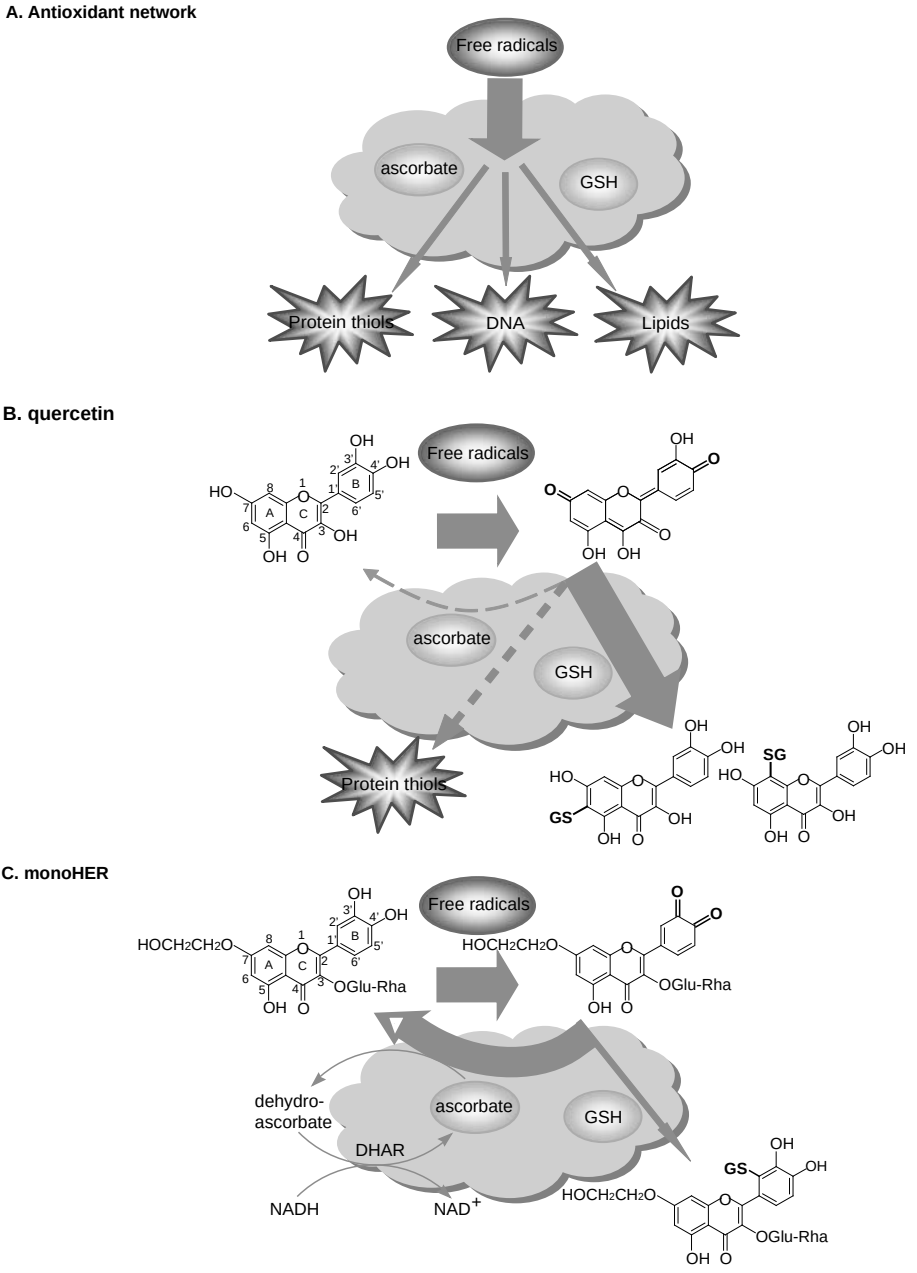

Figure 7. Interplay of monoHER and quercetin with the endogenous antioxidant network. (A) Schematic representation of the endogenous antioxidant network. Free radicals are scavenged by antioxidants in the network, such as GSH and ascorbate. In this way, free radicals are neutralized. Free radicals that are not neutralized can damage e.g. proteins, lipids and DNA. (B) The flavonoid quercetin is an excellent radical scavenger. During the scavenging of free radicals quercetin becomes oxidized. After oxidation of quercetin, four tautomeric forms of the oxidation product can

be formed. In the figure the tautomer which has an abundance of more than 99% is shown. When ascorbate and GSH are present in the same concentration, oxidized quercetin reacts much faster with GSH than with ascorbate, thereby forming 6-GSH-quercetin and 8-GSH-quercetin. Because of its high reactivity towards thiols, oxidized quercetin is also prone to react with protein thiols, as was seen in human blood plasma. This reaction of oxidized quercetin is not prevented by ascorbate and can lead to toxicity. (C) The oxidation product formed out of monoHER is an ortho-quinone. Ascorbate recycles this oxidation product to the parent compound monoHER, while GSH forms a conjugate with oxidized monoHER, i.e. 2'-GSH-monoHER. When both compounds are present in the same concentration, oxidized monoHER reacts rather with ascorbate (73%) than with GSH (27%). The oxidized ascorbate formed in this recycling can be regenerated in the network, e.g. by dehydroascorbate reductase (DHAR) that uses NADH as cofactor. Thus, the advantage of monoHER is that it can safely channel the non-specific reactivity of radicals toward ascorbate, which can be regenerated in the antioxidant network.

References

Amic D, Davidovic-Amic D, Beslo D, Rastija V, Lucic B, Trinajstic N (2007) SAR and QSAR of the antioxidant activity of flavonoids. *Curr Med Chem* **14:** 827-845

Bast A, Haenen GR (2002) The toxicity of antioxidants and their metabolites. *Environmental Toxicology and Pharmacology* **11:** 251-258

Bast A, Haenen GR, Doelman CJ (1991) Oxidants and antioxidants: state of the art. *Am J Med* **91:** 2S-13S

Boots AW, Haenen GR, Bast A (2008) Health effects of quercetin: from antioxidant to nutraceutical. *Eur J Pharmacol* **585:** 325-337

Boots AW, Kubben N, Haenen GR, Bast A (2003) Oxidized quercetin reacts with thiols rather than with ascorbate: implication for quercetin supplementation. *Biochem Biophys Res Commun* **308:** 560-565

Boots AW, Li H, Schins RP, Duffin R, Heemskerk JW, Bast A, Haenen GR (2007) The quercetin paradox. *Toxicol Appl Pharmacol* **222:** 89-96

Bowry VW, Ingold KU, Stocker R (1992) Vitamin E in human low-density lipoprotein. When and how this antioxidant becomes a pro-oxidant. *Biochem J* **288 (Pt 2):** 341-344

Brubacher D, Moser U, Jordan P (2000) Vitamin C concentrations in plasma as a function of intake: a meta-analysis. *Int J Vitam Nutr Res* **70:** 226-237

Bruynzeel AM, Niessen HW, Bronzwaer JG, van der Hoeven JJ, Berkhof J, Bast A, van der Vijgh WJ, van Groeningen CJ (2007) The effect of monohydroxyethylrutoside on doxorubicin-induced cardiotoxicity in patients treated for metastatic cancer in a phase II study. *Br J Cancer* **97:** 1084-1089

Formica JV, Regelson W (1995) Review of the biology of Quercetin and related bioflavonoids. *Food Chem Toxicol* **33:** 1061-1080

Galati G, Moridani MY, Chan TS, O'Brien PJ (2001) Peroxidative metabolism of apigenin and naringenin versus luteolin and quercetin: glutathione oxidation and conjugation. *Free Radic Biol Med* **30:** 370-382

Haenen GR, Bast A (2002) The use of vitamin supplements in self-medication. *Therapie* **57:** 119-122

Haenen GR, Jansen FP, Bast A (1993) The antioxidant properties of five O-(-β–Hydroxyethyl)-Rutosides of the flavonoid mixture Venoruton. *Phlebology* **Suppl.1:** 10-17

Hertog MG, Hollman PC, Katan MB, Kromhout D (1993) Intake of potentially anticarcinogenic flavonoids and their determinants in adults in The Netherlands. *Nutr Cancer* **20:** 21-29

Jacobs H, van der Vijgh WJ, Koek GH, Draaisma GJ, Moalin M, van Strijdonck GP, Bast A, Haenen GR (2009) Characterization of the glutathione conjugate of the semisynthetic flavonoid monoHER. *Free Radic Biol Med* **46:** 1567-1573

Kalyanaraman B, Premovic PI, Sealy RC (1987) Semiquinone anion radicals from addition of amino acids, peptides, and proteins to quinones derived from oxidation of catechols and catecholamines. An ESR spin stabilization study. *J Biol Chem* **262:** 11080-11087

Kuhnau J (1976) The flavonoids. A class of semi-essential food components: their role in human nutrition. *World Rev Nutr Diet* **24:** 117-191

Landis-Piwowar KR, Dou QP (2008) Polyphenols: biological activities, molecular targets, and the effect of methylation. *Curr Mol Pharmacol* **1:** 233-243

Liu HL, Jiang WB, Xie MX (2010) Flavonoids: recent advances as anticancer drugs. *Recent Pat Anticancer Drug Discov* **5:** 152-164

Meister A (1994a) Glutathione-ascorbic acid antioxidant system in animals. *J Biol Chem* **269:** 9397-9400

Meister A (1994b) Glutathione, ascorbate, and cellular protection. *Cancer Res* **54:** 1969s-1975s

Moore GA, Weis M, Orrenius S, O'Brien PJ (1988) Role of sulfhydryl groups in benzoquinone-induced Ca2+ release by rat liver mitochondria. *Arch Biochem Biophys* **267:** 539-550

Mukai K, Nishimura M, Kikuchi S (1991) Stopped-flow investigation of the reaction of vitamin C with tocopheroxyl radical in aqueous triton X-100 micellar solutions. The structure-activity relationship of the regeneration reaction of tocopherol by vitamin C. *J Biol Chem* **266:** 274-278

Niki E (1987) Interaction of ascorbate and alpha-tocopherol. *Ann N Y Acad Sci* **498:** 186-199

O'Brien PJ (1991) Molecular mechanisms of quinone cytotoxicity. *Chem Biol Interact* **80:** 1-41

Packer JE, Slater TF, Willson RL (1979) Direct observation of a free radical interaction between vitamin E and vitamin C. *Nature* **278:** 737-738

Pearson (1963) Hard and Soft Acids and Bases. *J. Am. Chem. Soc.* **85:** 3533-3539

Petruzzellis V, Troccoli T, Candiani C, Guarisco R, Lospalluti M, Belcaro G, Dugall M (2002) Oxerutins (Venoruton): efficacy in chronic venous insufficiency--a double-blind, randomized, controlled study. *Angiology* **53:** 257-263

Rathee P, Chaudhary H, Rathee S, Rathee D, Kumar V, Kohli K (2009) Mechanism of action of flavonoids as anti-inflammatory agents: a review. *Inflamm Allergy Drug Targets* **8:** 229-235

Upston JM, Terentis AC, Stocker R (1999) Tocopherol-mediated peroxidation of lipoproteins: implications for vitamin E as a potential antiatherogenic supplement. *Faseb J* **13:** 977-994

van Acker FA, van Acker SA, Kramer K, Haenen GR, Bast A, van der Vijgh WJ (2000) 7-monohydroxyethylrutoside protects against chronic doxorubicin-induced cardiotoxicity when administered only once per week. *Clin Cancer Res* **6:** 1337-1341

van Acker SA, Kramer K, Grimbergen JA, van den Berg DJ, van der Vijgh WJ, Bast A (1995) Monohydroxyethylrutoside as protector against chronic doxorubicin-induced cardiotoxicity. *Br J Pharmacol* **115:** 1260-1264

van Acker SA, Towart R, Husken BC, De Jong J, van der Vijgh WJ, Bast A (1993) The protective effect of Venoruton and its main constituents on acute doxorubicin-induced cardiotoxicity. *Phlebology* **Suppl. 1:** 31-32

Willems AM, Bruynzeel AM, Kedde MA, van Groeningen CJ, Bast A, van der Vijgh WJ (2006) A phase I study of monohydroxyethylrutoside in healthy volunteers. *Cancer Chemother Pharmacol* **57:** 678-684

Yen GC, Duh PD, Tsai HL, Huang SL (2003) Pro-oxidative properties of flavonoids in human lymphocytes. *Biosci Biotechnol Biochem* **67:** 1215-1222

Yu BP (1994) Cellular defenses against damage from reactive oxygen species. *Physiol Rev* **74:** 139-162

Chapter 5

The semisynthetic flavonoid monoHER sensitises human soft tissue sarcoma cells to doxorubicin-induced apoptosis via inhibition of nuclear factor-κB

Hilde Jacobs
Aalt Bast
Godefridus J. Peters
Wim J.F. van der Vijgh
Guido R.M.M. Haenen

British Journal of Cancer 2011; 10:437-440

Abstract

BACKGROUND: Despite therapeutic advances, the prognosis of patients with metastatic soft tissue sarcoma (STS) remains extremely poor. The results of a recent clinical phase II study, evaluating the protective effects of the semisynthetic flavonoid 7-mono-O-(β-hydroxyethyl)-rutoside (monoHER) on doxorubicin-induced cardiotoxicity, suggest that monoHER enhances the antitumour activity of doxorubicin in STSs.
METHODS: To molecularly explain this unexpected finding, we investigated the effect of monoHER on the cytotoxicity of doxorubicin, and the potential involvement of glutathione (GSH) depletion and nuclear factor-κB (NF-κB) inactivation in the chemosensitising effect of monoHER.
RESULTS: MonoHER potentiated the antitumour activity of doxorubicin in the human liposarcoma cell line WLS-160. Moreover, the combination of monoHER with doxorubicin induced more apoptosis in WLS-160 cells compared with doxorubicin alone. MonoHER did not reduce intracellular GSH levels. On the other hand, monoHER pretreatment significantly reduced doxorubicin-induced NF-κB activation.
CONCLUSION: These results suggest that reduction of doxorubicin-induced NF-κB activation by monoHER, which sensitises cancer cells to apoptosis, is involved in the chemosensitising effect of monoHER in human liposarcoma cells.

Introduction

Soft tissue sarcomas (STSs) comprise a rare and diverse group of malignancies from mesenchymal origin, accounting for ~ 1% of all adult malignancies (Jemal *et al.*, 2009). The only single agents that are consistently associated with response rates of about 25% in metastatic STS are doxorubicin and ifosfamide (Keohan and Taub, 1997; Santoro *et al.*, 1995).

In a clinical phase II study with metastatic cancer patients (Bruynzeel *et al.*, 2007), evaluating the protective effects of the semisynthetic flavonoid 7-mono-O-(β-hydroxyethyl)-rutoside (monoHER) on doxorubicin-induced cardiotoxicity (Bast *et al.*, 2007), we unexpectedly observed that of the four patients diagnosed with STS, three experienced objective remissions, whereas the fourth had stable disease. This observed 75% response rate is much better than the expected 25%. This prompted us to further study the sensitising effect of monoHER on doxorubicin-induced cytotoxicity.

MonoHER, like other flavonoids, may have an influence on the pathways that are involved in the development of resistance against doxorubicin (Kachadourian and Day, 2006; Sarkar and Li, 2007). Nuclear factor-κB (NF-κB) is one of the key factors involved in the development of chemoresistance (Baud and Karin, 2009; Karin, 2006; Sarkar and Li, 2008). It has been reported that chemotherapeutic agents, including doxorubicin, induce the activation of NF-κB in cancer cells (Chuang *et al.*, 2002), thereby inducing survival signals that inhibit apoptosis and promote cancer cell growth. Besides NF-κB activation, increased glutathione (GSH) levels in cancer cells have also been associated with multidrug resistance of many tumours, as GSH can conjugate with the chemotherapeutic agent, leading to drug inactivation and excretion (Estrela *et al.*, 2006).

Therefore, to support our clinical finding, we evaluated the effects of monoHER and doxorubicin on tumour cell growth, apoptosis, intracellular GSH levels and NF-κB activation in human STS cell lines.

Materials and methods

Cell culture and reagents

The human STS cell lines SKUT-1 (leiomyosarcoma), SKLMS-1 (leiomyosarcoma), HT-1080 (fibrosarcoma) and WLS-160 (liposarcoma) (Medical Oncology, VU University medical center, Amsterdam, The Netherlands) were cultured under standard conditions. Novartis Consumer Health (Nyon, Switzerland) kindly provided 7-mono-O-(β-hydroxyethyl)-rutoside (monoHER). From Sigma (St Louis, MO, USA), L-buthionine (SR)-sulphoximine (BSO) was purchased and doxorubicin HCl (2 mg ml^{-1}) was obtained from Pharmacia Upjohn BV (Woerden, the Netherlands). All other chemicals were of analytical grade.

Cell growth inhibition by sulphorhodamine B assay

The human STS cell lines were either untreated or pretreated with 50 μM monoHER. After 1 h incubation, medium was removed and replaced with fresh medium containing different concentrations of doxorubicin (0.001-10 μM). After 72 h of incubation, cell viability was examined by the sulphorhodamine B assay (Vichai and Kirtikara, 2006).

Caspase-3/7 assay for detecting apoptosis

WLS-160 cells were either untreated or pretreated with 50 μM monoHER for 1 h, and then exposed to 10 μM doxorubicin for an additional 6 h. After treatment, activation of caspase-3/7 was quantified by the Caspase-Glo 3/7 assay kit (Promega Corporation, Madison, WI, USA).

Measurement of intracellular GSH

WLS-160 cells were incubated with 50 μM monoHER or 50 μM BSO for 1, 6 or 24 h. After incubation, cells were washed with PBS, harvested by treatment with trypsin-EDTA (Gibco, Paisley, UK) and washed again with ice-cold PBS (Gibco). After centrifugation, cells were resuspended in ice-cold extraction buffer (0.1% Triton X-100 and 0.6% SSA, Sigma) and sonicated in icy water for 2-3 min. The extracts were used for determination of intracellular GSH using an enzymatic recycle method (Rahman *et al.*, 2006).

Nuclear factor-κB measurement

WLS-160 cells were treated with 10 μM doxorubicin for 1.5, 3, 6 or 24 h. In another experiment, the cells were either untreated or pretreated for 1 h with 50 μM monoHER before doxorubicin exposure (10 μM; 6 h). Nuclear factor-κB expression was determined in nuclear extracts of the cells (Hofmann *et al.*, 1999) using the TransAM NF-κB p50 transcription factor assay kit (Active Motif, Rixensart, Belgium). Protein concentrations were determined using the method of Bradford (Biorad, Veenendaal, The Netherlands).

Statistical analysis

All experiments were performed, at least, in triplicate. Results are given as mean ± s.d. or as a typical example. The statistical significance of the differences between experimental groups and controls was determined by Student's *t*-test. P-values ≤ 0.05 were considered statistically significant.

Results

As shown in Table 1, monoHER pretreatment did not significantly influence the antitumour activity of doxorubicin in SKUT-1, SKLMS-1 and HT-1080 cells. However, pretreatment of the liposarcoma cell line, WLS-160, with 50 μM monoHER for 1 h before doxorubicin exposure shifted the growth inhibition curve of doxorubicin to the left (Figure 1A). MonoHER alone did not affect tumour growth. These results indicate that monoHER potentiated the antitumour activity of doxorubicin in WLS-160 cells.

Table 1. IC_{50} values (μM) of growth inhibition by doxorubicin[a]

Human STS cell line	Doxorubicin	Doxorubicin + monoHER
SKLMS-1	0.063 ± 0.009	0.066 ± 0.007
SKUT-1	0.048 ± 0.008	0.045 ± 0.009
HT-1080	0.024 ± 0.005	0.027 ± 0.006
WLS-160	0.016 ± 0.003	0.0075 ± 0.001*

Abbreviations: IC_{50} = inhibitory concentration 50%; monoHER = 7-mono-O-(β-hydroxyethyl)-rutoside, [a] Data are expressed as mean ± s.d. * P ≤ 0.05.

The effect of monoHER on doxorubicin-induced apoptosis in WLS-160 cells as assessed by caspase-3/7 activation is shown in Figure 1B. Doxorubicin treat-

ment (10 µM; 6 h) strongly induced caspase-3/7 activity. Pretreatment of the cells with 50 µM monoHER for 1 h before doxorubicin exposure significantly enhanced the doxorubicin-induced caspase-3/7 activation. MonoHER alone had no effect on caspase-3/7 activity. These findings indicate that monoHER sensitised these cancer cells to doxorubicin-induced apoptosis.

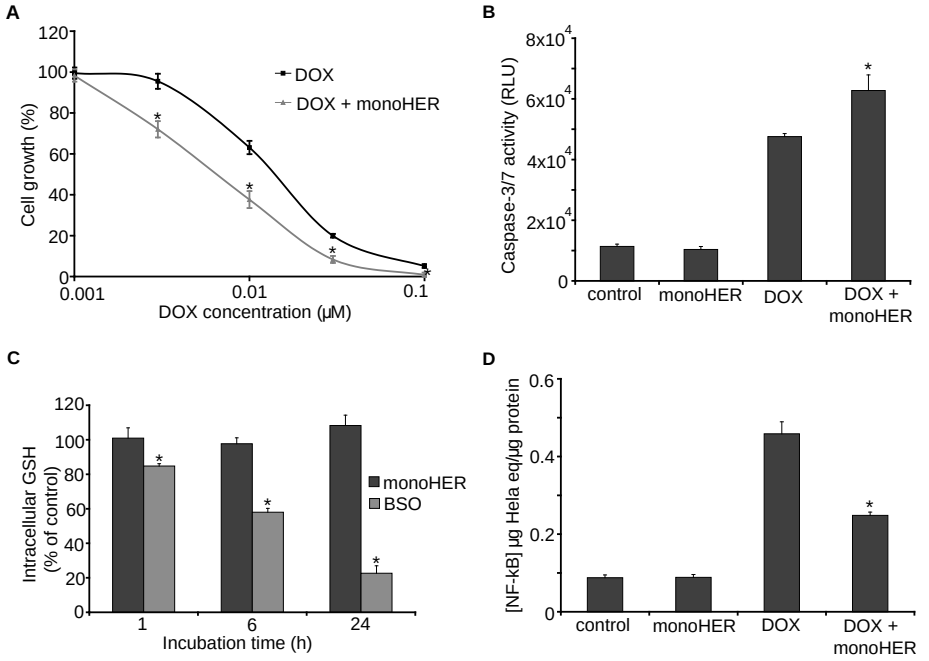

Figure 1. Effect of the semisynthetic flavonoid monoHER on the cytotoxic effects of doxorubicin in the liposarcoma cell line WLS-160. **(A)** MonoHER pretreatment (50 µM; 1 h) significantly enhances the cell growth inhibition induced by doxorubicin (0.001-0.1 µM; 72 h) (mean ± s.d. *P≤0.05 compared with doxorubicin treatment). **(B)** MonoHER pretreatment (50 µM; 1 h) significantly enhances the apoptosis induced by doxorubicin (10 µM; 6 h) (mean ± s.d. *P≤0.05 compared with doxorubicin treatment). Relative light units (RLUs); doxorubicin (DOX). **(C)** MonoHER treatment (50 µM; 1, 6 and 24 h) has no effect on the intracellular GSH concentration, whereas BSO (50 µM; 1, 6 and 24 h) reduces GSH levels in a time-dependent manner (mean ± s.d. *P≤0.05 compared with control). **(D)** MonoHER pretreatment (50 µM; 1 h) significantly prevents doxorubicin-induced (10 µM; 6 h) NF-κB activation (mean ± s.d. *P≤0.05 compared with doxorubicin treatment).

As shown in Figure 1C, treatment of WLS-160 cells with 50 µM monoHER for 1, 6 or 24 h did not affect intracellular GSH levels. In contrast, the GSH synthesis inhibitor BSO induced a time-dependent GSH depletion in WLS-160 cells. Moreover, BSO also enhanced the antitumour activity of doxorubicin (data not shown). These results indicate that intracellular GSH depletion can sensitise

WLS-160 cells to doxorubicin-induced apoptosis. However, this mechanism is not involved in the chemosensitising effects of monoHER.

Doxorubicin treatment (10 μM; 1.5, 3, 6 and 24 h) significantly induced NF-κB DNA-binding activity in WLS-160 cells compared with untreated controls. Within the measured time range, NF-κB activation was maximal at 6 h of drug exposure (data not shown). Figure 1D shows that pretreatment of cells with 50 μM monoHER for 1 h before 6 h of doxorubicin exposure significantly reduced doxorubicin-induced activation of NF-κB. MonoHER alone had no effect on the basal NF-κB level in WLS-160 cells. These results suggest that reduction of doxorubicin-induced NF-κB activation might be involved in the sensitising effect of monoHER on the antitumour effect of doxorubicin.

Discussion

In this paper, we show that monoHER can enhance the cytotoxicity of doxorubicin, possibly via modulation of NF-κB.

Four different human STS cell lines were investigated. Only in the liposarcoma cell line, WLS-160, pretreatment with monoHER resulted in a significantly greater inhibition of cancer cell growth. This different response on monoHER pretreatment between the different cell lines is possibly because of the known large diversity in STS and the subsequent response to chemotherapy (Van Glabbeke *et al.*, 1999; Verweij, 2009). The molecular mechanism behind the observed sensitising effect of monoHER in the responding liposarcoma cell line, WLS-160, was further explored.

First, we investigated how cytotoxicity of doxorubicin and the chemosensitising effect of monoHER were mediated. Doxorubicin as a single agent activated caspase-3/7 activity and thus induced apoptosis in WLS-160 cells. Pretreatment of these cells with monoHER resulted in a significantly greater induction of apoptosis. These results suggest that the greater degree of cancer cell death by the combination of monoHER with doxorubicin is mediated by the induction of an apoptotic pathway.

As multidrug resistance of many cancer cells is associated with increased intracellular GSH levels, GSH depletion is a potential strategy to sensitise tumour cells to chemotherapeutics and modify drug resistance (Estrela *et al.*, 2006; Meister, 1991). This can be achieved by inhibitors of GSH synthesis such as BSO, a selective and irreversible inhibitor of γ-glutamylcysteine synthase, the rate limiting enzyme of GSH synthesis (Han and Park, 2009). As also shown by our results, BSO efficiently enhances the effect of several chemotherapeutic drugs

including doxorubicin (Vanhoefer *et al.*, 1996). In addition, some flavonoids can also deplete GSH levels in cancer cells, thereby sensitising these cancer cells to chemotherapy (Kachadourian and Day, 2006; Kachadourian *et al.*, 2007; Ramos and Aller, 2008). Because monoHER is able to form a GSH-monoHER adduct that might deplete cells from GSH (Jacobs *et al.*, 2009), we examined whether monoHER can deplete GSH in WLS-160 cells. However, in contrast to BSO, monoHER did not significantly change GSH levels in WLS-160 cells, suggesting that the growth-inhibitory effect of monoHER is not mediated via GSH depletion.

Another crucial factor involved in drug resistance is NF-κB, an inducible and ubiquitously expressed transcription factor that regulates cell survival, inflammation and differentiation (Karin, 2006). Many chemotherapeutic agents induce the activity of NF-κB, which causes drug resistance in cancer cells (Sarkar and Li, 2008). Because doxorubicin rapidly induced NF-κB activity in WLS-160 cells within 6 h, inhibition of NF-κB was expected to enhance the antitumour activity of doxorubicin, similar to several *in vitro* and preclinical *in vivo* studies in which the regulation of NF-κB enhanced the efficacy of chemotherapy (Bava *et al.*, 2005; Li *et al.*, 2005; Nakanishi and Toi, 2005; Sung *et al.*, 2007). Our results show that monoHER prevented the NF-κB induction by doxorubicin in WLS-160 cells, suggesting that downregulation of NF-κB activation by monoHER may be responsible for the sensitisation of these cancer cells to doxorubicin. Figure 2 further illustrates this mechanism.

In conclusion, monoHER enhanced the cytotoxicity of doxorubicin in the human liposarcoma cell line WLS-160. This potentiation was not mediated by GSH depletion, but monoHER reduced doxorubicin-induced NF-κB activation, thereby sensitising tumour cells to apoptosis. Thus, the high response rate in the clinical phase II study may be mediated by reduction of doxorubicin-induced NF-κB activation. For certain STS patients, monoHER might improve chemotherapy and even decrease systemic toxicity. Moreover, monoHER might also be valuable for the treatment of other tumours that have developed chemoresistance through NF-κB activation. However, future studies are needed to further elucidate the value of adding monoHER to the chemotherapeutic treatment with doxorubicin.

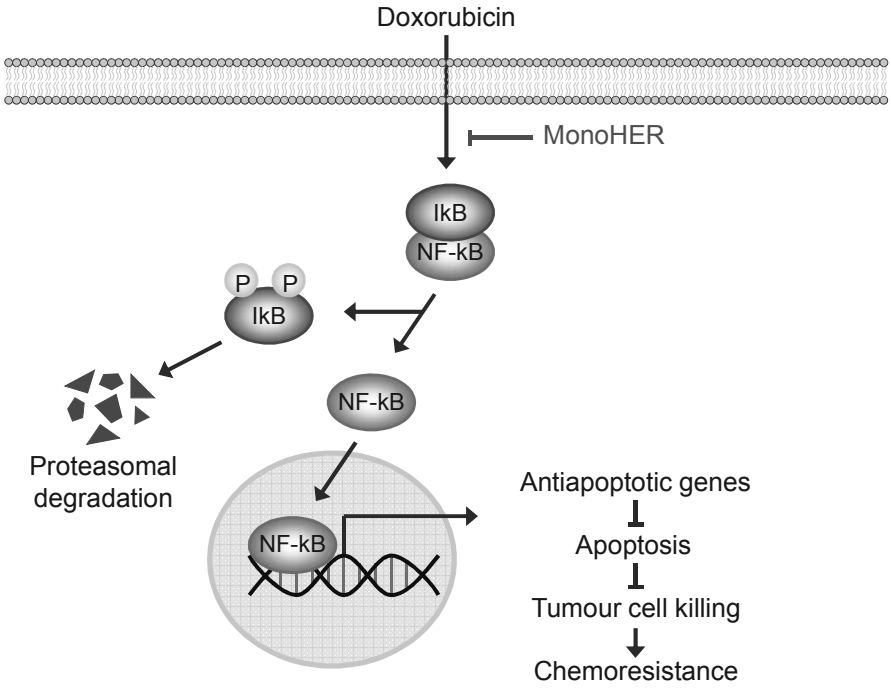

Figure 2. Suggested pathway illustrating the influence of monoHER on doxorubicin cytotoxicity in WLS-160 cells. Under resting conditions, NF-κB is maintained in an inactive state in the cytoplasm via interaction with the inhibitory protein, IκB. Doxorubicin can activate the NF-κB pathway, which involves the phosphorylation, ubiquitination and proteasomal degradation of IκB. Nuclear factor-κB is then free to translocate to the nucleus where it facilitates the transcription of, for example, antiapoptotic genes, resulting in less tumour cell killing and the development of drug resistance. MonoHER is able to reduce this doxorubicin-induced NF-κB activation, thereby sensitising WLS-160 cells to doxorubicin-induced apoptosis.

References

Bast A, Haenen GR, Bruynzeel AM, Van der Vijgh WJ (2007) Protection by flavonoids against anthracycline cardiotoxicity: from chemistry to clinical trials. *Cardiovasc Toxicol* **7:** 154-159

Baud V, Karin M (2009) Is NF-kappaB a good target for cancer therapy? Hopes and pitfalls. *Nat Rev Drug Discov* **8:** 33-40

Bava SV, Puliappadamba VT, Deepti A, Nair A, Karunagaran D, Anto RJ (2005) Sensitization of taxol-induced apoptosis by curcumin involves down-regulation of nuclear factor-kappaB and the serine/threonine kinase Akt and is independent of tubulin polymerization. *J Biol Chem* **280:** 6301-6308

Bruynzeel AM, Niessen HW, Bronzwaer JG, van der Hoeven JJ, Berkhof J, Bast A, van der Vijgh WJ, van Groeningen CJ (2007) The effect of monohydroxyethylrutoside on doxorubicin-induced cardiotoxicity in patients treated for metastatic cancer in a phase II study. *Br J Cancer* **97:** 1084-1089

Chuang SE, Yeh PY, Lu YS, Lai GM, Liao CM, Gao M, Cheng AL (2002) Basal levels and patterns of anticancer drug-induced activation of nuclear factor-kappaB (NF-kappaB), and its attenuation by tamoxifen, dexamethasone, and curcumin in carcinoma cells. *Biochem Pharmacol* **63:** 1709-1716

Estrela JM, Ortega A, Obrador E (2006) Glutathione in cancer biology and therapy. *Crit Rev Clin Lab Sci* **43:** 143-181

Han YH, Park WH (2009) The effects of N-acetyl cysteine, buthionine sulfoximine, diethyldithiocarbamate or 3-amino-1,2,4-triazole on antimycin A-treated Calu-6 lung cells in relation to cell growth, reactive oxygen species and glutathione. *Oncol Rep* **22:** 385-391

Hofmann MA, Schiekofer S, Isermann B, Kanitz M, Henkels M, Joswig M, Treusch A, Morcos M, Weiss T, Borcea V, Abdel Khalek AK, Amiral J, Tritschler H, Ritz E, Wahl P, Ziegler R, Bierhaus A, Nawroth PP (1999) Peripheral blood mononuclear cells isolated from patients with diabetic nephropathy show increased activation of the oxidative-stress sensitive transcription factor NF-kappaB. *Diabetologia* **42:** 222-232

Jacobs H, van der Vijgh WJ, Koek GH, Draaisma GJ, Moalin M, van Strijdonck GP, Bast A, Haenen GR (2009) Characterization of the glutathione conjugate of the semisynthetic flavonoid monoHER. *Free Radic Biol Med* **46:** 1567-1573

Jemal A, Siegel R, Ward E, Hao Y, Xu J, Thun MJ (2009) Cancer statistics, 2009. *CA Cancer J Clin* **59:** 225-249

Kachadourian R, Day BJ (2006) Flavonoid-induced glutathione depletion: potential implications for cancer treatment. *Free Radic Biol Med* **41:** 65-76

Kachadourian R, Leitner HM, Day BJ (2007) Selected flavonoids potentiate the toxicity of cisplatin in human lung adenocarcinoma cells: a role for glutathione depletion. *Int J Oncol* **31:** 161-168

Karin M (2006) Nuclear factor-kappaB in cancer development and progression. *Nature* **441:** 431-436

Keohan ML, Taub RN (1997) Chemotherapy for advanced sarcoma: therapeutic decisions and modalities. *Semin Oncol* **24:** 572-579

Li Y, Ahmed F, Ali S, Philip PA, Kucuk O, Sarkar FH (2005) Inactivation of nuclear factor kappaB by soy isoflavone genistein contributes to increased apoptosis induced by chemotherapeutic agents in human cancer cells. *Cancer Res* **65:** 6934-6942

Meister A (1991) Glutathione deficiency produced by inhibition of its synthesis, and its reversal; applications in research and therapy. *Pharmacol Ther* **51:** 155-194

Nakanishi C, Toi M (2005) Nuclear factor-kappaB inhibitors as sensitizers to anticancer drugs. *Nat Rev Cancer* **5:** 297-309

Rahman I, Kode A, Biswas SK (2006) Assay for quantitative determination of glutathione and glutathione disulfide levels using enzymatic recycling method. *Nat Protoc* **1:** 3159-3165

Ramos AM, Aller P (2008) Quercetin decreases intracellular GSH content and potentiates the apoptotic action of the antileukemic drug arsenic trioxide in human leukemia cell lines. *Biochem Pharmacol* **75:** 1912-1923

Santoro A, Tursz T, Mouridsen H, Verweij J, Steward W, Somers R, Buesa J, Casali P, Spooner D, Rankin E, et al. (1995) Doxorubicin versus CYVADIC versus doxorubicin plus ifosfamide in first-line treatment of advanced soft tissue sarcomas: a randomized study of the European Organization for Research and Treatment of Cancer Soft Tissue and Bone Sarcoma Group. *J Clin Oncol* **13:** 1537-1545

Sarkar FH, Li Y (2008) NF-kappaB: a potential target for cancer chemoprevention and therapy. *Front Biosci* **13:** 2950-2959

Sarkar FH, Li YW (2007) Targeting multiple signal pathways by chemopreventive agents for cancer prevention and therapy. *Acta Pharmacol Sin* **28:** 1305-1315

Sung B, Pandey MK, Aggarwal BB (2007) Fisetin, an inhibitor of cyclin-dependent kinase 6, down-regulates nuclear factor-kappaB-regulated cell proliferation, antiapoptotic and metastatic gene products through the suppression of TAK-1 and receptor-interacting protein-regulated IkappaBalpha kinase activation. *Mol Pharmacol* **71:** 1703-1714

Van Glabbeke M, van Oosterom AT, Oosterhuis JW, Mouridsen H, Crowther D, Somers R, Verweij J, Santoro A, Buesa J, Tursz T (1999) Prognostic factors for the outcome of chemotherapy in advanced soft tissue sarcoma: an analysis of 2,185 patients treated with anthracycline-containing first-line regimens--a European Organization for Research and Treatment of Cancer Soft Tissue and Bone Sarcoma Group Study. *J Clin Oncol* **17:** 150-157

Vanhoefer U, Cao S, Minderman H, Toth K, Skenderis BS, 2nd, Slovak ML, Rustum YM (1996) d,l-buthionine-(S,R)-sulfoximine potentiates in vivo the therapeutic efficacy of doxorubicin against multidrug resistance protein-expressing tumors. *Clin Cancer Res* **2:** 1961-1968

Verweij J (2009) Soft tissue sarcoma trials: one size no longer fits all. *J Clin Oncol* **27:** 3085-3087

Vichai V, Kirtikara K (2006) Sulforhodamine B colorimetric assay for cytotoxicity screening. *Nat Protoc* **1:** 1112-1116

Chapter 6

Identification of the metabolites of the antioxidant flavonoid 7-mono-O-(β-hydroxyethyl)-rutoside in mice

Hilde Jacobs
Ron Peters
Gertjan J.M. den Hartog
Wim J.F. van der Vijgh
Aalt Bast
Guido R.M.M. Haenen

Drug Metabolism and Disposition 2011; 39:750-756

Abstract

The clinical use of the anticancer drug doxorubicin is limited by severe cardiotoxicity. In mice, the semisynthetic antioxidant flavonoid 7-mono-O-(β-hydroxyethyl)-rutoside (monoHER) has been successfully used as a protector against doxorubicin-induced cardiotoxicity. However, most monoHER has already been cleared from the body at the time that doxorubicin concentrations are still high. This result suggests that not only the parent compound monoHER itself but also monoHER metabolites could be responsible for the observed cardioprotective effects in mice. Therefore, in the present study, we investigated the metabolism of monoHER in mice. Mice were administered 500 mg/kg monoHER intraperitoneally. At different time points after monoHER administration, bile was collected and analyzed for the presence of monoHER metabolites. The formed metabolites were identified by liquid chromatography-diode array detection-time of flight-mass spectrometry. Thirteen different metabolites were identified. The observed routes of monoHER metabolism are methylation, glucuronidation, oxidation of its hydroxyethyl group, GSH conjugation, and hydrolysis of its disaccharide. In line with other flavonoids, methylated monoHER and the monoHER glucosides are expected to have relatively high cellular uptake and low clearance from the body. Therefore, these metabolites might contribute to the observed protection of monoHER against doxorubicin-induced cardiotoxicity.

Introduction

Doxorubicin is a very effective antitumor agent, widely used in the treatment of different types of cancer. Unfortunately, treatment with doxorubicin is limited by a cumulative dose-dependent cardiotoxicity, which manifests itself as congestive heart failure (Bast *et al.*, 2007; Lipshultz *et al.*, 2005; Singal and Iliskovic, 1998). Although the mechanism of doxorubicin-induced cardiotoxicity is still not fully understood, the formation of free radicals by doxorubicin semiquinones seems to be implicated (Horenstein *et al.*, 2000; Xu *et al.*, 2001). Cardiac tissue is particularly vulnerable to free radical-induced injury because its antioxidant protection by enzymes such as superoxide dismutase and catalase is markedly reduced compared with that of other tissues in the body (Doroshow *et al.*, 1980; Iarussi *et al.*, 2000; Julicher *et al.*, 1988).

The semisynthetic flavonoid 7-mono-O-(β-hydroxyethyl)-rutoside (monoHER) is a constituent of the registered drug Venoruton, which is used in the treatment of chronic venous insuffiency (Petruzzellis *et al.*, 2002). In a series of structurally related flavonoids, monoHER was found to be the most potent antioxidant (Haenen *et al.*, 1993). As for most flavonoids, monoHER consists of three rings referred to as the A, B and C rings (Figure 1). It also contains a 3',4'-catechol moiety in the B ring and a C2-C3 double bond and 4-oxo function in the C ring, which contribute to its high antioxidant activity. Further characteristic structural features of monoHER are the rutinose group (glucose + rhamnose) at the 3-O position in the C ring and the hydroxyethyl group at the 7-O position in the A ring.

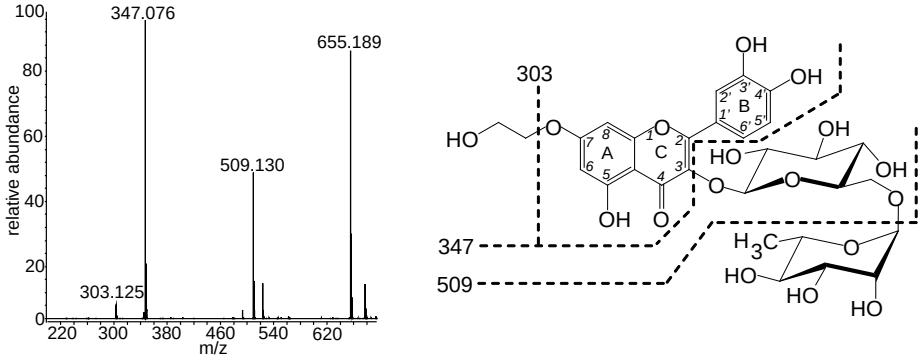

Figure 1. Structural formula of monoHER, including its fragmentation as shown by its mass spectrum obtained by tandem mass spectrometry.

Preclinical experiments in mice have shown that monoHER administration before doxorubicin effectively protects against doxorubicin-induced cardiotoxicity, without interfering with its antitumor activity (van Acker *et al.*, 2000; van Acker *et al.*, 1997). Of interest, the half-lives of monoHER in plasma and heart tissue (11.8 and 16.2 min, respectively) are much lower than those of doxorubicin (12.6 and 11.5 h, respectively) (Abou El Hassan *et al.*, 2003a; Abou El Hassan *et al.*, 2003b). In addition, monoHER cannot be detected for longer than 2 h after administration, whereas doxorubicin is present in plasma for at least 48 h after administration. This result means that monoHER has already been cleared from the body at the time that doxorubicin concentrations are still relatively high and suggests that not only the parent compound monoHER itself but also monoHER metabolites might be responsible for the observed cardioprotective effects in mice. Moreover, evidence with other polyphenols that metabolites may mediate or substantially contribute to the pharmacological efficacy of the parent molecule is accumulating, as is observed with flavonoids in grapes and wine (Forester and Waterhouse, 2009; Gescher and Steward, 2003). Therefore, identifying the metabolites of compounds is of great importance. Up to the present no metabolites were found in plasma or urine from mice and humans in our studies with monoHER (Abou El Hassan *et al.*, 2003b; Willems *et al.*, 2006). Earlier studies with radiolabeled monoHER in mice and rats reported that the liver was the main drug-eliminating organ. A major unidentified metabolite was found in bile, which was suggested to be a glucuronide of monoHER (Barrow and Griffiths, 1974; Hackett and Griffiths, 1977a). In addition, enterohepatic cycling has been described previously (Hackett and Griffiths, 1977b).

To further elucidate the protective effect of monoHER, the objective of this study was to investigate the metabolism of monoHER in mice and characterize its metabolites. This was realized by analyzing the bile fluid of mice that received monoHER for the presence of monoHER and possible monoHER metabolites using LC-DAD-TOF-MS analysis.

Materials and methods

Chemicals

7-Mono-O-(β-hydroxyethyl)-rutoside was provided by Novartis Consumer Health (Nyon, Switzerland). MonoHER was dissolved in 36 mM NaOH in sterile water, giving a final concentration of 33 mg/ml. Catechol-*O*-methyltransferase (COMT), S-adenosyl-L-methionine (SAM), dithiothreitol, and $MgCl_2$ were ob-

tained from Sigma-Aldrich (St. Louis, MO). Trifluoroacetic acid (TFA) and NaOH were purchased from Sigma-Aldrich (Steinheim, Germany). Acetonitrile HPLC grade, methanol, and dimethyl sulfoxide were obtained from Biosolve (Valkenswaard, The Netherlands).

Animals

Eighteen male BALB/c mice (8 weeks old, 20-25 g) purchased from Charles River (Maastricht, The Netherlands) were kept in a light- and temperature-controlled room (21-22 °C, humidity 60-65%). The animals were fed a standard diet and were allowed to eat and drink tap water ad libitum. The animals were allowed to adapt to the laboratory housing conditions for at least 1 week before the experiment was started.

Experimental design

The protocol was approved by the Ethics Committee for Animal Experiments of Maastricht University (Maastricht, The Netherlands). The mice were administered 500 mg/kg monoHER intraperitoneally. At different time points after monoHER administration (15, 60, 120, 180, and 240 min), three mice were sacrificed, and the gallbladder was collected. One group of mice received no monoHER; the bile of these mice served as a blank. Immediately after collection, the gallbladder was transferred into polypropylene micro-test tubes and frozen at - 80°C until analysis.

Sample preparation

Each gallbladder was perforated and mixed with 50 µl of dimethyl sulfoxide-methanol (1:4, v/v). The mixture was vortexed and centrifuged (17060g, 15 min). The supernatant was removed and injected onto the LC column.

LC-DAD analysis

LC-DAD of the bile samples was performed on an Agilent 1100 series LC-DAD system (Agilent Technologies, Santa Clara, CA). Analytical separations were achieved using an ODS-3 column (5 µm, 250 x 3 mm) (Inertsil; Varian Inc., Palo Alto, CA) at 40 °C. The mobile phase consisted of ultrapure water containing 0.1% (v/v) TFA (mobile phase A) and acetonitrile containing 0.1% (v/v) TFA (mobile phase B). The gradient was started at t = 0 min with 85% (v/v) A, was changed linearly over the first 20 min to 30% (v/v) B followed by an increase to

90% (v/v) B at t = 25 min, and was then stationary for 1 min. The column was reequilibrated with 15% (v/v) B for 5 min. A flow rate of 1 ml/min and an injection volume of 10 µl were used. Detection was performed with a DAD. The chromatograms presented are based on detection at 355 nm.

LC-DAD-TOF-MS analysis

LC-DAD-TOF-MS, including fragmentation and exact mass measurements, was performed using an Agilent 1100 LC-DAD-TOF-MS system (Agilent Technologies) to further characterize the peaks in the LC chromatogram. The UV signal at 355 nm was collected. Electrospray ionization was performed in positive mode with the following conditions: *m/z* range 50 to 3000, 175 V fragmentor (varied for fragmentation experiments), 0.1 *m/z* step size, 1.013 cycles/s, 350°C drying gas temperature, 10 liters of N_2/min drying gas, 35 psig nebulizer pressure, and 2 kV capillary voltage. The MS data were collected using internal reference mass correction. The reference substances [purine at 121.050873 Da and hexakis-(1*H*,1*H*,3*H*-tetrafluoro-pentoxy)phosphazene (HP-921) at 922.009798 Da] were constantly injected in the electrospray ion source equipped with a dual-sprayer mechanism. The LC conditions were the same as described above. The LC-DAD-TOF-MS system was controlled using MassHunter qualitative analysis software (B03.01; Agilent Technologies).

Elemental composition calculations from the exact masses were performed off-line using MassHunter. This software was used to work with the spectrum manually generated for every peak. Potential assignments were calculated using the monoisotopic masses with specifications of a tolerance of 10 ppm deviation. The number and types of expected atoms were set as follows: carbons <60, hydrogens <120, oxygens <30, nitrogens <30, and sulfurs <5, whereas the double bond equivalent was set to <50.

Quantification of monoHER metabolites

Quantification of the different metabolites was achieved by their UV response at 355 nm. Quantification of metabolites is normally achieved using external calibration with reference standards. However, no commercial reference standards were available for these metabolites. Therefore, it was assumed that the UV response at 355 nm is equal to that of monoHER for all metabolites. This is a reasonable assumption because the UV spectra in the 355 nm region of all metabolites are similar to that of monoHER.

The relative amounts of the metabolites were estimated by calculating the area under the curve (AUC) from the concentration-time curve of each metabolite, using the trapezoidal rule, and expressing this as percentage of the total AUC of all detected compounds together.

Synthesis of 4'-methyl-monoHER

MonoHER was enzymatically methylated using the enzyme COMT and the methyl donor SAM. The reaction mixture for the enzymatic O-methylation of monoHER consisted of 100 µM monoHER, 20 U of COMT, 1 mM SAM, 1.2 mM $MgCl_2$, and 1 mM dithiothreitol in a final volume of 1 ml Tris-HCl buffer. The mixture was incubated at 37°C for 24 h and then analyzed by the LC-DAD procedure described above. ^{1}H NMR analysis identified the formed metabolite as 4'-methyl-monoHER. To verify the presence of 4'-methyl-monoHER in the collected bile samples, bile fluid was spiked with this metabolite and analyzed by LC-DAD.

Results

Bile samples collected after monoHER administration contain several compounds that are absent in the blank bile (Figure 2). The DAD spectra of these compounds and the absorption maxima at 355 nm are similar to those of monoHER, indicating that these compounds are metabolites of monoHER. LC-DAD-TOF-MS was used to further identify these metabolites. Six major metabolites (M1-M6), representing more than 90% of all detected compounds, and seven minor metabolites (M7-M13) were detected. The mass ($[M+H]^+$), main fragment ions, and the proposed compound name of each metabolite are listed in Table 1. In Table 2, the exact mass determination data and the corresponding chemical formulas are summarized.

Parent

The peak in the LC chromatogram with a retention time of 8.5 min elutes at the same retention time as the parent compound monoHER. LC-MS analysis revealed *m/z* of 655, which corresponds to a molecular mass of 654 Da (Table 1). Tandem mass spectrometry fragmentation produced three key fragments: *m/z* 509 (- 145, loss of rhamnose sugar), *m/z* 347 (- 307, loss of rhamnose and glucose sugar), and *m/z* 303 (- 351, loss of rhamnose, glucose, and the hydroxye-

thyl group of the A ring) (Figure 1). This fragmentation pattern is similar to the fragmentation of monoHER. In addition, the elemental composition ($C_{29}H_{34}O_{17}$) generated by exact mass measurements (Table 2) is identical to that of the parent compound, identifying this compound as monoHER.

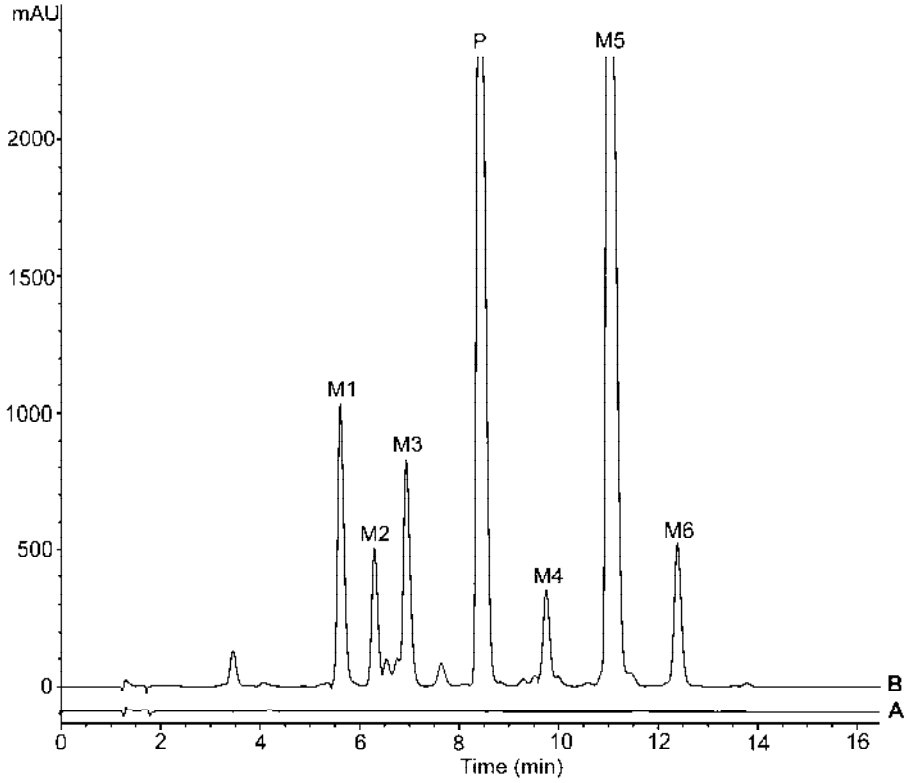

Figure 2. Representative LC chromatograms of (A) blank bile and (B) bile collected from mice 60 min after monoHER administration. The numbered peaks represent monoHER [parent (P)] and its six major metabolites (M1-M6). The chromatograms presented are based on detection at 355 nm.

Major metabolites

M1 and M2. Metabolites M1 and M2 have an *m/z* 176 Da higher than monoHER. This finding indicates that the metabolites are glucuronidated derivatives of monoHER. In addition, the fragments are similar to that of monoHER, only 176 Da higher (Table 1). The chemical formula ($C_{35}H_{42}O_{23}$) generated by exact mass measurements confirms the formation of monoHER glucuronide (Table 2).

M3. LC-MS analysis revealed that the main fragments of metabolite M3 are 14 Da higher than monoHER glucuronide (*m/z* 699, 537, 361, and 317) (Table 1).

Exact mass determination and the corresponding chemical composition ($C_{36}H_{44}O_{23}$) show the addition of a methyl group (+CH_2) to monoHER glucuronide (Table 2), identifying this peak as methyl-monoHER glucuronide.

Table 1. MonoHER and its metabolites identified in bile of mice by LC-DAD-TOF-MS.

	t_R (min)	Compound	$[M+H]^+$ (*m/z*)	Mass change from parent	Main fragment ions (*m/z*)
		Parent compound			
P	8.5	monoHER	655	0	509, 347, 303
		Major metabolites			
M1	5.6	monoHER glucuronide	831	+ 176	765, 685, 523, 347, 303
M2	6.3	monoHER glucuronide	831	+ 176	765, 685, 523, 347, 303
M3	6.9	methyl-monoHER glucuronide	845	+ 190	699, 537, 361, 317
M4	9.7	monoCER	669	+ 14	523, 463, 361
M5	11.1	methyl-monoHER	669	+ 14	523, 361, 317
M6	12.3	methyl-monoCER	683	+ 28	537, 375
		Minor metabolites			
M7	3.4	GSH-monoHER	960	+ 305	814, 705, 652, 523, 371
M8	7.1	monoHER diglucuronide	1007	+ 352	861, 845, 831, 699, 523, 347
M9	7.6	methyl-monoHEG	523	- 132	479, 361, 303
M10	7.8	monoCER glucuronide	845	+ 190	537, 361
M11	8.8	methyl-monoCER glucuronide	859	+ 204	551, 375
M12	12.5	dimethyl-monoHEG	537	- 118	375
M13	14.8	dimethyl-monoHER	683	+ 28	537, 375
		Impurities/metabolites			
M14	9.4	diHER	699	+ 44	655, 523, 347
M15	12.5	triHER	743	+ 88	622, 597, 435, 347
M16	13.3	methyl-diHER	713	+ 58	537, 361
M17	14.8	dimethyl-diHER	727	+ 72	537, 439, 361

M4. The main fragments of metabolite M4 are 14 Da higher than monoHER (*m/z* 523 and 361) (Table 1). The chemical formula ($C_{29}H_{32}O_{18}$) indicates that this metabolite has two hydrogen atoms less and one oxygen atom more (-H_2 + O) than monoHER (Table 2). This finding points to the oxidation of the hydroxyethyl group in the A ring of monoHER to a carboxyethyl group, thereby generating 7-mono-O-(β-carboxyethyl)-rutoside (monoCER).

M5. Metabolite M5 shows main fragments similar to monoHER, only 14 Da higher (*m/z* 523, 361, and 317) (Table 1). On the basis of the mass spectral data and the chemical formula ($C_{30}H_{36}O_{17}$), this metabolite was identified as the me-

thylated metabolite of monoHER (Table 2). Moreover, the peak area of M5 in the chromatogram increased after the bile sample was spiked with enzymatically synthesized 4'-methyl-monoHER.

M6. Metabolite M6 has an *m/z* 28 Da higher than monoHER (Table 1). From its chemical formula ($C_{30}H_{34}O_{18}$) it was deduced that the hydroxyethyl group in the A ring was oxidized together with the methylation of one of the hydroxyl groups of the catechol of monoHER (Table 2). This metabolite was therefore identified as methyl-monoCER.

Minor metabolites

M7. LC-MS analysis of metabolite M7 shows an *m/z* 305 Da higher than monoHER, which is indicative of GSH conjugation (Table 1). The peak area of M7 in the chromatogram increased after the bile sample was spiked with the synthetic reference standard, 2'-GSH-monoHER (Jacobs *et al.*, 2009), identifying the peak as such.

M8. Metabolite M8 shows an *m/z* 352 (or 2 x 176) Da higher than the parent compound (Table 1). This indicates the addition of two glucuronic acid groups to monoHER and identifies this metabolite as monoHER diglucuronide.

M9. Metabolite M9 shows an *m/z* 146 Da lower than methylated monoHER (Table 1). The chemical formula ($C_{24}H_{26}O_{13}$) shows the loss of $C_6H_{10}O_4$ (rhamnose sugar) compared with methyl-monoHER (Table 2). This can be explained by hydrolysis of the sugar group (glucose-rhamnose), which is attached to the B ring of methyl-monoHER, thereby generating methyl-7-mono-O-(β-hydroxyethyl)-glucoside (methyl-monoHEG).

M10. On the basis of the exact mass determination data and the corresponding chemical composition ($C_{35}H_{40}O_{24}$) (Table 2), metabolite M10 was identified as monoCER glucuronide.

M11. LC-MS analysis of metabolite M11 shows the same main fragments as monoCER-glucuronide, only 14 Da higher (*m/z* 551 and 375) (Table 1). On the basis of the mass spectral data and its chemical composition ($C_{36}H_{42}O_{24}$) (Table 2), this metabolite was identified as methyl-monoCER glucuronide.

M12. Metabolite M12 shows an *m/z* 146 Da lower than dimethyl-monoHER (Table 1). Accurate mass measurements indicate the loss of the rhamnose sugar ($C_6H_{10}O_4$) compared with dimethyl-monoHER (Table 2). This metabolite was therefore identified as dimethyl-monoHEG.

M13. Metabolite M13 shows an *m/z* 28 Da higher than the parent compound (Table 1). The chemical formula ($C_{31}H_{38}O_{17}$) generated by exact mass

measurements shows the addition of two methyl groups (+ 2 x CH_2) (Table 2), identifying this metabolite as dimethyl-monoHER.

Table 2. Exact mass determinations (TOF-MS).

	Compound	Measured *m/z* ($[M+H]^+$)	Calculated *m/z* ($[M+H]^+$)	Error (ppm)	Elemental composition	DBE
P	monoHER	655.1872	655.1869	-0.6	$C_{29}H_{34}O_{17}$	13
M1/M2	monoHER glucuronide	831.2161	831.2189	3.41	$C_{35}H_{42}O_{23}$	15
M3	methyl-monoHER glucuronide	845.2352	845.2346	-0.73	$C_{36}H_{44}O_{23}$	15
M4	monoCER	669.1684	669.1661	-3.41	$C_{29}H_{32}O_{18}$	14
M5	methyl-monoHER	669.2028	669.2025	-0.38	$C_{30}H_{36}O_{17}$	13
M6	methyl-monoCER	683.1838	683.1818	-2.97	$C_{30}H_{34}O_{18}$	14
M7	GSH-monoHER	960.2537	960.2551	1.39	$C_{39}H_{49}N_3O_{23}S_1$	17
M8	monoHER diglucuronide	1007.2520	1007.2510	-1.04	$C_{41}H_{50}O_{29}$	17
M9	methyl-monoHEG	523.1457	523.1446	-2.07	$C_{24}H_{26}O_{13}$	12
M10	monoCER glucuronide	845.2029	845.1983	-5.53	$C_{35}H_{40}O_{24}$	16
M11	methyl-monoCER glucuronide	859.2094	859.2139	5.22	$C_{36}H_{42}O_{24}$	16
M12	dimethyl-monoHEG	537.1592	537.1603	1.99	$C_{25}H_{28}O_{13}$	12
M13	dimethyl-monoHER	683.2170	683.2182	1.72	$C_{31}H_{38}O_{17}$	13
M14	diHER	699.2129	699.2131	0.27	$C_{31}H_{38}O_{18}$	13
M15	triHER	743.2430	743.2393	-4.98	$C_{33}H_{42}O_{19}$	13
M16	methyl-diHER	713.2327	713.2288	-5.56	$C_{32}H_{40}O_{18}$	13
M17	dimethyl-diHER	727.2450	727.2444	-0.84	$C_{33}H_{42}O_{18}$	13

DBE, double bond equivalent.

Impurities/metabolites

Besides monoHER itself and monoHER metabolites, other compounds were also detected in bile, accounting for less than 0.5% of all compounds. On the basis of their mass spectral data, these compounds were identified as impurities of monoHER, and metabolites of these impurities, i.e., diHER (M14), triHER (M15), methyl-diHER (M16), and dimethyl-diHER (M17). MonoHER was isolated from the hydroxyethylrutoside mixture Venoruton (consisting of monoHER, diHER, triHER, and tetraHER). Analysis of monoHER used in the present study confirmed the presence of diHER and triHER in very small amounts.

Time course of monoHER metabolite formation

As shown in Figure 3, the concentrations of most metabolites peaked at 60 min after monoHER administration. Exceptions are the metabolites in which the disaccharide has been hydrolyzed, i.e., the glucosides methyl-monoHEG (M9) and dimethyl-monoHEG (M12). They are gradually formed over time, and 240 min after monoHER administration their concentrations are higher than those of the other metabolites.

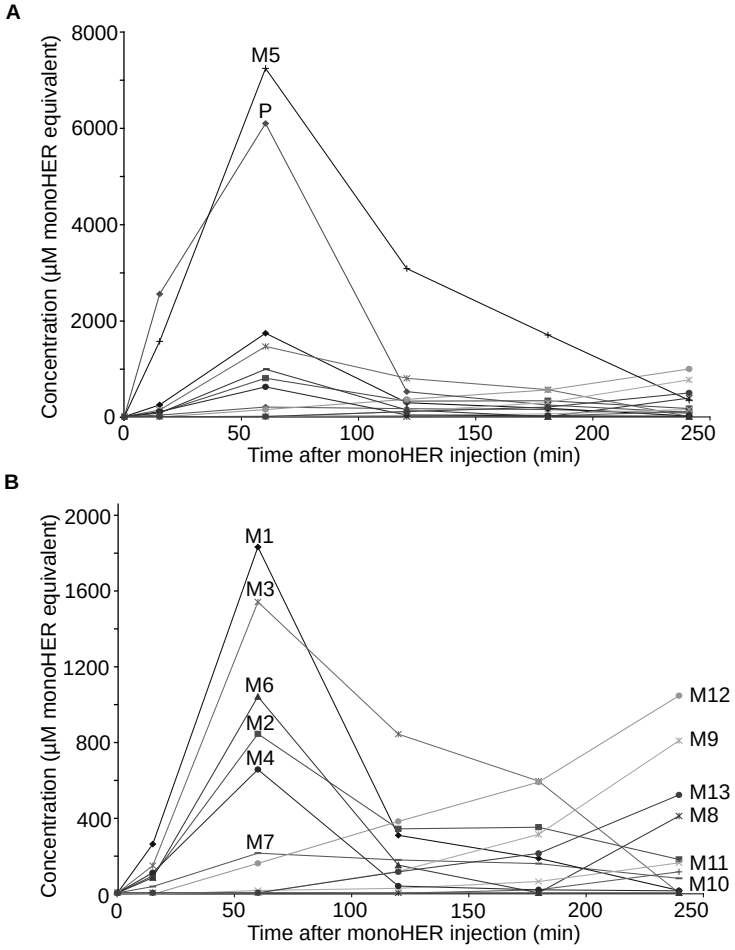

Figure 3. Metabolic profile of monoHER in mice. At 0, 15, 60, 120, 180, and 240 min after an intraperitoneal injection of monoHER (500 mg/kg), bile was collected in three mice and analyzed for the presence of monoHER metabolites. Panel A shows all detected monoHER metabolites. In panel B, the two compounds present in highest concentration (P and M5) are not shown, to more clearly visualize metabolites in the lower concentration range.The mean concentrations are expressed as micromolar monoHER equivalents. The S.D. was maximally 10% for all metabolites. Quantification of the different metabolites was achieved by their UV response at 355 nm.

Discussion

The main objective of the present study was to completely characterize the metabolites of the semisynthetic antioxidant flavonoid monoHER in mice. Because the liver is the main drug-eliminating organ, characterization was done in the bile fluid of mice. Our results show that monoHER is extensively metabolized. A scheme of the identified metabolites is shown in Figure 4. The observed routes of monoHER metabolism are methylation, glucuronidation, oxidation of its hydroxyethyl group, GSH conjugation, and hydrolysis of its disaccharide.

The primary metabolic route appeared to be methylation, yielding a 4'-*O*-methylated metabolite of monoHER (M5) that represents approximately 40% of all detected compounds. The O-methylation of catechols is mainly catalyzed by the enzyme COMT (Zhu, 2002). It has been shown that methylation of flavonoids makes them more lipophilic, thereby improving their transport over biological membranes and increasing their cellular uptake (Spencer *et al.*, 2004; Spencer *et al.*, 2003). Moreover, blocking the free hydroxyl group by methylation prevents other conjugation reactions such as glucuronidation at this group and thus increases the metabolic stability of flavonoids (Walle, 2009). Methylation of the hydroxyl group also decreases the antioxidant capacity of flavonoids (Spencer *et al.*, 2003). However, this decreased activity is compensated for by their increased intracellular concentration and metabolic stability (Spencer *et al.*, 2003). Moreover, after their uptake into the cells, cytochrome P450-dependent demethylation can take place, thereby generating the parent compound (Breinholt *et al.*, 2002). In addition, their high concentration formed and their relatively slow elimination suggests that the O-methylated metabolites of monoHER contribute to the antioxidant effect of monoHER.

Several hours after monoHER administration, the glucosides methyl-monoHEG (M9) and dimethyl-monoHEG (M12) have the highest concentrations of all metabolites. In addition to methylation, the rhamnose sugar has been removed in these metabolites. The time course of their formation indicates that they are primarily formed out of methyl-monoHER (M5) (Figure 3). These metabolites contain a terminal glucose moiety. Flavonoid glucosides are suggested to enter cardiac cells via the glucose transporter 4 (Passamonti *et al.*, 2009; Strobel *et al.*, 2005), which transports glucose in the heart (Huang and Czech, 2007). Because cellular access is required to exert a protective effect, the methylated metabolites of monoHER as well as the monoHER glucosides are believed to contribute to the protective effect of monoHER.

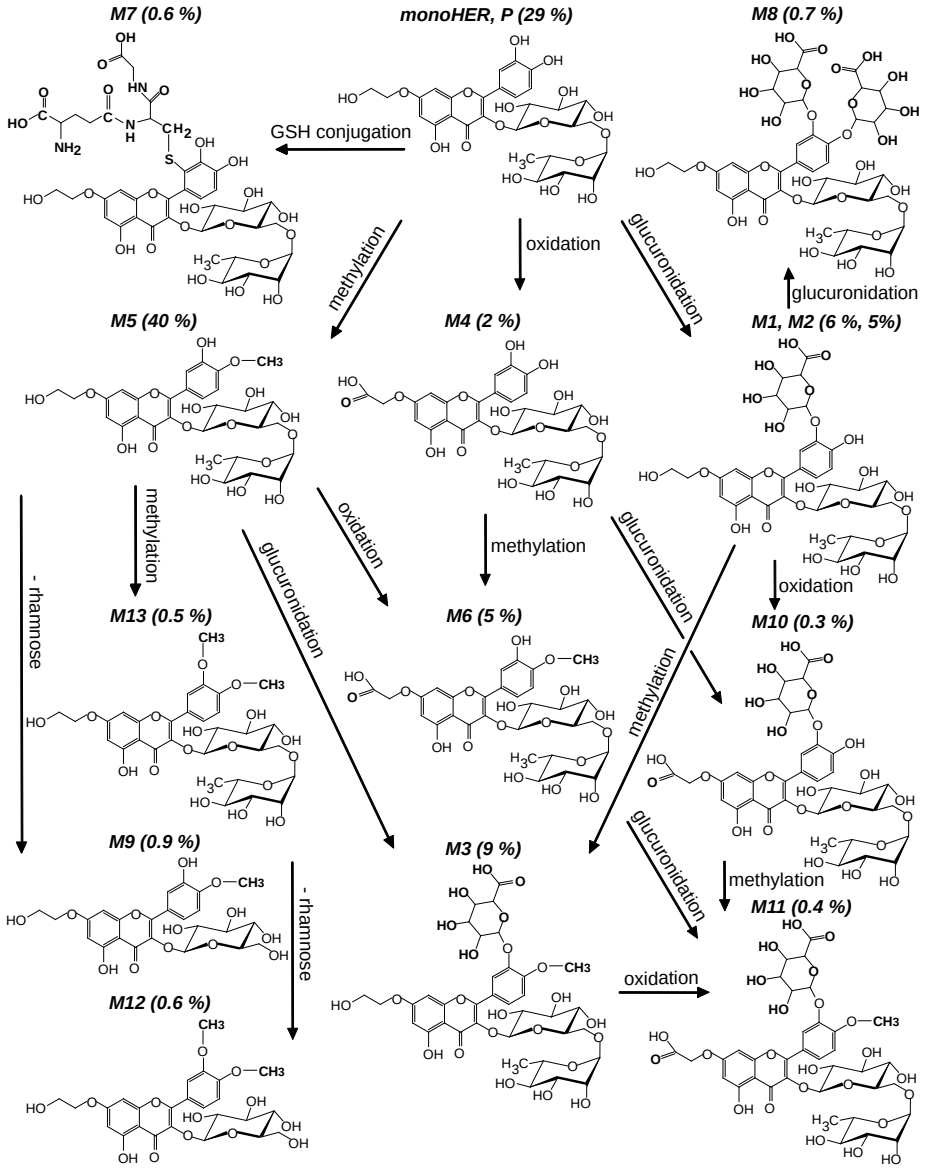

Figure 4. Proposed metabolism of monoHER in mice. The percentages in parentheses indicate the relative amounts of each metabolite. The relative amounts of the metabolites were estimated by calculating the AUC from the concentration-time curve of each metabolite, using the trapezoidal rule, and expressing this as a percentage of the total AUC of all detected compounds together.

The monoHER metabolites formed out of the other three conjugation reactions, i.e., glucuronidation, GSH conjugation, and oxidation, are charged at physiologi-

cal pH. These metabolites therefore probably have decreased cellular uptake and are unlikely to be involved in the protective effect of monoHER. In addition, Spencer et al. (2003) reported that the glucuronidated metabolites of flavonoids are unable to protect against oxidative stress-induced damage, presumably because of their inability to enter cells. The presence of GSH-monoHER conjugates indicates that monoHER has functioned as an antioxidant. GSH-monoHER formation is preceded by the oxidation of the catechol of monoHER, e.g., when it acts as an antioxidant by scavenging free radicals. Relatively low amounts of the GSH-monoHER conjugate were found, probably because there was no oxidative stress in these mice and because, as recently shown, the monoHER quinone reacts with the antioxidant ascorbate rather than with GSH (Jacobs *et al.*, 2010).

To summarize, it has been observed that even though monoHER is practically cleared from the body at the time that doxorubicin concentrations are still relatively high, the antioxidant monoHER does protect against doxorubicin-induced cardiotoxicity in mice (van Acker *et al.*, 2000). Three possible explanations can be given for this prolonged protective effect: first, it could mean that to have a protective effect monoHER only has to be present when the doxorubicin concentration peaks, i.e., shortly after doxorubicin administration; second, monoHER could have a "memory effect" on cells by inducing a protection that lasts after monoHER has been cleared from the body; or third, as the results of the present study suggest, monoHER metabolites might contribute to the observed cardioprotective effects. Although further research is needed, the methylated metabolites and the glucosides in particular are expected to contribute to the antioxidant activity of monoHER, which is involved in its protective effect against doxorubicin-induced cardiotoxicity.

References

Abou El Hassan MA, Kedde MA, Zwiers UT, Bast A, van der Vijgh WJ (2003a) The cardioprotector monoHER does not interfere with the pharmacokinetics or the metabolism of the cardiotoxic agent doxorubicin in mice. *Cancer Chemother Pharmacol* **51:** 306-310

Abou El Hassan MA, Kedde MA, Zwiers UT, Tourn E, Haenen GR, Bast A, van der Vijgh WJ (2003b) Bioavailability and pharmacokinetics of the cardioprotecting flavonoid 7-monohydroxyethyl-rutoside in mice. *Cancer Chemother Pharmacol* **52:** 371-376

Barrow A, Griffiths LA (1974) Metabolism of the hydroxyethylrutosides. II. Excretion and metabolism of 3',4',7-tri-O-(beta-hydroxyethyl) rutoside and related compounds in laboratory animals after parenteral administration. *Xenobiotica* **4:** 1-16

Bast A, Haenen GR, Bruynzeel AM, Van der Vijgh WJ (2007) Protection by flavonoids against anthracycline cardiotoxicity: from chemistry to clinical trials. *Cardiovasc Toxicol* **7:** 154-159

Breinholt VM, Offord EA, Brouwer C, Nielsen SE, Brosen K, Friedberg T (2002) In vitro investigation of cytochrome P450-mediated metabolism of dietary flavonoids. *Food Chem Toxicol* **40:** 609-616

Doroshow JH, Locker GY, Myers CE (1980) Enzymatic defenses of the mouse heart against reactive oxygen metabolites: alterations produced by doxorubicin. *J Clin Invest* **65:** 128-135

Forester SC, Waterhouse AL (2009) Metabolites are key to understanding health effects of wine polyphenolics. *J Nutr* **139:** 1824S-1831S

Gescher AJ, Steward WP (2003) Relationship between mechanisms, bioavailibility, and preclinical chemopreventive efficacy of resveratrol: a conundrum. *Cancer Epidemiol Biomarkers Prev* **12:** 953-957

Hackett AM, Griffiths LA (1977a) The disposition and metabolism of 3',4',7-tri-O-(beta-hydroxyethyl)rutoside and 7-mono-O-(beta-hydroxyethyl)rutoside in the mouse. *Xenobiotica* **7:** 641-651

Hackett AM, Griffiths LA (1977b) Enterohepatic cycling of O-(beta-hydroxyethyl) rutosides and their biliary metabolites in the rat. *Experientia* **33:** 161-163

Haenen GR, Jansen FP, Bast A (1993) The antioxidant properties of five O-(-β–Hydroxyethyl)-Rutosides of the flavonoid mixture Venoruton. *Phlebology* **Suppl.1:** 10-17

Horenstein MS, Vander Heide RS, L'Ecuyer TJ (2000) Molecular basis of anthracycline-induced cardiotoxicity and its prevention. *Mol Genet Metab* **71:** 436-444

Huang S, Czech MP (2007) The GLUT4 glucose transporter. *Cell Metab* **5:** 237-252

Iarussi D, Indolfi P, Galderisi M, Bossone E (2000) Cardiac toxicity after anthracycline chemotherapy in childhood. *Herz* **25:** 676-688

Jacobs H, Moalin M, Bast A, van der Vijgh WJ, Haenen GR (2010) An Essential Difference between the Flavonoids MonoHER and Quercetin in Their Interplay with the Endogenous Antioxidant Network. *PLoS One* **5:** e13880

Jacobs H, van der Vijgh WJ, Koek GH, Draaisma GJ, Moalin M, van Strijdonck GP, Bast A, Haenen GR (2009) Characterization of the glutathione conjugate of the semisynthetic flavonoid monoHER. *Free Radic Biol Med* **46:** 1567-1573

Julicher RH, Sterrenberg L, Haenen GR, Bast A, Noordhoek J (1988) The effect of chronic adriamycin treatment on heart kidney and liver tissue of male and female rat. *Arch Toxicol* **61:** 275-281

Lipshultz SE, Lipsitz SR, Sallan SE, Dalton VM, Mone SM, Gelber RD, Colan SD (2005) Chronic progressive cardiac dysfunction years after doxorubicin therapy for childhood acute lymphoblastic leukemia. *J Clin Oncol* **23:** 2629-2636

Passamonti S, Terdoslavich M, Franca R, Vanzo A, Tramer F, Braidot E, Petrussa E, Vianello A (2009) Bioavailability of flavonoids: a review of their membrane transport and the function of bilitranslocase in animal and plant organisms. *Curr Drug Metab* **10:** 369-394

Petruzzellis V, Troccoli T, Candiani C, Guarisco R, Lospalluti M, Belcaro G, Dugall M (2002) Oxerutins (Venoruton): efficacy in chronic venous insufficiency--a double-blind, randomized, controlled study. *Angiology* **53:** 257-263

Singal PK, Iliskovic N (1998) Doxorubicin-induced cardiomyopathy. *N Engl J Med* **339:** 900-905

Spencer JP, Abd-el-Mohsen MM, Rice-Evans C (2004) Cellular uptake and metabolism of flavonoids and their metabolites: implications for their bioactivity. *Arch Biochem Biophys* **423:** 148-161

Spencer JP, Kuhnle GG, Williams RJ, Rice-Evans C (2003) Intracellular metabolism and bioactivity of quercetin and its in vivo metabolites. *Biochem J* **372:** 173-181

Strobel P, Allard C, Perez-Acle T, Calderon R, Aldunate R, Leighton F (2005) Myricetin, quercetin and catechin-gallate inhibit glucose uptake in isolated rat adipocytes. *Biochem J* **386:** 471-478

van Acker FA, van Acker SA, Kramer K, Haenen GR, Bast A, van der Vijgh WJ (2000) 7-monohydroxyethylrutoside protects against chronic doxorubicin-induced cardiotoxicity when administered only once per week. *Clin Cancer Res* **6:** 1337-1341

van Acker SA, Boven E, Kuiper K, van den Berg DJ, Grimbergen JA, Kramer K, Bast A, van der Vijgh WJ (1997) Monohydroxyethylrutoside, a dose-dependent cardioprotective agent, does not affect the antitumor activity of doxorubicin. *Clin Cancer Res* **3:** 1747-1754

Walle T (2009) Methylation of dietary flavones increases their metabolic stability and chemopreventive effects. *Int J Mol Sci* **10:** 5002-5019

Willems AM, Bruynzeel AM, Kedde MA, van Groeningen CJ, Bast A, van der Vijgh WJ (2006) A phase I study of monohydroxyethylrutoside in healthy volunteers. *Cancer Chemother Pharmacol* **57:** 678-684

Xu MF, Tang PL, Qian ZM, Ashraf M (2001) Effects by doxorubicin on the myocardium are mediated by oxygen free radicals. *Life Sci* **68:** 889-901

Zhu BT (2002) Catechol-O-Methyltransferase (COMT)-mediated methylation metabolism of endogenous bioactive catechols and modulation by endobiotics and xenobiotics: importance in pathophysiology and pathogenesis. *Curr Drug Metab* **3:** 321-349

Chapter 7

Differences in the metabolic profile of the antioxidant flavonoid 7-mono-O-(β-hydroxyethyl)-rutoside between men and mice. Possible implications for its cardioprotective effect

Hilde Jacobs
Ger H. Koek
Ron Peters
Mohamed Moalin
Jan Tack
Wim J.F. van der Vijgh
Aalt Bast
Guido R.M.M. Haenen

Submitted

Abstract

Despite its well-known cardiotoxicity, the anthracycline doxorubicin continues to be a widely used chemotherapeutic agent. The antioxidant flavonoid 7-mono-O-(β-hydroxyethyl)-rutoside (monoHER) showed protection against doxorubicin-induced cardiotoxicity in mice. This protection could however not be observed in humans. A possible explanation for this different effect in mice and humans may be a difference in monoHER metabolism between both species. This prompted us to investigate the metabolism of monoHER in humans and to compare this with its metabolism in mice. Five healthy volunteers received monoHER by intravenous infusion. Up to three hours after infusion bile fluid was collected in which monoHER metabolites were identified by LC-DAD-TOF-MS and ^{1}H NMR. Thirteen different metabolites could be identified. The observed routes of monoHER metabolism were glucuronidation, methylation, oxidation of its hydroxyethyl group, GSH conjugation, and hydrolysis of its disaccharide group. In mice the major metabolic route appeared to be methylation, thereby forming bioactive metabolites that are implicated in the cardioprotective effect of monoHER. In humans monoHER is predominantly converted into inactive glucuronidated metabolites. Our data indicate that the different pharmacological effect of monoHER in mice and men might be explained by a difference in monoHER metabolism between both species. This study adds to the growing appreciation of flavonoid metabolites as bioactive compounds.

Introduction

Doxorubicin is a very effective antitumour agent, widely applied in the treatment of various types of cancer. Unfortunately, treatment with doxorubicin is limited by a cumulative dose-dependent cardiotoxicity, which manifests itself as congestive heart failure (Bast *et al.*, 2007; Lipshultz *et al.*, 2005; Singal and Iliskovic, 1998). Doxorubicin-induced cardiotoxicity mainly results from free radicals, which are produced during redox-cycling of doxorubicin (Horenstein *et al.*, 2000; Xu *et al.*, 2001). Cardiac tissue is particularly vulnerable to free radical-induced injury because antioxidant enzymes such as superoxide dismutase and catalase, which protect against oxidative damage, are markedly reduced compared with other tissues in the body (Doroshow *et al.*, 1980; Iarussi *et al.*, 2000; Julicher *et al.*, 1988).

Flavonoids can be considered as potential protectors against doxorubicin-induced cardiotoxicity because of their excellent radical scavenging properties (Amic *et al.*, 2007; Rice-Evans *et al.*, 1996; van Acker *et al.*, 1995; van Acker *et al.*, 1996). In a series of structurally related flavonoids, the semisynthetic flavonoid 7-mono-O-(β-hydroxyethyl)-rutoside (monoHER, Figure 1), which is a constituent of the registered drug Venoruton, was found to be the most potent antioxidant (Haenen *et al.*, 1993).

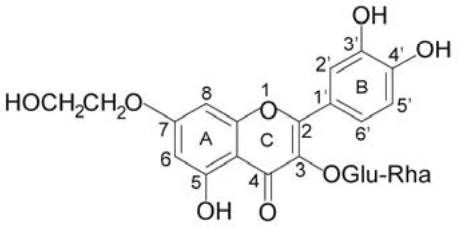

Figure 1. Structural formula of monoHER and numbering of relevant carbon atoms.

Preclinical experiments in mice have shown that monoHER effectively protects against doxorubicin-induced cardiotoxicity, without interfering with the antitumour activity of doxorubicin (van Acker *et al.*, 2000; van Acker *et al.*, 1997). Recent experiments revealed that monoHER metabolites are likely to contribute to these cardioprotective effects in mice (Jacobs *et al.*, 2011b). On the basis of their time course of formation and chemical characteristics, especially the methylated metabolites and the monoHER glucosides seem to be involved in the protective effect of monoHER (Jacobs *et al.*, 2011b). In a clinical phase II trial

with metastatic cancer patients, monoHER did not significantly protect against the cardiotoxicity induced by doxorubicin (Bruynzeel *et al.*, 2007). It can be excluded that this difference between mice and humans is due to a difference in monoHER levels because the pharmacokinetic end points (C_{max} and AUC^{∞}) of monoHER were similar in both species (Abou El Hassan *et al.*, 2003; Willems *et al.*, 2006). Therefore, to explain the different pharmacological effect of monoHER in humans and mice, we hypothesized that metabolites of monoHER, which contribute to its cardioprotection, are formed in mice but not (or to a lesser extend) in humans.

The objective of the present study was to characterize the metabolites of monoHER in humans and compare the identified metabolites with those previously found in mice. Our data show that there is a difference in the metabolism of monoHER between men and mice, which might explain the different pharmacological effect of monoHER in both species.

Materials and methods

Chemicals

7-Mono-O-(β-hydroxyethyl)-rutoside (monoHER) was provided by Novartis Consumer Health (Nyon, Switzerland). 2'-GSH-monoHER and 4'-methyl-monoHER were synthesized as described previously (Jacobs *et al.*, 2011b; Jacobs *et al.*, 2009). β-Glucuronidase from Helix pomatia (type H-5), sulphatase from Helix pomatia (type H-1), trifluoroacetic acid (TFA), deuterated water (D_2O) and sodium acetate were purchased from Sigma-Aldrich (Steinheim, Germany). Acetonitrile HPLC grade, methanol and dimethyl sulfoxide (DMSO) were obtained from Biosolve (Valkenswaard, The Netherlands).

Study population

Five healthy volunteers (three men and two women) with a mean age of 34 years took part in this study. Exclusion criteria were: diagnosed hepatic diseases like chronic hepatitis B and C, gallstones disease and bile excretion disturbances like Primary Biliary Cirrhosis and Primary Sclerosing Cholangitis, fat storage disease like non-alcoholic steatohepatitis (NASH), use of any medication (except oral anticonception), consumption of 4 or more glasses of alcohol per day. Before the start of the study, blood was taken to verify adequate liver function.

Ethical Considerations

This study was approved by the Medical Ethical Review Committee of the University Hospital Gasthuisberg (Leuven, Belgium). The outline of the study was explained to the volunteers before obtaining their written informed consent.

Treatment

Formulation of the drug
The monoHER infusion was formulated under aseptic conditions by the Department of Pharmacy, University Hospital Gasthuisberg, Leuven, Belgium. The required amount of monoHER was dissolved in 100 ml 5% dextrose for intravenous use, adjusted to pH 9.3 using 4 M sodium hydroxide. After dissolution of the drug, the solution was readjusted to pH 8.4 with 1 M hydrochloric acid. The final solution was filtered through a 0.2-µm filter. The solution is chemically stable for at least 24 hour at room temperature (Abou El Hassan *et al.*, 2000) and therefore the volunteers received the drug within 24 h after preparation.

Administration of the drug
MonoHER was administered as an intravenous infusion for 15 minutes at a dose of 1500 mg/m^2.

Bile aspiration
Before monoHER infusion and every 10 minutes over a period of 3 hours after the start of monoHER infusion, bile fluid from the healthy volunteers was collected via oral intubation of a tube with a balloon, which was maneuvered into the second part of the duodenum under fluoroscopic control (Koek *et al.*, 2004). The balloon served to prevent mixing of gastric contents or food with duodenal contents. After the balloon was inflated with air, a high caloric drink (200 ml Nutridrink®; 300 Kcal: 13% proteins, 48% carbohydrates and 39% lipids. Nutricia, Belgium) was given to stimulate bile excretion. At each time-point, the aspiration was performed until about 10 ml was collected. The bile fluid was divided into portions of 1 ml and frozen at -80°C.

Blood sampling
Venous blood samples (10 ml) were collected from the healthy volunteers just before monoHER infusion (blank) and 30, 45, 60, and 120 minutes after the start of monoHER infusion. Blood was collected in a sodium heparin-containing glass tube. Blood cells were spun down in a centrifuge at 4000 rpm for 5 minutes. Aliquots of 1 ml plasma (supernatant) were transferred into polypropy-

lene micro-test tubes. Each sample was frozen immediately at -80°C until analysis.

Sample preparation

Samples of bile fluid or plasma were mixed with twice the volume of DMSO/methanol (1/4, v/v). The mixture was vortexed and centrifuged (17060 g, 15 min). The supernatant was collected and injected onto the LC column.

To identify the presence of glucuronide and sulphate conjugates in the bile fluid, β-glucuronidase solution (40 U in 0.1 M sodium acetate pH 4.0) and sulphatase solution (40 U in 0.1 M sodium acetate pH 6.2) were respectively added to a sample of bile fluid. Incubations were carried out for 30 minutes at 37°C, which provides maximal deconjugation (cleavage of ether-bonds of glucuronides and sulphates, respectively) (Bartholome *et al.*, 2010). Following incubation, the samples were extracted as described above and analyzed by LC-DAD.

Bile samples were also spiked with reference compounds (monoHER, 2'-GSH-monoHER, and 4'-methyl-monoHER) to examine the possible presence of these compounds in the bile fluid.

LC-DAD analysis

LC-DAD of the bile and plasma samples was performed on an Agilent 1100 series LC-DAD system (Agilent Technologies, Santa Clara, CA, USA). Analytical separations were achieved using an ODS-3 column (5 µm, 250 x 3 mm) (Inertsil; Varian Inc., Palo Alto, CA, USA) at 40°C. The mobile phase consisted of ultrapure water containing 0.1% (v/v) TFA (mobile phase A) and acetonitrile containing 0.1% (v/v) TFA (mobile phase B). The gradient was started at t = 0 min with 15% (v/v) B, was changed linearly over the first 20 min to 30% (v/v) B followed by an increase to 90% (v/v) B at t = 25 min, and was then stationary for 1 min. The column was reequilibrated with 15% (v/v) B for 5 min. A flow rate of 1 ml/min and an injection volume of 10 µl were used. Detection was performed with a diode array detector (DAD). The chromatograms presented are based on detection at 355 nm. The LC-DAD system was controlled using ChemStation software (A09.03, Agilent).

LC-DAD-TOF-MS analysis

LC-DAD-TOF-MS, including fragmentation and exact mass measurements, was performed using an Agilent 1100 LC-DAD-TOF-MS system (Agilent Technologies)

to further characterize the peaks in the LC chromatogram. The UV signal at 355 nm was collected. Electrospray ionization (ESI) was performed in positive mode with the following conditions: *m/z* range 50 to 3000, 175 V fragmentor (varied for fragmentation experiments), 0.1 *m/z* step size, 1.013 cycles/s, 350°C drying gas temperature, 10 liters of N_2/min drying gas, 35 psig nebulizer pressure, and 2 kV capillary voltage. The MS data were collected using internal reference mass correction. The reference substances [purine at 121.050873 Da and hexakis-(1*H*,1*H*,3*H*-tetrafluoro-pentoxy)phosphazene (HP-921) at 922.009798 Da] were continuously injected into the electrospray ion source equipped with a dual-sprayer mechanism. The LC conditions were the same as described above. The LC-DAD-TOF-MS system was controlled using MassHunter qualitative analysis software (B03.01; Agilent Technologies).

Elemental composition calculations from the exact masses were performed off-line using MassHunter. This software was used to work with the MS spectrum manually generated for every peak. Potential assignments were calculated using the monoisotopic masses with specifications of a tolerance of 10 ppm deviation. The number and types of expected atoms were set as follows: carbons <60, hydrogens <120, oxygens <30, nitrogens <30, and sulfurs <5, whereas the double bond equivalent (DBE) was set to <50.

Preparative high-performance liquid chromatography

Preparative HPLC was carried out on a Gilson system (Gilson Inc., Middleton, WI, USA), which comprised a pump (model 305), a manometric module (model 806), a dynamic mixer (model 811B) and a UV detector (Water 2487). The detection wavelength was 355 nm. A Zorbax SB C18 column (21.2 x 250 mm) (Agilent) was used with a mobile phase of (A) H_2O and (B) acetonitrile, both containing 0.1% TFA. The gradient was started at t = 0 min with 20% (v/v) B, changed linearly over 26 min to 90% (v/v) B and was stationary for 4 min. The column was reequilibrated with 20% acetonitrile for 5 min. The flow rate was 20 ml/min and the injection volume 600 µl.

^{1}H NMR measurements

^{1}H NMR measurements were performed in D_2O at 25 °C on a Bruker Avance 300 MHz NMR equipped with a 5-mm QNP probe (Varian, Mulgrave Victoria, Australia). A 10 s scan time and a 54 min acquisition time were used. Chemical shifts are reported in ppm relative to tetramethylsilane. The results were confirmed by the software program ACD/HNMR Predictor (version 8.09).

Quantification of monoHER metabolites

Bile and plasma concentrations of the different metabolites were determined by their UV response at 355 nm (area of the peak in the chromatogram). Because no commercial reference standards were available for these metabolites, it was assumed that the UV response at 355 nm is equal to that of monoHER for all metabolites. This is a reasonable assumption because they all have the same chromophore and the UV spectra in the 355 nm region of all metabolites are similar to that of monoHER.

The relative amounts of the metabolites were estimated by calculating the area under the curve (AUC) from the concentration-time curve of each metabolite, using the trapezoidal rule, and expressing this as percentage of the total AUC of all detected compounds together.

Results

Metabolites in bile

Representative LC chromatograms of bile samples, collected from the healthy volunteers before the start of monoHER infusion (blank bile) and 65 min after i.v. administration of 1500 mg/m^2 monoHER, are shown in Figure 2.

The chromatogram of bile collected after monoHER administration shows several additional peaks compared with that of the blank bile. The DAD spectra of these peaks and the absorption maxima at 355 nm are similar to those of monoHER, indicating that these peaks correspond to metabolites of monoHER. Six major metabolites (M1-M6), representing more than 90% of all detected compounds, and seven minor metabolites (M7-M13) were detected. Also other compounds that could be traced as impurities of monoHER and their metabolites (M14-M18) were detected in bile, accounting for less than 1% of all compounds.

Metabolites in plasma

In the plasma samples collected from the healthy volunteers after monoHER infusion, analyzed by LC-DAD, the parent compound monoHER (96.5%) and three major metabolites M2 (2%), M3 (0.5%) and M5 (1.0%) could be detected.

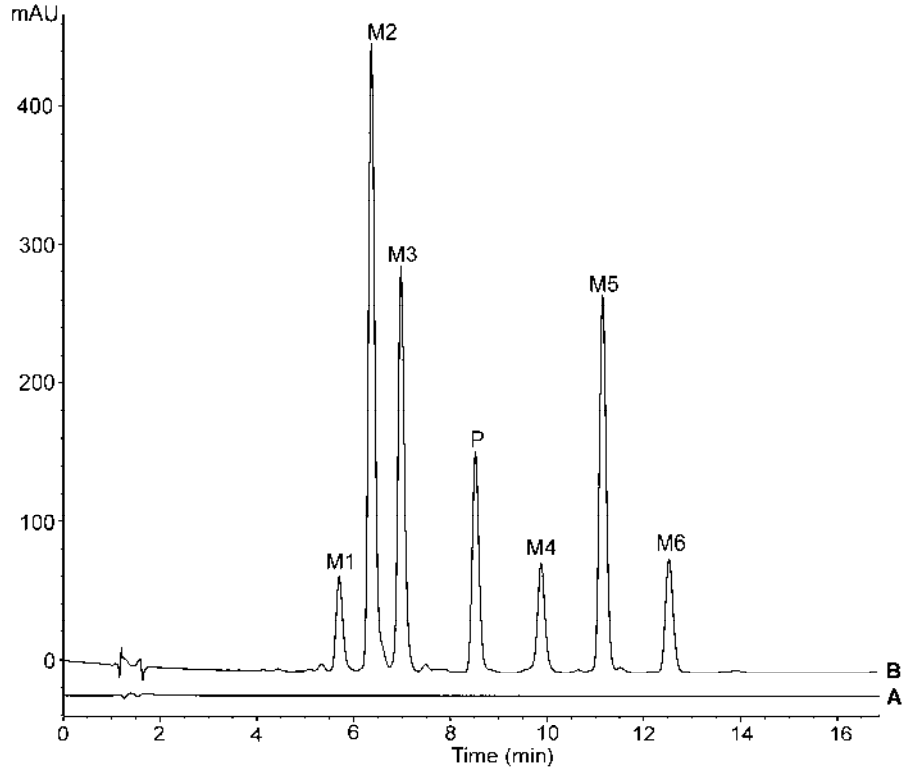

Figure 2. Representative LC chromatogram of (A) bile collected from a human volunteer just before monoHER administration and (B) bile collected from the same volunteer 65 min after i.v. administration of monoHER. The numbered peaks represent monoHER [parent(P)] and its six major metabolites (M1-M6). The chromatograms presented are based on detection at 355 nm.

Identification of metabolites

Tandem mass spectrometry fragmentation of the parent compound produced three key fragments: *m/z* 509 (- 145, loss of rhamnose sugar), *m/z* 347 (- 307, loss of rhamnose and glucose sugar), and *m/z* 303 (- 351, loss of rhamnose, glucose, and the hydroxyethyl group of the A ring) (Figure 3).

Identification of the different metabolites was done based on their mass-to-charge ratio (*m/z)* values, mass change from the parent compound, main fragment ions, and elemental composition (obtained by accurate mass measurements). Further details about the identification of the metabolites have been published previously (Jacobs *et al.*, 2011b). The results are summarized in Table 1 and Table 2. The four major metabolites (M2, M3, M5 and M6) were collected by preparative HPLC and further characterized by ^{1}H NMR (Table 3). An over-

view of the chemical structures of the metabolites and their mutual relationships are given in Figure 4.

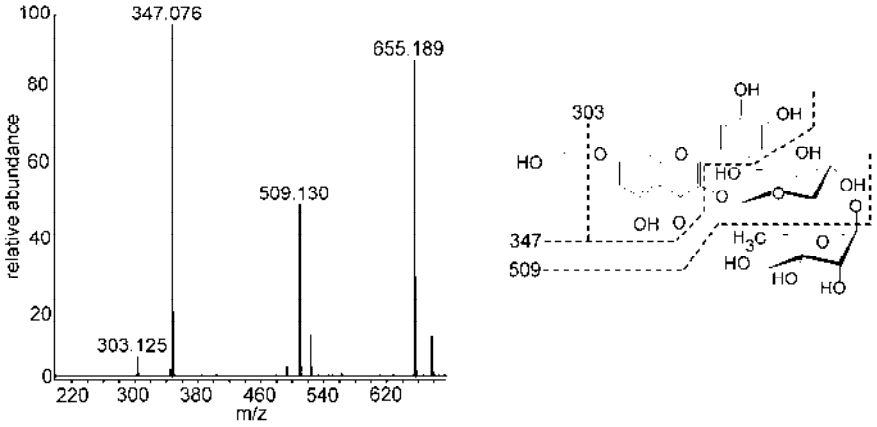

Figure 3. Mass spectrum of monoHER obtained by tandem mass spectrometry, and the proposed origin of the key fragment ions.

Table 1. MonoHER and its metabolites identified in bile of the volunteers by LC-DAD-TOF-MS.

	t_R (min)	Compound	$[M+H]^+$ (*m/z*)	Mass change from parent	Main fragment ions (*m/z*)
		Parent compound			
P	8.5	monoHER	655	0	509, 347, 303
		Major metabolites			
M1	5.6	monoHER glucuronide	831	+ 176	765, 685, 523, 347, 303
M2	6.3	monoHER glucuronide	831	+ 176	765, 685, 523, 347, 303
M3	6.9	methyl-monoHER glucuronide	845	+ 190	699, 537, 361, 317
M4	9.7	monoCER	669	+ 14	523, 463, 361
M5	11.1	methyl-monoHER	669	+ 14	523, 361, 317
M6	12.3	methyl-monoCER	683	+ 28	537, 375
		Minor metabolites			
M7	3.4	GSH-monoHER	960	+ 305	814, 705, 652, 523, 371
M8	7.1	monoHER diglucuronide	1007	+ 352	861, 845, 831, 699, 523, 347
M9	7.6	methyl-monoHEG	523	- 132	479, 361, 303
M10	7.8	monoCER glucuronide	845	+ 190	537, 361
M11	8.8	methyl-monoCER glucuronide	859	+ 204	551, 375
M12	12.5	dimethyl-monoHEG	537	- 118	375
M13	14.8	dimethyl-monoHER	683	+ 28	537, 375

		Impurities/metabolites			
M14	9.4	diHER	699	+ 44	655, 523, 347
M15	12.5	triHER	743	+ 88	622, 597, 435, 347
M16	13.3	methyl-diHER	713	+ 58	537, 361
M17	14.8	dimethyl-diHER	727	+ 72	537, 439, 361

Abbreviations: HER = hydroxyethyl-rutoside, CER = carboxyethyl-rutoside, HEG = hydroxyethyl-glucoside.

Table 2. Exact mass determinations (TOF-MS).

	Compound	Measured *m/z* ($[M+H]^+$)	Calculated *m/z* ($[M+H]^+$)	Error (ppm)	Elemental composition	DBE
P	monoHER	655.1872	655.1869	-0.6	$C_{29}H_{34}O_{17}$	13
M1/M2	monoHER glucuronide	831.2161	831.2189	3.41	$C_{35}H_{42}O_{23}$	15
M3	methyl-monoHER glucuronide	845.2352	845.2346	-0.73	$C_{36}H_{44}O_{23}$	15
M4	monoCER	669.1684	669.1661	-3.41	$C_{29}H_{32}O_{18}$	14
M5	methyl-monoHER	669.2028	669.2025	-0.38	$C_{30}H_{36}O_{17}$	13
M6	methyl-monoCER	683.1838	683.1818	-2.97	$C_{30}H_{34}O_{18}$	14
M7	GSH-monoHER	960.2537	960.2551	1.39	$C_{39}H_{49}N_3O_{23}S_1$	17
M8	monoHER diglucuronide	1007.2520	1007.2510	-1.04	$C_{41}H_{50}O_{29}$	17
M9	methyl-monoHEG	523.1457	523.1446	-2.07	$C_{24}H_{26}O_{13}$	12
M10	monoCER glucuronide	845.2029	845.1983	-5.53	$C_{35}H_{40}O_{24}$	16
M11	methyl-monoCER glucuronide	859.2094	859.2139	5.22	$C_{36}H_{42}O_{24}$	16
M12	dimethyl-monoHEG	537.1592	537.1603	1.99	$C_{25}H_{28}O_{13}$	12
M13	dimethyl-monoHER	683.2170	683.2182	1.72	$C_{31}H_{38}O_{17}$	13
M14	diHER	699.2129	699.2131	0.27	$C_{31}H_{38}O_{18}$	13
M15	triHER	743.2430	743.2393	-4.98	$C_{33}H_{42}O_{19}$	13
M16	methyl-diHER	713.2327	713.2288	-5.56	$C_{32}H_{40}O_{18}$	13
M17	dimethyl-diHER	727.2450	727.2444	-0.84	$C_{33}H_{42}O_{18}$	13

Abbreviations: HER = hydroxyethyl-rutoside, CER = carboxyethyl-rutoside, HEG = hydroxyethyl-glucoside, DBE = double bond equivalent.

Table 3. ^{1}H NMR characteristics of monoHER and its main metabolites identified in human bile.

	Compound	Proton	Chemical shift (ppm)	Multiplicity	Number of protons
P	monoHER	H2’	7.45	B	1
		H6’	7.49	B	1
		H5’	6.79	D	1
		H6	6.22	D	1
		H8	6.47	D	1
		OH5	4.32	S	1
		CH_2CH_2O7	3.66	T	4
		Gluc-H1	-	-	-
		Methyl	-	-	-
M2	monoHER-3’-glucuronide	H2’	7.59	B	1
		H6’	7.59	B	1
		H5’	6.84	D	1
		H6	6.13	S	1
		H8	6.22	S	1
		OH5	4.39	S	1
		CH_2CH_2O7	3.66	T	4
		Gluc-H1	5.05	D	1
		Methyl	-	-	-
M3	3’-methyl-monoHER-4’-glucuronide	H2’	7.50	S	1
		H6’	7.64	D	1
		H5’	6.90	D	1
		H6	6.15	S	1
		H8	6.28	S	1
		OH5	4.34	S	1
		CH_2CH_2O7	3.66	T	4
		Gluc-H1	5.10	D	1
		Methyl	3.85	S	3
M5	4’-methyl-monoHER	H2’	7.52	D	1
		H6’	7.60	DD	1
		H5’	6.98	D	1
		H6	6.30	D	1
		H8	6.57	D	1
		OH5	4.37	S	1
		CH_2CH_2O7	3.70	T	4
		Gluc-H1	-	-	-
		Methyl	3.77	S	3
M6	4’-methyl-monoCER	H2’	7.67	S	1
		H6’	7.72	D	1
		H5’	7.08	D	1
		H6	6.26	S	1
		H8	6.51	S	1
		OH5	4.51	S	1
		CH_2CH_2O7	-	-	-
		Gluc-H1	-	-	-
		Methyl	3.86	S	3

Abbreviations: S = singlet, D = doublet, DD = double doublet, T = triplet, B = Broad.

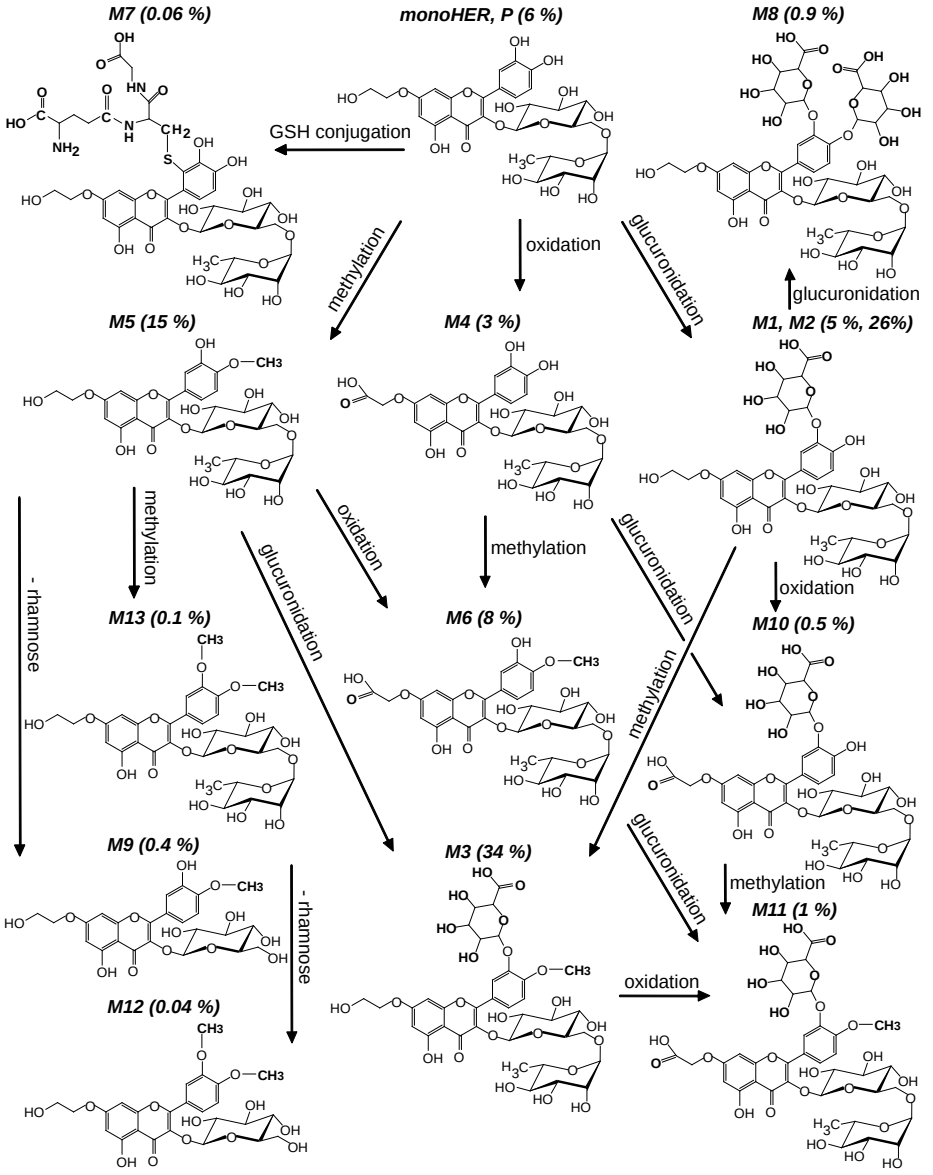

Figure 4. Proposed metabolism of monoHER in humans. The percentages in parentheses indicate the relative amounts of each metabolite. The relative amounts of the metabolites were estimated by calculating the AUC from the concentration-time curve of each metabolite, using the trapezoidal rule, and expressing this as a percentage of the total AUC of all detected compounds together.

Concentration-time profiles

Figure 5 shows the concentrations of the parent compound and each metabolite in bile at different time points after monoHER administration. From this figure it can be seen that monoHER is rapidly metabolized. The major metabolic pathway is glucuronidation. Incubation of bile with the enzyme β-glucuronidase, which cleaves the ether bond between glucuronic acid and the parent compound, caused the peaks of the glucuronide metabolites in the chromatogram to disappear with a concomitant increase in the area of the monoHER peak (data not shown). Other observed routes of monoHER metabolism are methylation, oxidation of its hydroxyethyl group, GSH conjugation, and hydrolysis of its disaccharide.

Comparison of the relative amounts of the different metabolites reveals that both monoHER glucuronide (M2) and the methylated conjugate of monoHER glucuronide (M3) are the major metabolites, accounting for 26% and 34% of the total amount of all detected compounds, respectively. The relative amounts of all detected compounds, compared with those in mice, are presented in Table 4.

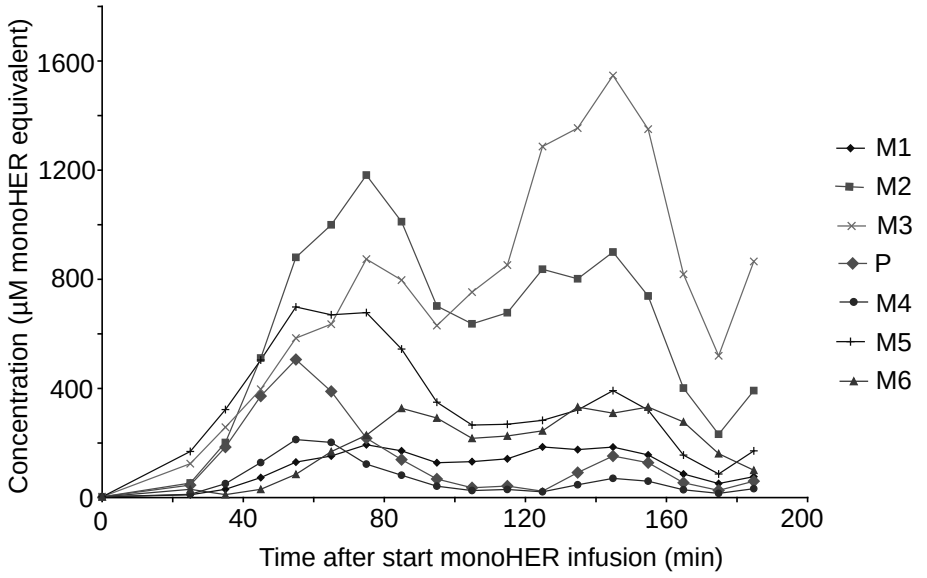

Figure 5. Metabolic profile of monoHER in humans. Every 10 minutes after monoHER administration (1500 mg/m^2, i.v.), bile was collected and analyzed for the presence of monoHER metabolites. The concentrations are expressed as micromolar monoHER equivalents.

Discussion

The results of this study suggest that the different pharmacological effect of monoHER in mice and humans may originate from a difference in monoHER metabolism between the two species. We characterized the metabolites of monoHER that are formed in humans and compared them with those previously found in mice. Because the liver is the main drug-eliminating organ characterization was done in the bile fluid of healthy volunteers who received monoHER by intravenous infusion. This appeared to be a successful strategy because we were able to identify up to thirteen different metabolites.

In humans, the same metabolites were found as in mice (Jacobs *et al.*, 2011b). However, in mice especially methylation was detected, while in humans mainly glucuronidation was observed (Table 4). Other observed metabolic reactions were oxidation, GSH conjugation, and hydrolysis of the disaccharide.

Table 4. Relative amount of each monoHER metabolite (% of total) detected in bile of humans and mice.

	Compound	Humans	Mice
	Parent compound		
P	monoHER	5.8 ± 2.3	29.2 ± 4.0
	Major metabolites[a]		
M1	monoHER glucuronide	5.4 ± 1.1	6.3 ± 0.4
M2	monoHER glucuronide	26.4 ± 5.2	4.7 ± 0.2
M3	methyl-monoHER glucuronide	34.2 ± 6.3	8.6 ± 0.3
M4	monoCER	2.6 ± 1.8	2.1 ± 0.1
M5	methyl-monoHER	14.8 ± 3.2	39.9 ± 1.4
M6	methyl-monoCER	7.6 ± 3.4	5.4 ± 1.2
	Minor metabolites[b]		
M7	GSH-monoHER	0.06	0.56
M8	monoHER diglucuronide	0.93	0.67
M9	methyl-monoHEG	0.44	0.86
M10	monoCER glucuronide	0.52	0.32
M11	methyl-monoCER glucuronide	1.07	0.35
M12	dimethyl-monoHEG	0.04	0.56
M13	dimethyl-monoHER	0.14	0.48

[a] Quantification with LC-DAD (mean ± S.D., humans: n = 5, mice: n = 3).

[b] Quantification with LC-MS based on one AUC of each compound.

For other flavonoids also sulfation has been described, however no sulphates were detected for monoHER. This is probably because a relatively high dose (~ 3 gram) of monoHER was administered intravenously. At high doses the relative importance of sulfation decreases since this conjugation route becomes saturated at a relative low concentration, which will result in a shift from sulfation toward glucuronidation (Koster *et al.*, 1981). For other polyphenols, the limited data that are available on the proportions of the various types of conjugates indicate that the main metabolites in humans are glucuronides (Baba *et al.*, 2000; Doerge *et al.*, 2000; Lee *et al.*, 2002; Manach *et al.*, 2003; Setchell *et al.*, 2001; Shelnutt *et al.*, 2002; Zhang *et al.*, 2003).

Conjugation with glucuronic acid is mainly catalyzed by the liver enzyme uridine 5'-diphospho(UDP)-glucuronosyltransferase (UGT) (Radominska-Pandya *et al.*, 1999). The resulting glucuronide is much more hydrophilic than the original compound, making it unable to cross lipid membranes and enter cells (Miners and Mackenzie, 1991). Therefore, the glucuronidated metabolites of monoHER are unlikely to be involved in the cardioprotective effect of monoHER. In humans, the main metabolic route of monoHER appeared to be glucuronidation, which might contribute to the absence of cardioprotection in humans.

We were also able to detect GSH-monoHER conjugates. The presence of GSH conjugates indicates that monoHER has functioned as antioxidant. As a catechol, during the scavenging of reactive species, monoHER can be converted into a quinone and subsequently conjugate with glutathione (GSH) (Jacobs *et al.*, 2009). Relatively low amounts of GSH-monoHER conjugate were found compared with the other metabolites, probably because there was no oxidative stress in the healthy volunteers and because, as recently shown, the monoHER quinone rather reacts with the antioxidant ascorbate than with GSH (Jacobs *et al.*, 2010). Like the glucuronides and the oxidized metabolites, the GSH conjugates are charged at physiological pH, which will decrease their cellular uptake. Also taking into account the relatively low concentration of these metabolites, it is unlikely that these metabolites contribute to the protective effect of monoHER.

Another metabolic route was methylation. The *O*-methylation of catechols is catalyzed by the enzyme catechol-*O*-methyltransferase (COMT) (Zhu, 2002). It has been shown that methylation makes flavonoids more lipophilic, thereby facilitating their transport over biological membranes and increasing their cellular uptake (Spencer *et al.*, 2004; Spencer *et al.*, 2003). Moreover, blocking the free hydroxyl group by methylation, prevents other conjugation reactions such as glucuronidation at this position, and thus increases the metabolic stability of flavonoids (Walle, 2009). It has been shown that the methylated metabolites of

the flavonoid quercetin provided significant protection against oxidative stress-induced cellular damage (Spencer *et al.*, 2003). Also the methylated metabolite of epicatechin, i.e. 3'-O-methylepicatechin, has been shown to exert protective effects (Spencer *et al.*, 2001). In line with these findings, the methylated conjugates of monoHER are considered as active metabolites that contribute to the cardioprotective effect of monoHER. In contrast to humans, the major metabolic pathway in mice is methylation. This might also explain why monoHER efficiently protects the heart against doxorubicin-induced cardiotoxicity in mice and not in humans.

The monoHER-glucosides are a group of compounds that might be of special interest. These metabolites are formed by hydrolysis of the disaccharide, thereby removing the rhamnose sugar. They contain a terminal glucose moiety and are also methylated. Flavonoid glucosides are reported to rapidly enter cells via GLUT-transporters (Passamonti *et al.*, 2009; Strobel *et al.*, 2005), which also transport glucose (Huang and Czech, 2007). This will increase the intracellular antioxidant concentration and enhance their effect. The role of these metabolites in the protective effect of monoHER needs to be further investigated. In mice, these metabolites are gradually formed over time and several hours after monoHER administration they have the highest concentrations compared with all other metabolites. This suggests that these metabolites might be of importance, particularly in the late protection against doxorubicin-induced cardiotoxicity in mice. In humans, the concentration of these metabolites (M9 and M12) remains relatively low.

Another remarkable finding in the clinical phase II study with monoHER was that monoHER enhances the antitumour activity of doxorubicin in certain types of cancer (Bruynzeel *et al.*, 2007). This has not been observed in animals thus far (van Acker *et al.*, 1997). It has been shown that monoHER sensitizes cancer cells to apoptosis by preventing doxorubicin-induced NF-κB activation (Jacobs *et al.*, 2011a). The possible contribution of metabolites in this potentiating effect of monoHER has to be determined.

To conclude, in humans monoHER is predominantly converted into inactive glucuronides. In mice, on the other hand, monoHER is mainly converted into an active metabolite, i.e methyl-monoHER. In addition, monoHER glucosides might be relevant. These metabolites are formed more extensively (especially at later time-points) in mice compared with humans. Thus, the difference in the metabolic profile between men and mice might explain why the cardioprotective effect of monoHER in mice was not observed in humans. These results underscore that flavonoid metabolites are bioactive compounds that play a crucial role in the beneficial health effects of flavonoids.

Acknowledgements

The authors would like to thank Rita Vos and Lieselot Holvoet (Department of Gastroenterology, University Hospital Gasthuisberg, Belgium) for the help with the bile sampling. We are also thankful to the volunteers who participated in this study. We also like to thank Jef Vekemans (Laboratory of Macromolecular and Organic Chemistry, Eindhoven University of Technology, the Netherlands) for assistance with the ^{1}H NMR measurements.

References

Abou El Hassan MA, Kedde MA, Zwiers UT, Tourn E, Haenen GR, Bast A, van der Vijgh WJ (2003) Bioavailability and pharmacokinetics of the cardioprotecting flavonoid 7-monohydroxyethylrutoside in mice. *Cancer Chemother Pharmacol* **52:** 371-376

Abou El Hassan MA, Touw DJ, Wilhelm AJ, Bast A, van der Vijgh WJ (2000) Stability of monoHER in an aqueous formulation for i.v. administration. *Int J Pharm* **211:** 51-56

Amic D, Davidovic-Amic D, Beslo D, Rastija V, Lucic B, Trinajstic N (2007) SAR and QSAR of the antioxidant activity of flavonoids. *Curr Med Chem* **14:** 827-845

Baba S, Osakabe N, Yasuda A, Natsume M, Takizawa T, Nakamura T, Terao J (2000) Bioavailability of (-)-epicatechin upon intake of chocolate and cocoa in human volunteers. *Free Radic Res* **33:** 635-641

Bartholome R, Haenen G, Hollman CH, Bast A, Dagnelie PC, Roos D, Keijer J, Kroon PA, Needs PW, Arts CW (2010) Deconjugation kinetics of glucuronidated phase II flavonoid metabolites by beta-glucuronidase from neutrophils. *Drug Metab Pharmacokinet* **25:** 379-387

Bast A, Haenen GR, Bruynzeel AM, Van der Vijgh WJ (2007) Protection by flavonoids against anthracycline cardiotoxicity: from chemistry to clinical trials. *Cardiovasc Toxicol* **7:** 154-159

Bruynzeel AM, Niessen HW, Bronzwaer JG, van der Hoeven JJ, Berkhof J, Bast A, van der Vijgh WJ, van Groeningen CJ (2007) The effect of monohydroxyethylrutoside on doxorubicin-induced cardiotoxicity in patients treated for metastatic cancer in a phase II study. *Br J Cancer* **97:** 1084-1089

Doerge DR, Chang HC, Churchwell MI, Holder CL (2000) Analysis of soy isoflavone conjugation in vitro and in human blood using liquid chromatography-mass spectrometry. *Drug Metab Dispos* **28:** 298-307

Doroshow JH, Locker GY, Myers CE (1980) Enzymatic defenses of the mouse heart against reactive oxygen metabolites: alterations produced by doxorubicin. *J Clin Invest* **65:** 128-135

Haenen GR, Jansen FP, Bast A (1993) The antioxidant properties of five O-(-β–Hydroxyethyl)-Rutosides of the flavonoid mixture Venoruton. *Phlebology* **Suppl.1:** 10-17

Horenstein MS, Vander Heide RS, L'Ecuyer TJ (2000) Molecular basis of anthracycline-induced cardiotoxicity and its prevention. *Mol Genet Metab* **71:** 436-444

Huang S, Czech MP (2007) The GLUT4 glucose transporter. *Cell Metab* **5:** 237-252

Iarussi D, Indolfi P, Galderisi M, Bossone E (2000) Cardiac toxicity after anthracycline chemotherapy in childhood. *Herz* **25:** 676-688

Jacobs H, Bast A, Peters GJ, van der Vijgh WJ, Haenen GR (2011a) The semisynthetic flavonoid monoHER sensitises human soft tissue sarcoma cells to doxorubicin-induced apoptosis via inhibition of nuclear factor-kappaB. *Br J Cancer* **104**: 437-440

Jacobs H, Moalin M, Bast A, van der Vijgh WJ, Haenen GR (2010) An Essential Difference between the Flavonoids MonoHER and Quercetin in Their Interplay with the Endogenous Antioxidant Network. *PLoS One* **5:** e13880

Jacobs H, Peters R, den Hartog GJ, van der Vijgh WJ, Bast A, Haenen GR (2011b) Identification of the metabolites of the antioxidant flavonoid 7-mono-O-({beta}-hydroxyethyl)-rutoside in mice. *Drug Metab Dispos* **39:**750-756

Jacobs H, van der Vijgh WJ, Koek GH, Draaisma GJ, Moalin M, van Strijdonck GP, Bast A, Haenen GR (2009) Characterization of the glutathione conjugate of the semisynthetic flavonoid monoHER. *Free Radic Biol Med* **46:** 1567-1573

Julicher RH, Sterrenberg L, Haenen GR, Bast A, Noordhoek J (1988) The effect of chronic adriamycin treatment on heart kidney and liver tissue of male and female rat. *Arch Toxicol* **61:** 275-281

Koek GH, Vos R, Flamen P, Sifrim D, Lammert F, Vanbilloen B, Janssens J, Tack J (2004) Oesophageal clearance of acid and bile: a combined radionuclide, pH, and Bilitec study. *Gut* **53:** 21-26

Koster H, Halsema I, Scholtens E, Knippers M, Mulder GJ (1981) Dose-dependent shifts in the sulfation and glucuronidation of phenolic compounds in the rat in vivo and in isolated hepatocytes. The role of saturation of phenolsulfotransferase. *Biochem Pharmacol* **30:** 2569-2575

Lee MJ, Maliakal P, Chen L, Meng X, Bondoc FY, Prabhu S, Lambert G, Mohr S, Yang CS (2002) Pharmacokinetics of tea catechins after ingestion of green tea and (-)-epigallocatechin-3-gallate by humans: formation of different metabolites and individual variability. *Cancer Epidemiol Biomarkers Prev* **11:** 1025-1032

Lipshultz SE, Lipsitz SR, Sallan SE, Dalton VM, Mone SM, Gelber RD, Colan SD (2005) Chronic progressive cardiac dysfunction years after doxorubicin therapy for childhood acute lymphoblastic leukemia. *J Clin Oncol* **23:** 2629-2636

Manach C, Morand C, Gil-Izquierdo A, Bouteloup-Demange C, Remesy C (2003) Bioavailability in humans of the flavanones hesperidin and narirutin after the ingestion of two doses of orange juice. *Eur J Clin Nutr* **57:** 235-242

Miners JO, Mackenzie PI (1991) Drug glucuronidation in humans. *Pharmacol Ther* **51:** 347-369

Passamonti S, Terdoslavich M, Franca R, Vanzo A, Tramer F, Braidot E, Petrussa E, Vianello A (2009) Bioavailability of flavonoids: a review of their membrane transport and the function of bilitranslocase in animal and plant organisms. *Curr Drug Metab* **10:** 369-394

Radominska-Pandya A, Czernik PJ, Little JM, Battaglia E, Mackenzie PI (1999) Structural and functional studies of UDP-glucuronosyltransferases. *Drug Metab Rev* **31:** 817-899

Rice-Evans CA, Miller NJ, Paganga G (1996) Structure-antioxidant activity relationships of flavonoids and phenolic acids. *Free Radic Biol Med* **20:** 933-956

Setchell KD, Brown NM, Desai P, Zimmer-Nechemias L, Wolfe BE, Brashear WT, Kirschner AS, Cassidy A, Heubi JE (2001) Bioavailability of pure isoflavones in healthy humans and analysis of commercial soy isoflavone supplements. *J Nutr* **131:** 1362S-1375S

Shelnutt SR, Cimino CO, Wiggins PA, Ronis MJ, Badger TM (2002) Pharmacokinetics of the glucuronide and sulfate conjugates of genistein and daidzein in men and women after consumption of a soy beverage. *Am J Clin Nutr* **76:** 588-594

Singal PK, Iliskovic N (1998) Doxorubicin-induced cardiomyopathy. *N Engl J Med* **339:** 900-905

Spencer JP, Abd-el-Mohsen MM, Rice-Evans C (2004) Cellular uptake and metabolism of flavonoids and their metabolites: implications for their bioactivity. *Arch Biochem Biophys* **423:** 148-161

Spencer JP, Kuhnle GG, Williams RJ, Rice-Evans C (2003) Intracellular metabolism and bioactivity of quercetin and its in vivo metabolites. *Biochem J* **372:** 173-181

Spencer JP, Schroeter H, Rechner AR, Rice-Evans C (2001) Bioavailability of flavan-3-ols and procyanidins: gastrointestinal tract influences and their relevance to bioactive forms in vivo. *Antioxid Redox Signal* **3:** 1023-1039

Strobel P, Allard C, Perez-Acle T, Calderon R, Aldunate R, Leighton F (2005) Myricetin, quercetin and catechin-gallate inhibit glucose uptake in isolated rat adipocytes. *Biochem J* **386:** 471-478

van Acker FA, van Acker SA, Kramer K, Haenen GR, Bast A, van der Vijgh WJ (2000) 7-monohydroxyethylrutoside protects against chronic doxorubicin-induced cardiotoxicity when administered only once per week. *Clin Cancer Res* **6:** 1337-1341

van Acker SA, Boven E, Kuiper K, van den Berg DJ, Grimbergen JA, Kramer K, Bast A, van der Vijgh WJ (1997) Monohydroxyethylrutoside, a dose-dependent cardioprotective agent, does not affect the antitumor activity of doxorubicin. *Clin Cancer Res* **3:** 1747-1754

van Acker SA, Tromp MN, Haenen GR, van der Vijgh WJ, Bast A (1995) Flavonoids as scavengers of nitric oxide radical. *Biochem Biophys Res Commun* **214:** 755-759

van Acker SA, van den Berg DJ, Tromp MN, Griffioen DH, van Bennekom WP, van der Vijgh WJ, Bast A (1996) Structural aspects of antioxidant activity of flavonoids. *Free Radic Biol Med* **20:** 331-342

Walle T (2009) Methylation of dietary flavones increases their metabolic stability and chemopreventive effects. *Int J Mol Sci* **10:** 5002-5019

Willems AM, Bruynzeel AM, Kedde MA, van Groeningen CJ, Bast A, van der Vijgh WJ (2006) A phase I study of monohydroxyethylrutoside in healthy volunteers. *Cancer Chemother Pharmacol* **57:** 678-684

Xu MF, Tang PL, Qian ZM, Ashraf M (2001) Effects by doxorubicin on the myocardium are mediated by oxygen free radicals. *Life Sci* **68:** 889-901

Zhang Y, Hendrich S, Murphy PA (2003) Glucuronides are the main isoflavone metabolites in women. *J Nutr* **133:** 399-404

Zhu BT (2002) Catechol-O-Methyltransferase (COMT)-mediated methylation metabolism of endogenous bioactive catechols and modulation by endobiotics and xenobiotics: importance in pathophysiology and pathogenesis. *Curr Drug Metab* **3:** 321-349

Chapter 8

Summary and general discussion

Preclinical experiments have shown that the antioxidant flavonoid monoHER has several beneficial pharmacological actions (**Chapter 1**). One of its most important actions is that it protects the heart against doxorubicin-induced damage in mice. Unexpectedly, this protection could not clearly be observed in a clinical phase II study with metastatic cancer patients. In addition, the results of this clinical study suggest that monoHER enhances the antitumour activity of doxorubicin. The aim of this thesis was to explain these unexpected clinical findings. This was done by further investigating the antioxidant properties of monoHER and its interaction with endogenous antioxidants. Also the possible molecular mechanisms behind the antitumour effect of monoHER were studied. Moreover, to explain the different biological effects of monoHER in men and mice, the metabolism of monoHER was studied in both species and its metabolites were characterized.

Antioxidant function of monoHER

During the scavenging of highly reactive species, antioxidants donate an electron or a hydrogen atom to the radical involved. In this way the reactivity of the radical is annihilated. However, in this reaction the antioxidant itself is converted into an oxidation product that takes over part of the reactivity of the radical. In **Chapter 2**, it was shown that in the process of offering protection against free radicals, monoHER is likewise converted into a quinone. This monoHER quinone is reactive towards thiols, e.g. it reacts with glutathione (GSH), thereby forming a GSH-monoHER adduct. Characterization of this adduct by MS and ^{1}H NMR revealed that GSH binds to the C2' position in the B ring of the monoHER quinone, identifying it as 2'-GSH-monoHER. Molecular quantum chemical calculations revealed that the C2' of the monoHER quinone has the highest LUMO (lowest unoccupied molecular orbital) value, which underscores that the C2' atom is most susceptible to nucleophilic attack by GSH. The GSH-monoHER adduct could also be detected in the bile fluid of a healthy volunteer who received monoHER by intravenous infusion. To our knowledge we were the first to detect a GSH-flavonoid conjugate *in vivo*. The formation of the electrophilic monoHER quinone is potentially harmful because when it reacts with GSH it might lower GSH levels and thus the antioxidant defense. In addition to the reaction with GSH, it is assumed that the quinone is also prone to react with e.g. essential thiol groups of proteins or enzymes, which might cause damage. Thus, the supposed beneficial effect of monoHER as an antioxidant could be eclipsed by the formation of quinone-like products with an electrophilic, toxic potential.

In **Chapter 3** the reactivity of the 2'-GSH-monoHER adduct was studied and compared with that of the 6- or 8-GSH-quercetin adduct. It was found that GSH-quercetin reacts with the thiol N-acetyl-L-cysteine (NAC) to form NAC-quercetin, whereas GSH-monoHER does not react with NAC. In addition, the adduct of the monoHER quinone with the dithiol dithiothreitol (DTT) is relatively stable, whereas the DTT-quercetin adduct is readily converted into quercetin and DTT disulfide. These differences in reactivity of the thiol-flavonoid adducts demonstrate that GSH-monoHER is relatively stable, whereas GSH-quercetin is not. This difference in reactivity was corroborated by molecular quantum chemical calculations. Thus, although both flavonoid quinones are rapidly scavenged by GSH, the advantage of monoHER is that it forms a stable conjugate with GSH, thereby preventing the possible spread of toxicity. These findings demonstrate that even structurally comparable flavonoids behave differently, which should be considered when evaluating the health effects of flavonoids.

To prevent damage by reactive oxidation products of antioxidants, the human body has an intricate network of antioxidants that pass over the reactivity from one antioxidant to another in a controlled way, thereby gradually diminishing the reactivity of the radical and recycling the antioxidants. In **Chapter 4**, it was investigated how monoHER fits into this antioxidant network. This position was compared with that of quercetin. Both the monoHER quinone and the quercetin quinone are reactive towards thiols of both GSH and proteins. However, in human blood plasma where GSH is practically absent, oxidized quercetin readily reacts with protein thiols, whereas oxidized monoHER does not react with plasma protein thiols. This could be explained by the presence of ascorbate in plasma, because ascorbate is able to reduce oxidized monoHER to the parent compound monoHER before oxidized monoHER can react with thiols. This is a major difference with oxidized quercetin that preferentially reacts with thiols rather than ascorbate (Boots *et al.*, 2003). The difference in selectivity between monoHER and quercetin originates from an intrinsic difference in the chemical nature of their oxidation products, which was confirmed by molecular quantum chemical calculations. The reactivity is directed in different ways by the two flavonoids studied. The advantage of monoHER is that it can safely channel the reactivity of radicals into the antioxidant network where the reactivity is neutralized. Thus, structurally related flavonoids belonging to the same subgroup and displaying a comparable radical scavenging activity, may have a different impact on health.

Antitumour effect of monoHER

The results of the clinical phase II study, evaluating the protective effects of monoHER on doxorubicin-induced cardiotoxicity, suggest that monoHER enhances the antitumour activity of doxorubicin in soft tissue sarcomas. This effect was investigated *in vitro* using soft tissue sarcoma cell lines (**Chapter 5**). In one (WLS-160) of the four cell lines monoHER potentiated the antitumour activity of doxorubicin. In this cell line it appeared that the effect is mediated by the induction of an apoptotic pathway. Because monoHER is able to form a GSH-monoHER adduct, it was investigated whether monoHER can deplete GSH in the soft tissue sarcoma cell lines. In contrast to the known GSH depleter L-buthionine sulfoximine (BSO), monoHER did not significantly change GSH levels in these cancer cells. This suggests that the growth inhibitory effect of monoHER in WLS-160 cells is not mediated via GSH depletion, which is in contrast to the GSH depletion observed in some cancer cells by some other flavonoids (Kachadourian and Day, 2006; Kachadourian *et al.*, 2007; Ramos and Aller, 2008). It is known that many chemotherapeutic agents induce the transcription factor NF-κB, which causes drug resistance in cancer cells (Sarkar and Li, 2008). Accordingly, doxorubicin rapidly induced NF-κB activity in WLS-160 cells, which was prevented by monoHER. Thus, down-regulation of NF-κB activation by monoHER may be responsible for the sensitization of these cancer cells to doxorubicin. From this study it may be assumed that monoHER might improve chemotherapy for certain soft tissue sarcoma patients. Moreover, it cannot be excluded that monoHER may also be valuable for the treatment of other tumours that have developed resistance through NF-κB activation.

Metabolism of monoHER in mice and men

In mice, monoHER has been successfully used as a protector against doxorubicin-induced cardiotoxicity. However, most monoHER has already been cleared from the body at the time that doxorubicin concentrations are still high. This suggests that not only the parent compound monoHER itself, but also monoHER metabolites could be responsible for the observed cardioprotective effects in mice. In **Chapter 6**, the metabolism of monoHER was investigated in the bile fluid of mice. This led to the characterization of thirteen different metabolites. The observed routes of monoHER metabolism were methylation, glucuronidation, oxidation of its hydroxyethyl group, GSH conjugation, and hydrolysis of its disaccharide. In line with other flavonoids, methylated monoHER and the monoHER glucosides were expected to have a relatively high cellular uptake and a low clearance from the body. Therefore, it is suggestive that these metabolites

might contribute to the observed protection of monoHER against doxorubicin-induced cardiotoxicity.

The observed preclinical protection of monoHER against doxorubicin-induced cardiotoxicity in mice could however not be observed in the clinical phase II study with metastatic cancer patients (Bruynzeel *et al.*, 2007). It could be that metabolites of monoHER, which contribute to its cardioprotection, are formed in mice but not (or to a lesser extend) in men. Therefore, the metabolism of monoHER was also investigated in the bile fluid of healthy volunteers **(Chapter 7)**. The same metabolites were found in men as previously in mice; however the relative amounts of the metabolites were quite different. The major metabolic route in mice appeared to be methylation while in humans especially glucuronidation was observed. It has been shown that methylation of flavonoids makes them more lipophilic, thereby improving their transport over biological membranes and increasing their cellular uptake (Spencer *et al.*, 2004; Spencer *et al.*, 2003). It is therefore suggestive that the methylated conjugates of monoHER are active metabolites that contribute to the observed cardioprotective effect of monoHER in mice. Glucuronidation, on the other hand, leads to reduced cellular uptake and accelerated elimination (Miners and Mackenzie, 1991) and thus does not contribute to the cardioprotective effect of monoHER. Moreover in mice, in contrast to men, monoHER metabolites in which the disaccharide is cleaved -and thus contain a free glucose moiety- were formed at later time-points and to a greater extend. These metabolites are possibly taken up by cardiac cells via glucose transporters, thereby increasing the intracellular antioxidant concentration and contributing to the protective effect of monoHER. From this study it could be concluded that the difference in the metabolic profile between men and mice might possibly explain the different biological activity of monoHER in both species.

Implications and further research

MonoHER and its metabolites are good candidates for further investigations. Besides the favourable properties of monoHER described in the introductory chapter, the research described in this thesis added some more advantages, i.e., the oxidation product of monoHER (in contrast to that of quercetin) can more easily be reduced to monoHER and is therefore relatively harmless, monoHER can reduce NF-κB activation in certain tumour cells, and certain monoHER metabolites may contribute to cardioprotection and possibly to antitumour activity.

Therefore, several interesting research lines are open for the future:

- Concerning the antitumour properties of monoHER, it would be interesting to investigate whether monoHER also sensitises other tumours that have developed resistance to chemotherapy through NF-κB activation.
- It would also be valuable to study the antioxidant and antitumour activities of the newly identified monoHER metabolites.
- Promising active metabolites can then be further investigated in a tumour bearing nude mouse model.
- Because it is likely that the methylated metabolites of monoHER contribute to its cardioprotective effects, it would be interesting to measure their effects in our mouse atrium model and to measure the pharmacokinetics of the active metabolites in plasma and heart tissue of mice.
- In a next step, the cardioprotective metabolites have to be investigated in mice.
- If results are promising, clinical study/studies may be proposed regarding the antitumour and/or cardioprotective effect.

References

Boots AW, Kubben N, Haenen GR, Bast A (2003) Oxidized quercetin reacts with thiols rather than with ascorbate: implication for quercetin supplementation. *Biochem Biophys Res Commun* **308:** 560-565

Bruynzeel AM, Niessen HW, Bronzwaer JG, van der Hoeven JJ, Berkhof J, Bast A, van der Vijgh WJ, van Groeningen CJ (2007) The effect of monohydroxyethylrutoside on doxorubicin-induced cardiotoxicity in patients treated for metastatic cancer in a phase II study. *Br J Cancer* **97:** 1084-1089

Kachadourian R, Day BJ (2006) Flavonoid-induced glutathione depletion: potential implications for cancer treatment. *Free Radic Biol Med* **41:** 65-76

Kachadourian R, Leitner HM, Day BJ (2007) Selected flavonoids potentiate the toxicity of cisplatin in human lung adenocarcinoma cells: a role for glutathione depletion. *Int J Oncol* **31:** 161-168

Miners JO, Mackenzie PI (1991) Drug glucuronidation in humans. *Pharmacol Ther* **51:** 347-369

Ramos AM, Aller P (2008) Quercetin decreases intracellular GSH content and potentiates the apoptotic action of the antileukemic drug arsenic trioxide in human leukemia cell lines. *Biochem Pharmacol* **75:** 1912-1923

Sarkar FH, Li Y (2008) NF-kappaB: a potential target for cancer chemoprevention and therapy. *Front Biosci* **13:** 2950-2959

Spencer JP, Abd-el-Mohsen MM, Rice-Evans C (2004) Cellular uptake and metabolism of flavonoids and their metabolites: implications for their bioactivity. *Arch Biochem Biophys* **423:** 148-161

Spencer JP, Kuhnle GG, Williams RJ, Rice-Evans C (2003) Intracellular metabolism and bioactivity of quercetin and its in vivo metabolites. *Biochem J* **372:** 173-181

Samenvatting en algemene discussie

Uit preklinische experimenten is gebleken dat het antioxidant flavonoïde monoHER verschillende gunstige farmacologische eigenschappen bezit **(Hoofdstuk 1)**. Eén opmerkelijke eigenschap is de bescherming tegen doxorubicine geïnduceerde hartschade in muizen. Deze bescherming kon helaas niet duidelijk worden bevestigd in een klinische fase II studie met een kleine groep kankerpatiënten met een metastatische ziekte. De resultaten van deze klinische studie suggereerden wel dat monoHER de antitumor activiteit van doxorubicine versterkt. Het doel van dit proefschrift was om deze onverwachte klinische bevindingen nader te verklaren. Hiertoe werden de antioxidant eigenschappen van monoHER en de interactie met endogene antioxidanten nader bestudeerd. Ook werden de mogelijke moleculaire mechanismen achter het gunstige effect van monoHER op de antitumor werking van doxorubicine onderzocht. Om de verschillende biologische effecten van monoHER in muis en mens te verklaren, werd bovendien het metabolisme van monoHER in zowel muis als mens bestudeerd en werden de monoHER metabolieten gekarakteriseerd.

Antioxidant functie van monoHER

Tijdens het wegvangen van reactieve deeltjes (radicalen) doneren antioxidanten een elektron of een waterstofatoom aan het betrokken radicaal. Op deze manier wordt de reactiviteit van het radicaal tenietgedaan. Tijdens deze reactie wordt het antioxidant echter zelf omgezet in een oxidatieproduct, dat een deel van de reactiviteit van het radicaal overneemt. In **Hoofdstuk 2** werd aangetoond dat monoHER ook wordt omgezet in een oxidatieproduct (quinon) wanneer het beschermt tegen vrije radicalen. Dit monoHER quinon is reactief met thiolen, het reageert met glutathion (GSH) waarbij een GSH-monoHER adduct wordt gevormd. Opheldering van de structuur van dit adduct met MS en ^{1}H NMR toonde aan dat GSH op de C2' plaats in de B ring van het monoHER quinon bindt, waardoor het als 2'-GSH-monoHER geïdentificeerd werd. Moleculair kwantum chemische berekeningen toonden aan dat het C2' atoom van het monoHER quinon de hoogste LUMO (laagst onbezette moleculaire orbitaal) waarde heeft. Dit verklaart dat het C2' atoom de meest waarschijnlijke plaats is voor nucleofiele aanval van GSH. Het GSH-monoHER adduct werd ook teruggevonden in de galvloeistof van een gezonde vrijwilliger die monoHER kreeg toegediend via een intraveneus infuus. Voor zover wij weten, zijn wij de eersten die een GSH-flavonoïde adduct hebben gedetecteerd *in vivo*. De vorming van het elektrofiele monoHER quinon is mogelijk schadelijk omdat het, wanneer het met GSH reageert, de GSH concentraties en dus het antioxidant verdedigingsmechanisme verlaagt. Bovendien wordt verondersteld dat het quinon, naast

GSH, ook met essentiële thiolgroepen van eiwitten, zoals enzymen, kan reageren. Het veronderstelde positieve effect van monoHER als antioxidant kan dus worden overschaduwd door de vorming van quinon producten met een elektrofiel en potentieel toxisch karakter.

In **Hoofdstuk 3** werd de reactiviteit van het 2'-GSH-monoHER adduct bestudeerd en vergeleken met dat van het 6- of 8-GSH-quercetine adduct. Er werd gevonden dat GSH-quercetine met het thiol N-acetyl-L-cysteine (NAC) reageert, waarbij NAC-quercetine wordt gevormd. Het GSH-monoHER adduct daarentegen reageerde niet met NAC. Bovendien werd gevonden dat het adduct van het monoHER quinon met de dithiol dithiothreitol (DTT) relatief stabiel is, terwijl het DTT-quercetine adduct snel wordt omgezet in quercetine en DTT disulfide. Deze verschillen in reactivitieit van de thiol-flavonoïde adducten tonen aan dat GSH-monoHER veel stabieler is dan GSH-quercetine. Dit verschil in reactiviteit werd bevestigd door moleculair kwantum chemische berekeningen. Hoewel beide quinonen van monoHER en quercetine snel ingevangen worden door GSH, is het voordeel van monoHER t.o.v. quercetine dat het een stabiel adduct vormt met GSH en daarbij de mogelijke verspreiding van toxiciteit voorkomt. Deze bevindingen tonen aan dat zelfs flavonoïden met een zeer vergelijkbare structuur zich veschillend gedragen. Dit kan tot uiting komen in de biologische effecten van deze flavonoïden.

Om schade veroorzaakt door reactieve oxidatieproducten van antioxidanten te voorkomen, heeft het menselijk lichaam een intrinsiek netwerk van antioxidanten, die op een gecontroleerde manier de reactiviteit van het ene naar het andere antioxidant overbrengen. Op deze manier wordt de reactiviteit van het radicaal geleidelijk verminderd en worden de antioxidanten telkens terug gevormd. In **Hoofdstuk 4** werd onderzocht hoe monoHER in dit antioxidantnetwerk past. Deze positie werd vergeleken met die van quercetine. Zowel het monoHER quinon als het quercetine quinon zijn reactief met thiolen van zowel GSH als eiwitten. In humaan bloed plasma, dat bijna geen GSH bevat, reageert geoxideerd quercetine echter snel met eiwitthiolen, terwijl geoxideerd monoHER niet met plasma eiwitthiolen reageert. Dit kon worden verklaard door de aanwezigheid van vitamine C in plasma. Vitamine C is in staat het geoxideerde monoHER te reduceren tot monoHER voordat het geoxideerde monoHER met thiolen kan reageren. Dit is in tegenstelling met het geoxideerde quercetine dat eerder met thiolen reageert dan met vitamine C. Het verschil in deze selectiviteit tussen monoHER en quercetine, komt door een intrinsiek verschil in de chemische aard van hun oxidatieproducten. Dit werd bevestigd door moleculair kwantum chemische berekeningen. De reactiviteit wordt door de twee bestudeerde flavonoïden op verschillende manieren gereguleerd. Het voordeel van

monoHER is dat het de reactiviteit van de radicalen veilig het antioxidantnetwerk in kan sturen, zodat de reactiviteit geneutralizeerd wordt. Dit toont wederom aan dat structuur gerelateerde flavonoïden, die tot dezelfde subgroep behoren en een vergelijkbare radicaal vangende activiteit hebben, een heel verschillende impact op de gezondheid kunnen hebben.

Antitumor effect van monoHER

De resultaten van de klinische fase II studie, waarin de beschermende effecten van monoHER op doxorubicine geïnduceerde cardiotoxicitieit geëvalueerd werden, suggereren dat monoHER het antitumor effect van doxorubicine in weke delen sarcomen versterkt. Dit effect werd *in vitro* verder onderzocht door gebruik te maken van weke delen sarcomen cellijnen **(Hoofdstuk 5)**. In één (WLS-160) van de vier onderzochte cellijnen, versterkte monoHER het antitumor effect van doxorubicine. In deze cellijn bleek het effect van monoHER gemedieerd te worden door de inductie van apoptose. Omdat monoHER in staat is een GSH-monoHER adduct te vormen, werd er onderzocht of monoHER het GSH-niveau in de weke delen sarcomen cellijnen kan verlagen. In tegenstelling tot de bekende GSH verlagende stof, L-buthionine sulfoximine (BSO), had monoHER geen significante invloed op de GSH-niveaus in deze kankercellen. Dit suggereert dat, in tegenstelling tot de GSH-depletie die werd waargenomen in sommige kankercellen veroorzaakt door enkele andere flavonoïden, de groeiremmende effecten van monoHER in WLS-160 cellen niet gemedieerd werden door GSH depletie. Het is bekend dat vele chemotherapeutische middelen de transcriptiefactor NF-κB activeren, hetgeen resistentie tegen deze middelen veroorzaakt in kankercellen. Zo activeerde doxorubicine ook snel NF-κB in WLS-160 cellen, wat voorkomen werd door monoHER. Vermindering van NF-κB activatie door monoHER zou dus verantwoordelijk kunnen zijn voor het gevoelig maken van deze kankercellen voor doxorubicine. Uit deze studie kan geconcludeerd worden dat monoHER de chemotherapie voor bepaalde patiënten met een weke delen sarcoom mogelijk kan verbeteren. Vervolgonderzoek moet aantonen of monoHER ook waardevol kan zijn voor de behandeling van andere tumoren die resistentie ontwikkeld hebben via NF-κB activatie.

Metabolisme van monoHER in muis en mens

In muizen werd monoHER met succes gebruikt als een beschermer tegen doxorubicine geïnduceerde cardiotoxiciteit. Het merendeel van monoHER is echter al verdwenen uit het lichaam op het moment dat de doxorubicine con-

centraties nog hoog zijn. Dit suggereert dat, naast monoHER zelf, ook monoHER metabolieten betrokken kunnen zijn bij het vastgestelde hartbeschermende effect van monoHER in muizen. In **Hoofdstuk 6** werd het metabolisme van monoHER onderzocht door de galvloeistof van muizen, die monoHER kregen toegediend, te verzamelen. Dit leidde tot de karakterisatie van dertien verschillende metabolieten. De volgende metabole routes van monoHER werden waargenomen: methylering, glucuronidering, oxidatie van de hydroxyethyl groep, GSH conjugatie en hydrolyse van het disaccharide. Op grond van bevindingen met andere flavonoïden wordt verwacht dat gemethyleerd monoHER en de monoHER glucosiden een relatief hoge cellulaire opname en relatief lage klaring uit het lichaam hebben. Het is daarom aannemelijk dat deze metabolieten kunnen bijdragen aan de waargenomen bescherming van monoHER tegen doxorubicine geïnduceerde cardiotoxiciteit.

De in muizen gevonden bescherming van monoHER tegen doxorubicine geïnduceerde cardiotoxiciteit kon niet duidelijk worden bevestigd in de klinische fase II studie met kankerpatiënten met een gemetastaseerde ziekte. Mogelijk worden monoHER metabolieten, die bijdragen tot de bescherming, wel gevormd in muizen, maar niet (of in mindere mate) in mensen. Daarom werd het monoHER metabolisme ook onderzocht in de galvloeistof van gezonde vrijwilligers (**Hoofdstuk 7**). In deze mensen werden dezelfde metabolieten teruggevonden als eerder in muizen. De relatieve hoeveelheden van de metabolieten verschilden wel in hoge mate tussen beide soorten. De belangrijkste metabole route in muizen bleek methylering te zijn, terwijl in mensen vooral glucuronidering werd waargenomen. Methylering maakt flavonoïden lipofieler, waardoor ze beter over biologische membranen getransporteerd kunnen worden en hun cellulaire opname verhoogd wordt. Het is daarom aannemelijk dat de gemethyleerde metabolieten van monoHER bijdragen aan het hartbeschermende effect van monoHER, dat werd waargenomen in muizen. Glucuronidering, daarentegen, vermindert de opname in de cel en versnelt de eliminatie. De geglucuronideerde metabolieten zullen daarom niet bijdragen aan het hartbeschermende effect van monoHER. Bovendien werden er in muizen, in tegenstelling tot in mensen, meer monoHER metabolieten gevormd die een vrije glucose groep bevatten (monoHER glucosiden). Verondersteld wordt dat deze metabolieten actief worden opgenomen door hartcellen via glucose transporters, wat de intracellulaire antioxidant concentratie verhoogt en dus bijdraagt aan het beschermende effect van monoHER. Uit deze studie kon geconcludeerd worden dat het verschil in het metabole profiel tussen muis en mens mogelijk de verschillende biologische activitieit van monoHER in beide species verklaart.

Implicaties en verder onderzoek

MonoHER en de metabolieten van monoHER zijn goede kandidaten voor verder onderzoek. Aan de positieve eigenschappen van monoHER, die werden beschreven in het inleidende hoofdstuk, heeft het onderzoek beschreven in dit proefschrift er nog enkele toegevoegd. Zo kan het oxidatieproduct van monoHER (in tegenstelling tot dat van quercetine) gemakkelijker gereduceerd worden tot monoHER waardoor het minder schadelijk is, monoHER kan NF-κB activatie verminderen in bepaalde kankercellen en verondersteld wordt dat bepaalde monoHER metabolieten bijdragen tot de hartbescherming en mogelijk de antitumor activiteit.
Er staan daarom verschillende interessante onderzoekslijnen open voor de toekomst:

- Wat het antitumor effect van monoHER betreft, zou het interessant zijn om te onderzoeken of monoHER, naast de bestudeerde liposarcoma WLS-160, ook andere tumoren, die resistentie voor chemotherapie ontwikkeld hebben door NF-κB activatie, terug gevoeliger kan maken voor chemotherapie.
- Het zou ook waardevol zijn om de antioxidant en antitumor activiteiten van de nieuw geïdentificeerde monoHER metabolieten te onderzoeken.
- Veelbelovende actieve metabolieten kunnen dan verder onderzocht worden in ons tumordragende naakte muizenmodel.
- Gebaseerd op de veronderstelling dat de gemethyleerde metabolieten van monoHER het hart beschermen, zou het interessant zijn om deze stoffen te onderzoeken in ons muis atrium model en om de farmacokinetiek van de actieve metabolieten te bepalen in plasma en hartweefsel van muizen.
- In een volgende stap zullen de hartbeschermende metabolieten onderzocht moeten worden in muizen, *in vivo*.
- Als de resulaten veelbelovend zijn, kan het antitumor en/of hartbeschermende effect van de monoHER metabolieten klinisch worden onderzocht.

Dankwoord

Eindelijk! Mijn boekje is klaar! Ik was echter nooit zover gekomen zonder de hulp van een groot aantal mensen. Daarom wil ik in dit laatste hoofdstuk iedereen bedanken die op de een of andere manier heeft bijgedragen aan de totstandkoming van dit proefschrift en de fijne promotietijd.

Allereerst wil ik mijn promotor Prof. dr. A. Bast en copromotores Dr. G.R.M.M. Haenen en Prof. dr. W.J.F. van der Vijgh bedanken voor de kans die ze me hebben gegeven om dit promotieonderzoek te starten. Beste Aalt, bedankt voor je enthousiaste en motiverende begeleiding! Ik apprecieer het erg dat je elke week weer tijd vrij wist te maken om samen met Guido de resultaten (en vaak ook andere dingen..) te bespreken. Je hield onze onderzoekslijn altijd goed in de gaten en je zorgde voor de juiste bijsturing en advies op het juiste moment. Beste Guido, ik kan me geen betere directe begeleider voorstellen dan jou. Bedankt dat je deur altijd voor me open stond. Ondanks je drukke agenda wist je toch altijd tijd vrij te maken om data te bekijken, mee te denken aan proefopzetten en je kennis te delen. Ook bedankt voor het snelle corrigeren van manuscripten. Als ik je weer eens 'huiswerk' mee gaf, lag het 's morgens, voorzien van jouw commentaren, al weer terug op mijn bureau. Bedankt voor je toewijding en uitstekende begeleiding! Beste Wim, ik bewonder uw passie en grenzeloze enthousiasme voor onderzoek. Ook al had u geen vaste werkplek in Maastricht, via e-mail, telefoon, post, fax en natuurlijk uw regelmatige bezoekjes aan Maastricht wist u mij toch een bijzonder goede begeleiding te geven. Mede dankzij uw zorgvuldigheid en kritische kijk, hebben we mooie resultaten bekomen. Hiervoor wil ik u hartelijk bedanken.
Aalt, Guido en Wim, ik heb veel van jullie geleerd. Jullie zijn een geweldig promotieteam!

Ik had het geluk om tijdens mijn promotieonderzoek samen te mogen werken met verschillende mensen uit verschillende vakgebieden.
Dr. G.H. Koek (AzM, Maastricht), beste Ger, bedankt voor je hulp bij de humane studie in Leuven. Door jouw ervaring verliep het verzamelen van de gal bij de proefpersonen bijzonder gesmeerd! Ook wil ik graag Prof. dr. J. Tack, Rita Vos en Lieselot Holvoet (Gasthuisberg, Leuven) bedanken voor hun hulp bij deze studie. En natuurlijk ook alle vrijwilligers die bereid waren aan deze studie deel te nemen.
Dr. R. Peters (DSM Resolve, Geleen), beste Ron, bedankt voor alle hulp bij de LC-MS analyses. Voor de identificatie van de verschillende monoHER metabolieten was jouw kennis onmisbaar. Het was gezellig om een paar dagen bij jullie op het lab door te brengen. Leuk dat je nu ook in mijn beoordelingscommissie zit!

Dr. G.P.F. van Strijdonck (Hoge school Zuyd, Heerlen), beste Gino, jou wil ik samen met je toenmalige student Guy Draaisma graag bedanken voor de hulp bij de identificatie van het GSH-monoHER adduct. Dit heeft een mooie publicatie opgeleverd!
Prof. dr. G.J. Peters (VU, Amsterdam), beste Frits, hartelijk bedankt voor het aanleveren van de humane cellijnen en uw hulp bij het schrijven van het celkweek artikel. Ook dit leidde tot een mooie publicatie!

Ik wil ook graag alle leden van de beoordelingscommissie hartelijk bedanken voor het beoordelen van mijn proefschrift.

Vervolgens wil ik graag mijn Toxicologie collega's bedanken voor de aangename werksfeer en de geweldig leuke tijd de afgelopen jaren. Om zeker niemand te vergeten ga ik best even één voor één alle kamers af. Ik heb mijn eigen kamer mogen delen met verschillende toffe mensen. Els, mijn allereerste kamergenootje, ik weet nog goed hoe ik viereneenhalf jaar geleden als AIO kwam binnenwandelen. Je was toen zelf druk bezig met alles te regelen voor je eigen promotie. Toch vond je regelmatig de tijd voor een gezellige babbel. Bedankt om me zo goed op te vangen, mede dankzij jou voelde ik me direct thuis op onze afdeling. Na een tijdje werd het iets 'drukker' op onze kamer.. Agnes, we zijn maar kort kamergenootjes geweest, maar het was een leuke tijd! Fijn dat je nu weer terug in Maastricht werkt. En dan mijn twee huidige kamergenootjes, Daniëlle en Bregje. Het is echt gezellig bij ons op de kamer (Zou ons plantje daar voor iets tussen zitten? Of jullie regelmatige meezingen met de radio? Of zou het toch komen door onze gezamenlijke jeugdidolen ;-)...) Daniëlle, jou moet ik nog extra bedanken voor het dagelijks ophalen van onze post. Zo bezorgde je me onlangs net op tijd een toch wel belangrijke brief ;-)
Dan onze twee toffe buurvrouwen, Jiska en Merel. Jiska, bedankt voor je luisterende oor en de handige promotietips. Merel, bedankt voor de gezelligheid (wanneer gaan we die cocktails nu nog eens shaken?).
De volgende kamer is al vaak van eigenaar veranderd. Eerst Saskia, Liesbeth en Erik C (zelf een kersverse doctor). Ondertussen druk bezet door: Nuria (gracias..!), Kristien (fijn dat jij mijn opvolgster bent, zo blijft het monoHER onderzoek toch in belgische handen ;-)), Erik R (je chocoladecake is echt overheerlijk!, en nog gezond ook.. toch?) en Max, jij verdient nog een speciaal woordje van dank voor alle hulp bij de chemische aspecten van mijn proefschrift, van Spartan berekeningen tot NMR analyses. Echt super hoe je telkens heel enthousiast een chemische verklaring wist te geven aan mijn biologische bevindingen. Bedankt hiervoor!

Vervolgens een iets rustigere kamer.. alhoewel ik hoor toch regelmatig een luid gelach uit die richting komen. Antje (bedankt voor al je kritische vragen tijdens onze werkbesprekingen) en Gertjan (nogmaals bedankt voor je hulp bij de muizenstudie).
En dan, last but not least, volgens mij de drukst bezochte kamer van onze afdeling (door mij in ieder geval toch..). Marie-José, Roger, Esther (en vroeger ook Marc en Vanessa), bedankt dat ik altijd bij jullie terecht kon als ik weer eens ergens hulp bij nodig had of gewoon voor een gezellige babbel. Marie-José, bedankt voor je helpende hand op het lab! Marc, bedankt voor me wegwijs te maken met de HPLC en voor de hulp bij het opzetten van mijn eerste HPLC methode. Vanessa, je was een toffe collega! Esther, DUS.. het is altijd gezellig met jou in de buurt (eetmaatje, feestmaatje,..), bedankt voor de leuke koffiepauzes, je behulpzaamheid en interesse. Roger, bedankt voor al je hulp, je gezelligheid en het organiseren van onze Tox-borrels. Dit zorgde voor de nodige ontspanning tijdens onze drukke werkzaamheden.. en bracht een gezellige sfeer op onze afdeling. Volgens mij zijn we echt wel de leukste afdeling van de uni. Tox rules! ;-)
Er zijn de afgelopen jaren ook een aantal stagiaires de revue gepasseerd: Guy, Arthur, Mick, Marike en Raymon. Bedankt voor jullie inzet!
Verder wil ik ook nog Els en Akke bedanken voor hun administratieve hulp, alle ex-collega's van Farmacologie en alle nieuwe Toxicologie collega's.

Dan nog een speciaal woordje van dank voor mijn paranimfen, Els en Roger. Eerst en vooral heel erg bedankt dat jullie mijn paranimfen willen zijn. Echt fijn dat jullie op 1 juli naast mij zullen staan! Ik heb jullie daarnet al even genoemd. Maar, ook buiten het werk hebben we al verschillende leuke dingen gedaan. Denk maar aan de ooh zo foute Q-party's en andere feestjes. En natuurlijk onze skivakantie samen. Dat was echt super leuk.. vooral de après-ski.. ♫ ..*Und ich spring, spring..* ♫ ;-). Bedankt voor alles!

Gelukkig bleef er tijdens deze drukke promotietijd ook nog voldoende tijd over voor familie en vrienden.
Hanne, Mauro, Jan, Martin, Marga en Jelle, bedankt voor de gezellige etentjes en feestjes. Binnenkort is het onze beurt om een BBQ te organiseren. Echt fijn dat jullie er op 1 juli ook bij willen zijn om mij aan te moedigen!

Mijn lieve schoonfamilie: Martine, Daniel, Tiffany, mémé en bonpoes. Bedankt voor jullie welgemeende interesse en steun. Hopelijk wordt het over enkele weken duidelijk wat ik nu precies gedaan heb de afgelopen jaren!

Marga, je bent de beste zus die ik me kan voorstellen. Bedankt voor alles! Onze ontspannende weekendjes samen, onze talrijke shop-dates, het samen sporten en natuurlijk onze super leuke vakanties, samen met Jelle (mijn toffe schoonbroer) en Yannick, zorgden voor de nodige ontspanning. En natuurlijk niet te vergeten jullie lieve kleine meid. Roxan, ik ben een hele trotse meter!

Bomma en Bompa, hoe kan ik jullie ooit bedanken voor alles wat jullie voor mij gedaan hebben.. Bedankt dat ik altijd bij jullie terecht kan en voor jullie interesse en steun in alles wat ik doe!

Mama en papa, bedankt dat jullie altijd voor me klaar staan.. en dat ik nog zo lang heb mogen genieten van jullie warme nest. En natuurlijk ook Leedy en Lara (de liefste honden van de hele wereld), bedankt voor het altijd even enthousiaste onthaal bij het thuiskomen en voor de fijne ontspannende wandelingen na een drukke werkdag.

Liefste Yannick, bedankt voor alles (te veel om op te noemen), je liefde, interesse, hulp, gezelligheid,.. Ik kijk al uit naar het samenwonen in ons eigen huisje..!

Bedankt iedereen!!!

Hilde

Curriculum vitae

Curriculum vitae

Hilde Jacobs was born on May 4th 1984 in Lommel, Belgium. After finishing secondary school at the 'Sint-Jozefscollege' in Lommel, she started in 2002 with the study Biomedical Sciences at the transnational University Limburg (tUL, campus Diepenbeek, Belgium). She did her master internship at the Department of Molecular Genetics at Maastricht University where she investigated the role of the transcription factor NF-κB in atherosclerosis. In 2006 she graduated as a Master in Clinical Molecular Life Sciences. In January 2007, she started her PhD project at the Department of Toxicology at Maastricht University. The research performed during this project, under the supervision of Prof. dr. A. Bast, Dr. G.R.M.M. Haenen and Prof. dr. W.J.F. van der Vijgh, is described in the present thesis. Since January 2011 she is working as a postdoctoral fellow at the Department of Toxicology, Maastricht University.

List of publications

Full papers

Jacobs H, van der Vijgh WJF, Koek GH, Draaisma GJJ, Moalin M, van Strijdonck GPF, Bast A, Haenen GRMM. *Characterization of the glutathione conjugate of the semisynthetic flavonoid monoHER.* Free Radical Biology and Medicine 2009; **46**:1567-1573.

Jacobs H, Moalin M, van Gisbergen M, Bast A, van der Vijgh WJF, Haenen GRMM. *An essential difference in the reactivity of the glutathione adducts of the structurally closely related flavonoids monoHER and quercetin.* Submitted.

Jacobs H, Moalin M, Bast A, van der Vijgh WJF, Haenen GRMM. *An essential difference between the flavonoids monoHER and quercetin in their interplay with the endogenous antioxidant network.* PLoS One 2010; **5**:e13880.

Jacobs H, Bast A, Peters GJ, van der Vijgh WJF, Haenen GRMM. *The semisynthetic flavonoid monoHER sensitises human soft tissue sarcoma cells to doxorubicin-induced apoptosis via inhibition of nuclear factor-kB.* British Journal of Cancer 2011; **104**:437-440.

Jacobs H, Peters R, den Hartog GJM, van der Vijgh WJF, Bast A, Haenen GRMM. *Identification of the metabolites of the antioxidant flavonoid 7-mono-O-(β-hydroxyethyl)-rutoside in mice.* Drug Metabolism and Disposition 2011; **39**:750-756.

Jacobs H, Koek GH, Peters R, Moalin M, Tack J, van der Vijgh WJF, Bast A, Haenen GRMM. *Differences in the metabolic profile of the antioxidant flavonoid 7-mono-O-(β-hydroxyethyl)-rutoside between men and mice. Possible implications for its cardioprotective effect.* Submitted.

Abstracts

Jacobs H, Haenen GRMM, Draaisma GJJ, van Strijdonck GPF, van der Vijgh WJF, Bast A. *The reaction product formed during the antioxidant activity of monoHER is relatively harmless.* Poster presentation at the PhD student meeting of the Netherlands Society of Toxicology and Annual Meeting of the NVT, June 2008, Wageningen, The Netherlands.

Jacobs H, Haenen GRMM, Draaisma GJJ, van Strijdonck GPF, van der Vijgh WJF, Bast A. *The reaction product formed during the antioxidant action of monoHER is relatively nontoxic.* Poster presentation at the PhD student meeting of the Netherlands Federation of Innovative Drug Research (FIGON) and Annual Meeting of the NVF, October 2008, Lunteren, The Netherlands.

Jacobs H, Haenen GRMM, Draaisma GJJ, van Strijdonck GPF, van der Vijgh WJF, Bast A. *Characterization of the glutathione conjugate of the semisynthetic flavonoid monoHER.* Poster presentation at the Biomedica Life Science Summit, March 2010, Aachen, Germany.